AKADEMIA GÓRNICZO-HUTNICZA
IM. STANISŁAWA STASZICA W KRAKOWIE
AGH UNIVERSITY OF SCIENCE
AND TECHNOLOGY

SCALE TRANSPORT PROPERTIES

http://home.agh.edu.pl/~grzesik

Methods of studying scale defect structures and transport properties

1. Determining the crystalline sublattice with the predominant disorder (e.g. marker method)
2. Determining deviation from stoichiometry in the compound that constitutes the scale
3. Determining the type and concentration of point defects in the compound that constitutes the scale (defect structure)
4. Determining the mobility of the defects that constitute the scale (transport properties)

Methods of studying deviation from stoichiometry in compounds constituting a scale

- **Direct gravimetric method**
- **Rosenburg method**
- Volumetric or manometric method
- Chemical analysis of the scale composition
- Electrochemical method
- Redox method
- Roentgen method

Direct gravimetric method in deviation from stoichiometry studies

Example I:
MeX, predominant disorder in the cation sublattice

Experimental stages:

- Weighing the studied metal sample: m_{Me} – initial sample mass
- Complete oxidation of the metallic sample: m_X – sample mass change
- Determination of the molar ratio of the metal to the oxidation in the scale compound:

$$\frac{m_{Me} / M_{Me}}{m_X / M_X}$$

< 1	= 1	> 1
$Me_{1-y}X$	MeX	$Me_{1+y}X$

M_{Me} and M_X – molar mass of the metal and oxidant, respectively

Direct gravimetric method in deviation from stoichiometry studies

Example II:
MeX, predominant disorder in the anion sublattice

Experimental stages:

- Weighing the studied metal sample: m_{Me} – initial sample mass
- Complete oxidation of the metallic sample: m_X – sample mass change
- Determination of the molar ratio of the metal to the oxidation in the scale compound:

$$\frac{m_{Me} / M_{Me}}{m_X / M_X}$$

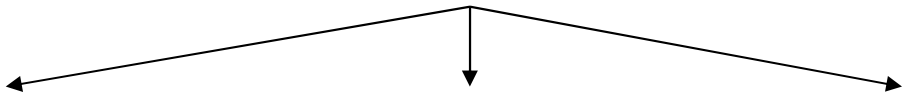

< 1	= 1	> 1
MeX_{1+y}	MeX	MeX_{1-y}

Direct gravimetric method in deviation from stoichiometry studies

Example III:
Me_aX_b, predominant disorder in the <u>cation sublattice</u>

Experimental stages:

- Weighing the studied metal sample: m_{Me} – initial sample mass
- Complete oxidation of the metallic sample: m_X – sample mass change
- Determination of the molar ratio of the metal to the oxidation in the scale compound:

$$\frac{m_{Me} / M_{Me}}{m_X / M_X}$$

< a/b	= a/b	> a/b
$Me_{a-y}X_b$	Me_aX_b	$Me_{a+y}X_b$

Direct gravimetric method in deviation from stoichiometry studies

Example III:

Me_aX_b, predominant disorder in the cation sublattice, cont.

$$\frac{m_{Me} / M_{Me}}{m_X / M_X} < \frac{a}{b} \qquad \Rightarrow \qquad Me_{a-y}X_b$$

$$\frac{a - y}{b} = \frac{m_{Me} / M_{Me}}{m_X / M_X}$$

$$y = a - \frac{b \cdot m_{Me} / M_{Me}}{m_X / M_X}$$

Rosenburg method in deviation from stoichiometry studies

This method will be presented in the section on scale transport property studies

Determining the type and concentration of point defects in the compound constituting a scale

Example:

$Mn_{1-y}S$, predominant disorder in the cation sublattice

$$y = 1 - \frac{m_{Mn} \cdot M_S}{m_S \cdot M_{Mn}}$$

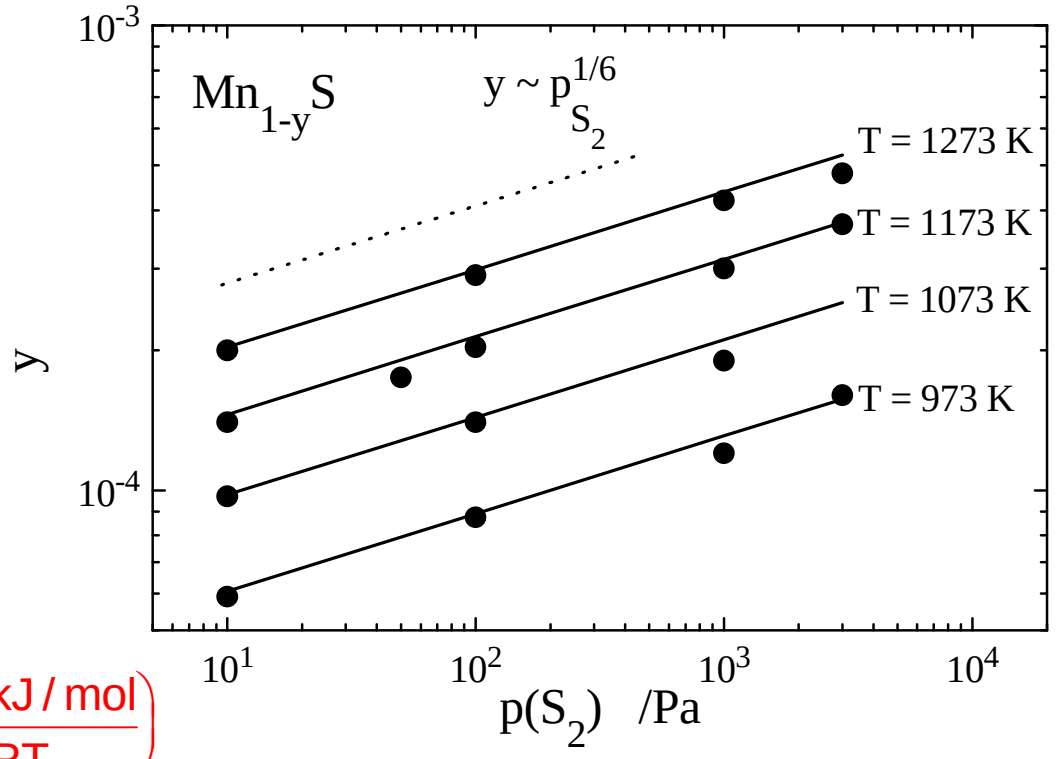

$$y = [V''_{Mn}] = 4{,}43 \cdot 10^{-2}\, p_{S_2}^{1/6} \exp\left(-\frac{41{,}0\ \text{kJ/mol}}{RT}\right)$$

S. Mrowec and Z. Grzesik, "Nonstoichiometry and self-diffusion in "α -MnS", Solid State Phenomena, **72**, 69-78 (2000).

S. Mrowec, Z. Grzesik, "Defect concentration and their mobility in nonstoichiometric manganous sulphide", Solid State Ionics, **143**, 25-29 (2001).

Determining the type and concentration of point defects in the compound constituting a scale

Example:

$Mn_{1-y}S$, predominant disorder in the cation sublattice, cont.

$$y = [V''_{Mn}] = 4{,}43 \cdot 10^{-2}\, p_{S_2}^{1/6} \exp\left(-\frac{41{,}0\ \text{kJ/mol}}{RT}\right)$$

$$\tfrac{1}{2}S_2 \Leftrightarrow V_{Mn}^{x} + S_S^{x} \qquad \tfrac{1}{2}S_2 \Leftrightarrow V_{Mn}^{'} + h^{\bullet} + S_S^{x} \qquad \tfrac{1}{2}S_2 \Leftrightarrow V_{Mn}^{''} + 2h^{\bullet} + S_S^{x}$$

$$K = [V_{Mn}^{x}] \cdot p_{S_2}^{-1/2} \qquad K = [V'_{Mn}] \cdot [h^{\bullet}] \cdot p_{S_2}^{-1/2} \qquad K = [V''_{Mn}] \cdot [h^{\bullet}]^2 \cdot p_{S_2}^{-1/2}$$

$$[V_{Mn}^{x}] = K \cdot p_{S_2}^{1/2} \qquad [V'_{Mn}] = [h^{\bullet}] \qquad 2[V''_{Mn}] = [h^{\bullet}]$$

$$[V'_{Mn}] = K^{1/2} \cdot p_{S_2}^{1/4} \qquad [V''_{Mn}] = 0.63 \cdot K^{1/3} \cdot p_{S_2}^{1/6}$$

Determining the type and concentration of point defects in the compound constituting a scale

Example:

$Mn_{1-y}S$, predominant disorder in the cation sublattice, cont.

$$y = [V''_{Mn}] = 4{,}43 \cdot 10^{-2}\, p_{S_2}^{1/6} \exp\left(-\frac{41{,}0\ \text{kJ/mol}}{RT}\right)$$

$$\frac{1}{2}S_2 \Leftrightarrow V''_{Mn} + 2h^{\bullet} + S_S^x$$

$$[V''_{Mn}] \cdot [h^{\bullet}]^2 \cdot p_{S_2}^{-1/2} = K = \exp\left(-\frac{\Delta G_f}{RT}\right) = \exp\left(\frac{\Delta S_f}{RT}\right) \cdot \exp\left(-\frac{\Delta H_f}{RT}\right)$$

$$2[V''_{Mn}] = [h^{\bullet}]$$

$$[V''_{Mn}] = \tfrac{1}{2}[h^{\bullet}] = 0.63 \cdot p_{S_2}^{1/6} \cdot \exp\left(\frac{\Delta S_f}{3R}\right) \cdot \exp\left(-\frac{\Delta H_f}{3RT}\right)$$

ΔS_f and ΔH_f – entropy and enthalpy of defect formation

Scale transport properties

D_d – defect diffusion coefficient [cm^2s^{-1}]; describes defect mobility in thermodynamic equilibrium conditions for the compound that constitutes the scale

$\tilde{D}$ – chemical diffusion coefficient [cm^2s^{-1}]; describes defect mobility in conditions of a defect concentration gradient, i.e. in non-equilibrium conditions

D_{Me} – self-diffusion coefficient [cm^2s^{-1}]; describes atom (ion) mobility in the compound that constitutes the scale

Correlations between the diffusion coefficients

$$D_{Me} = D_d \cdot N_d$$

$$D_{Me} \cdot C_{Me} = D_d \cdot C_d$$

$$D_{Me} \cdot \frac{C_{Me}}{C_{Me} + C_d} = D_d \cdot \frac{C_d}{C_{Me} + C_d}$$

$$C_{Me} >> C_d \quad \Rightarrow \quad D_{Me} = D_d \cdot N_d$$

$$D_d = 2\tilde{D}\frac{d \ln N_d}{d \ln p_{X_2}}$$

$$\tilde{D} = (1 + |p|) D_d$$

C_d – defect concentration
N_d – molar fraction of defect concentration
p – degree of defect ionization

Scale transport properties

$$D_d = \alpha a_0^2 \omega$$

$$\omega = \kappa \nu \exp\left(\frac{\Delta S_m}{R}\right) \exp\left(-\frac{\Delta H_m}{RT}\right)$$

$$D_d = \alpha a_0^2 \kappa \nu \exp\left(\frac{\Delta S_m}{R}\right) \exp\left(-\frac{\Delta H_m}{RT}\right)$$

$$\nu = \frac{2}{\pi a_0}\sqrt{\frac{\Delta H_m}{M}}$$

α – geometric coefficient
ω – jump frequency
a_o – distance traveled by an atom during a jump
κ – transition coefficient
ν – frequency coefficient
ΔH_m – activation enthalpy of defect diffusion
M – metal molar mass

Gravimetry in scale defect structure and transport property studies

Scheme of a thermogravimetric apparatus for studying metal sulphidation kinetics in sulfur vapors

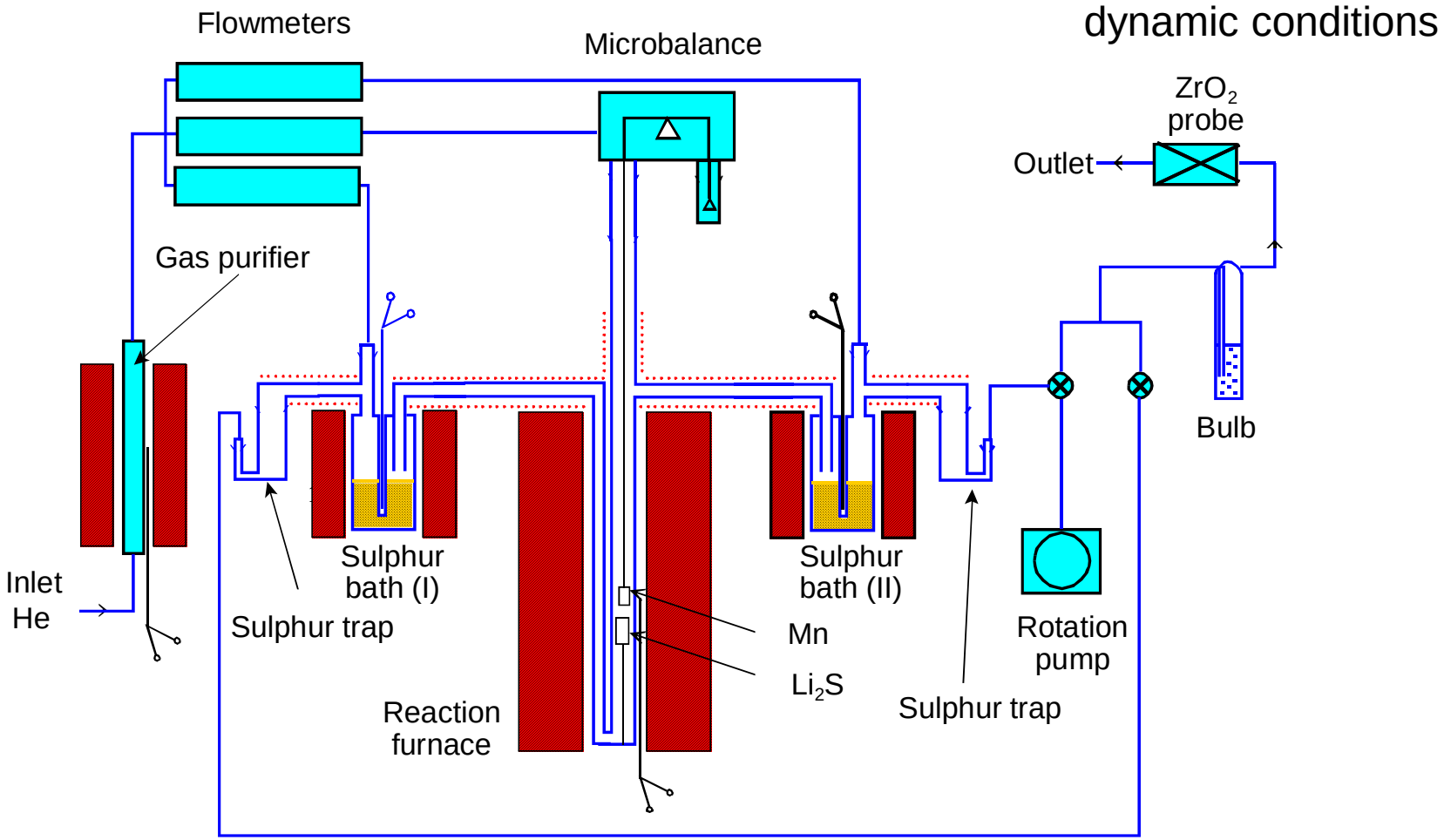

Z. Grzesik, S. Mrowec, T. Walec, J. Dąbek, J. Therm. Anal. Cal., **59** (2000) 985

Main advantages of the apparatus

- sensitivity: **0,1 µg**
- possibility of performing **rapid** sulfur vapor pressure changes
- possibility of performing **long-term** measurements

Pressure dependence of the manganese parabolic sulphidation rate constant

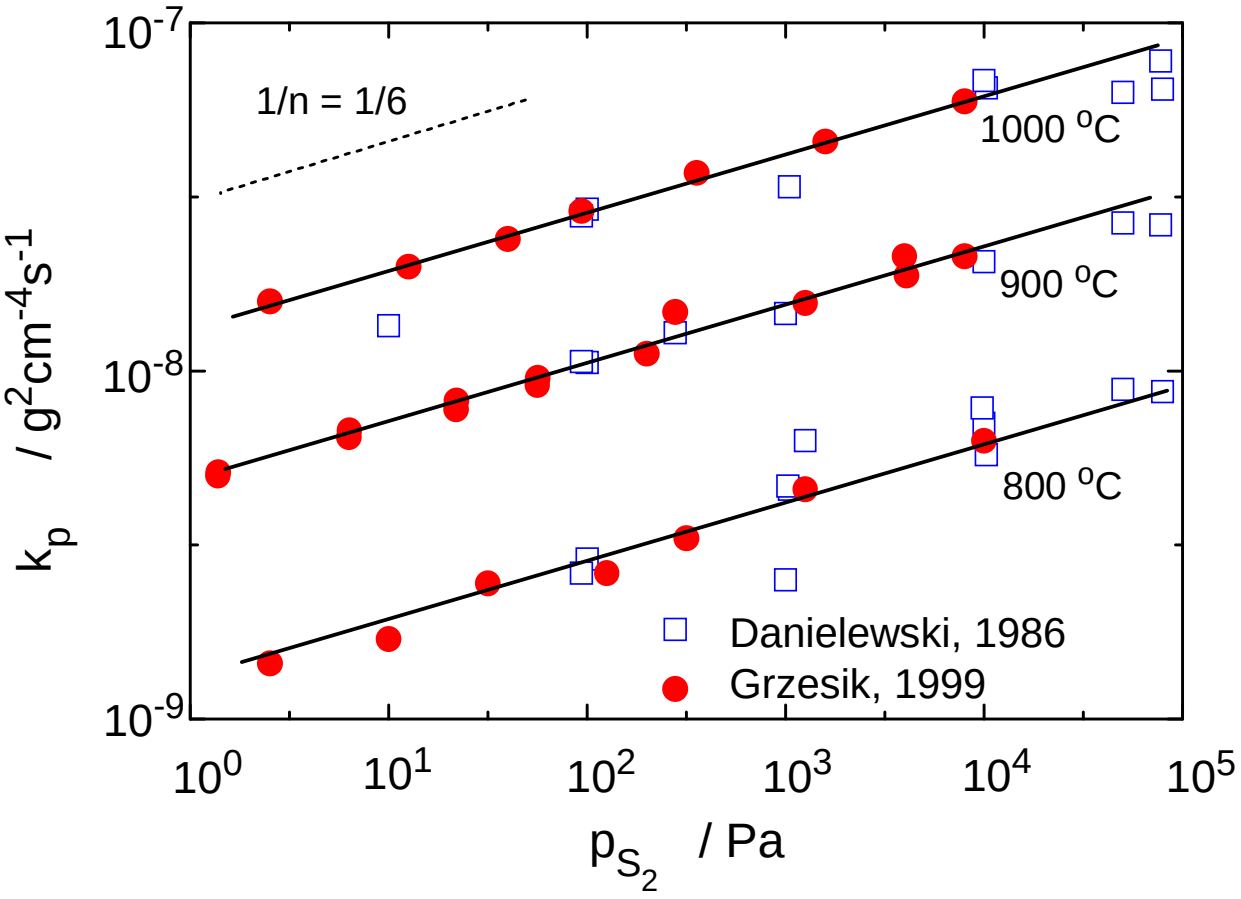

Z. Grzesik, S. Mrowec, T. Walec and J. Dąbek, "New microthermogravimetric apparatus, kinetics of metal sulphidation and transport properties of transition metal sulphides", Journal of Thermal Analysis and Calorimetry, **59**, 985-997 (2000).

Sulphidation kinetics of Mn during a rapid change in sulfur vapor pressure

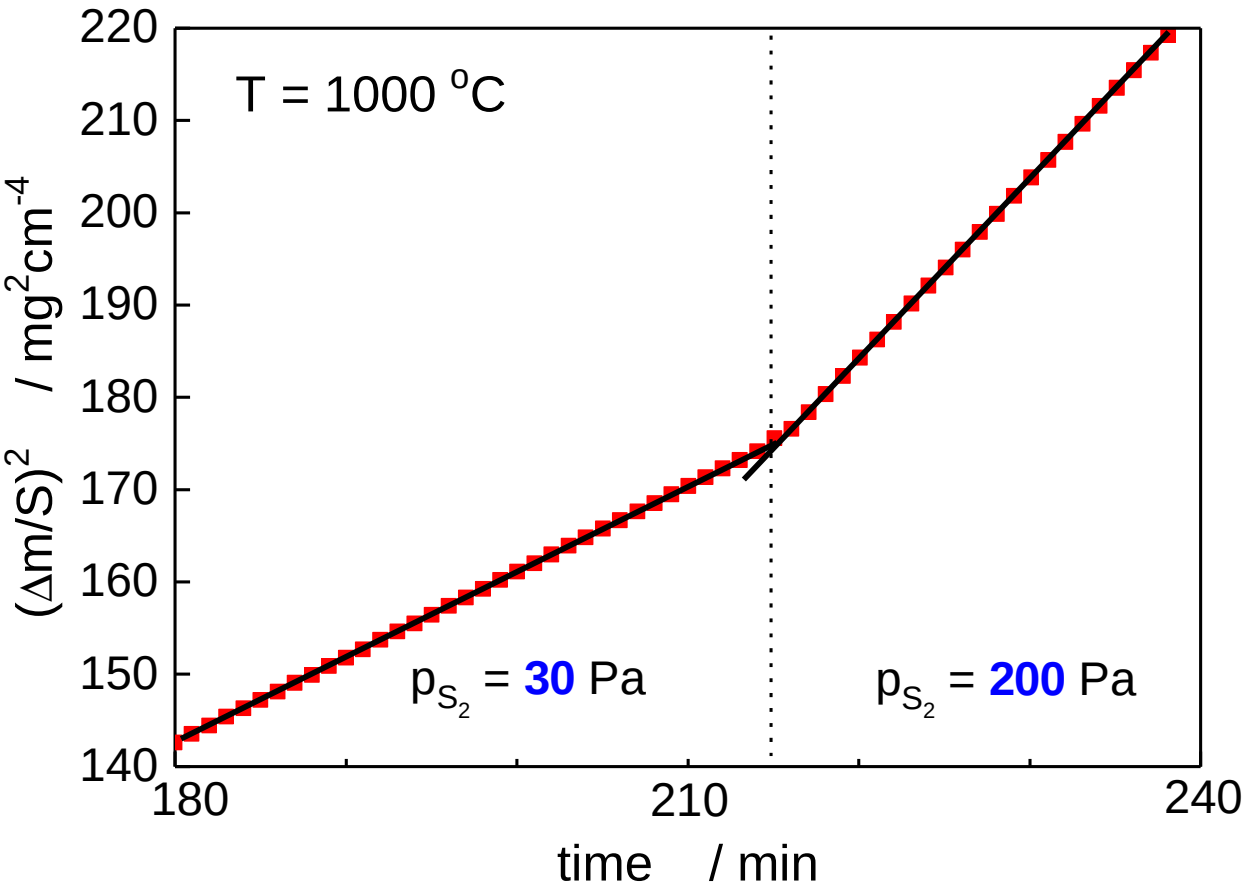

Z. Grzesik, "Własności transportowe zgorzelin siarczkowych powstających w procesie wysokotemperaturowej korozji metali", Ceramika, **87**, 1-124 (2005).

Schematic illustration of the microthermogravimetric apparatus for studies in H_2-H_2S mixtures

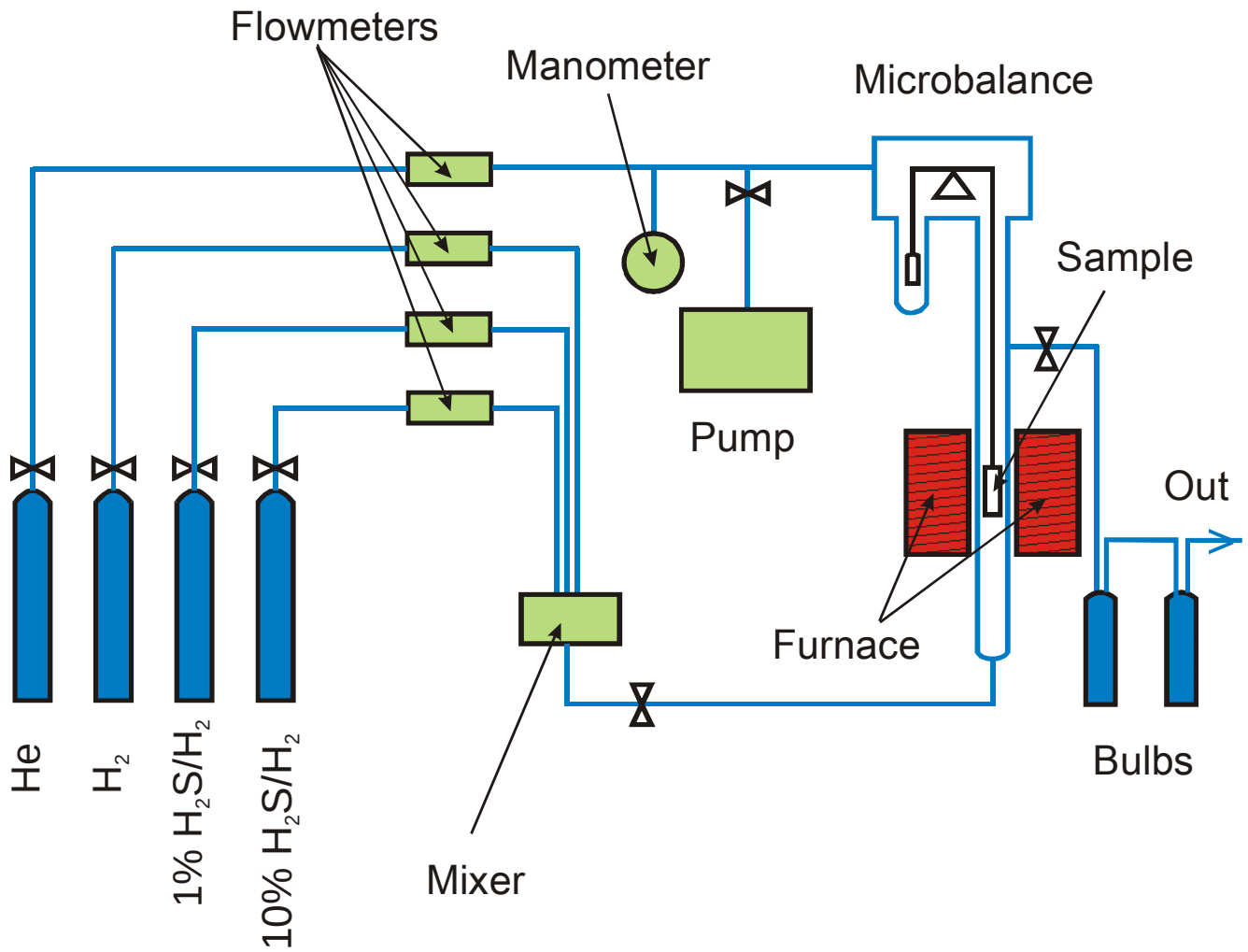

Z. Grzesik, "Własności transportowe zgorzelin siarczkowych powstających w procesie wysokotemperaturowej korozji metali", Ceramika, **87**, 1-124 (2005).

Methods of studying transport properties

- **reequilibration method (relaxation)**
- **two-stage oxidation method (Rosenburg)**

S. Mrowec and K. Hashimoto, J. Materials Sci., **30**, 4801 (1995)

Z. Grzesik and S. Mrowec, "Kinetics and thermodynamics of point defects in nonstoichiometric metal oxides and sulphides. Microthermogravimetric study", J. Therm. Anal. Cal., **90**, 269-282 (2007).

Z. Grzesik, S. Mrowec and T. Walec, J. Phys. Chem. Solids, **61**, 809 (2000).

Z. Grzesik, "Własności transportowe zgorzelin siarczkowych powstających w procesie wysokotemperaturowej korozji metali", Ceramika, **87**, 1-124 (2005).

A. J. Rosenburg, J. Electrochem. Soc., **107**, 795 (1960).

Point defect concentration distribution during reequilibration of a $Me_{1-y}X$-type compound

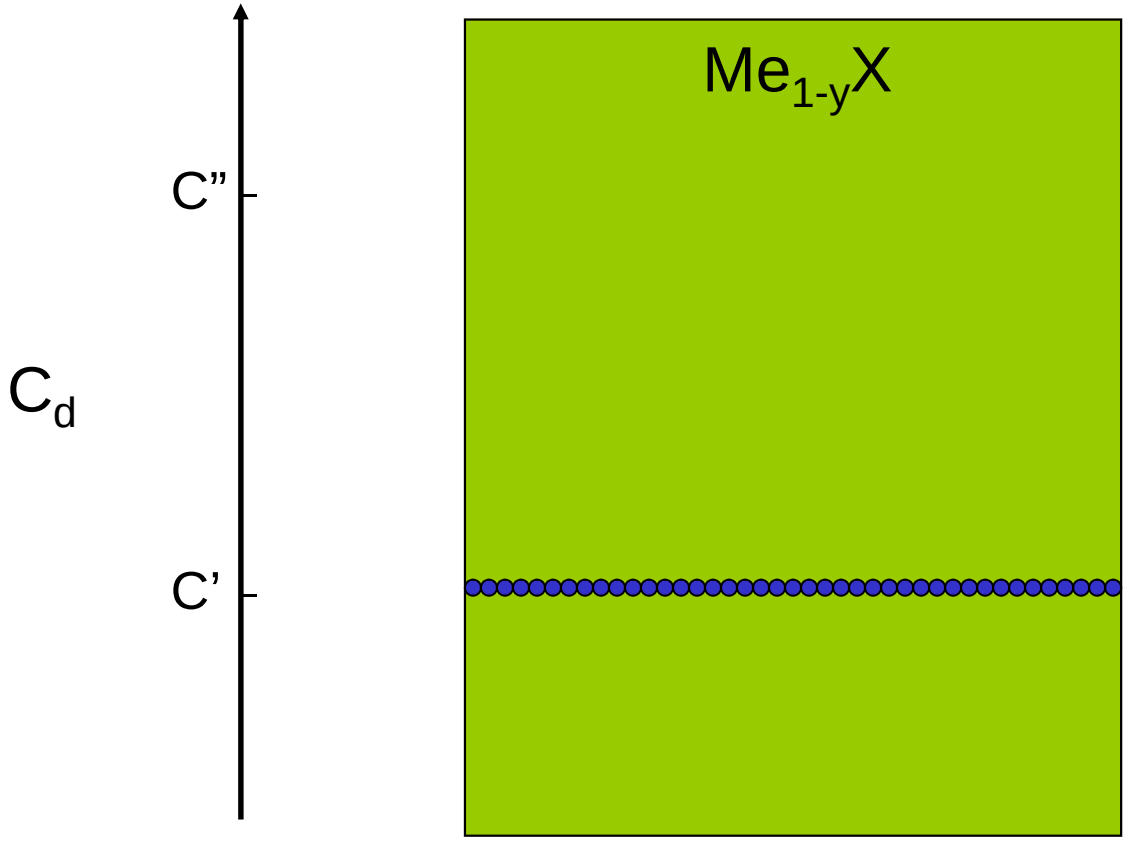

T = const; p’ = const

Point defect concentration distribution during reequilibration of a $Me_{1-y}X$-type compound

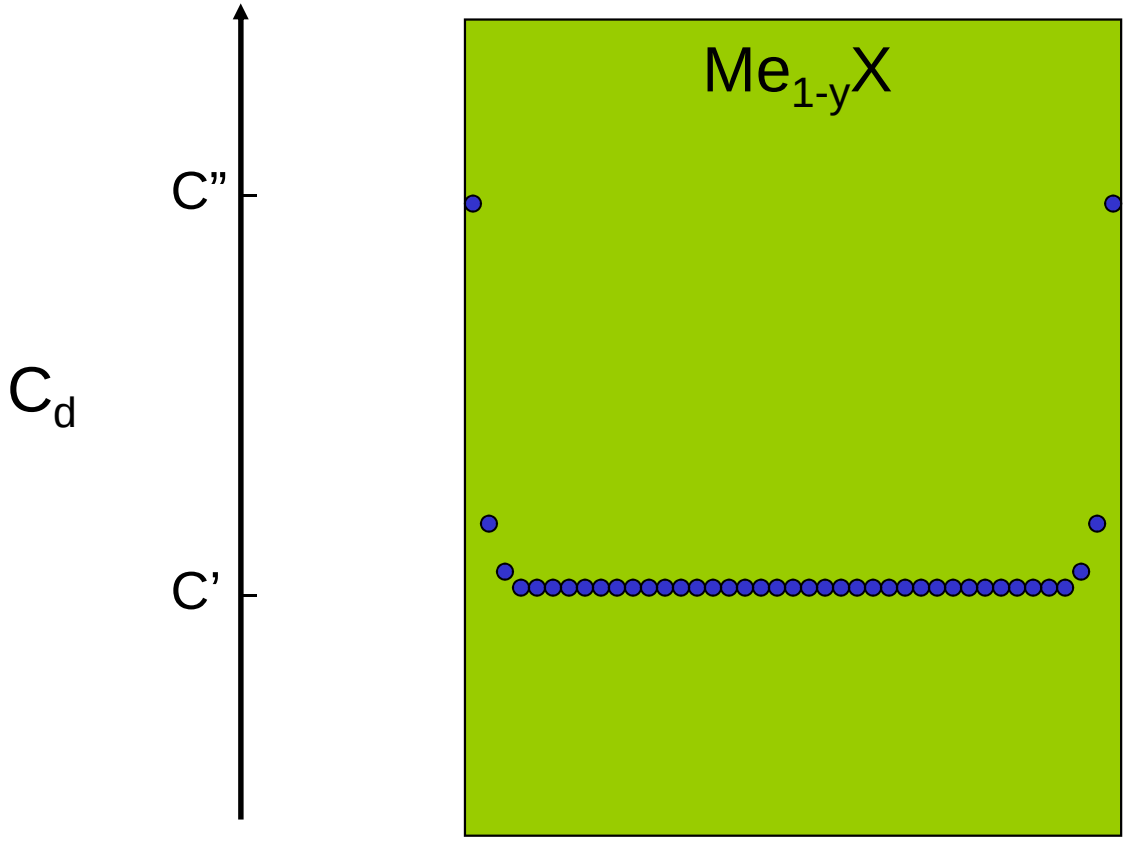

T = const; p” = const; p” > p’

Point defect concentration distribution during reequilibration of a $Me_{1-y}X$-type compound

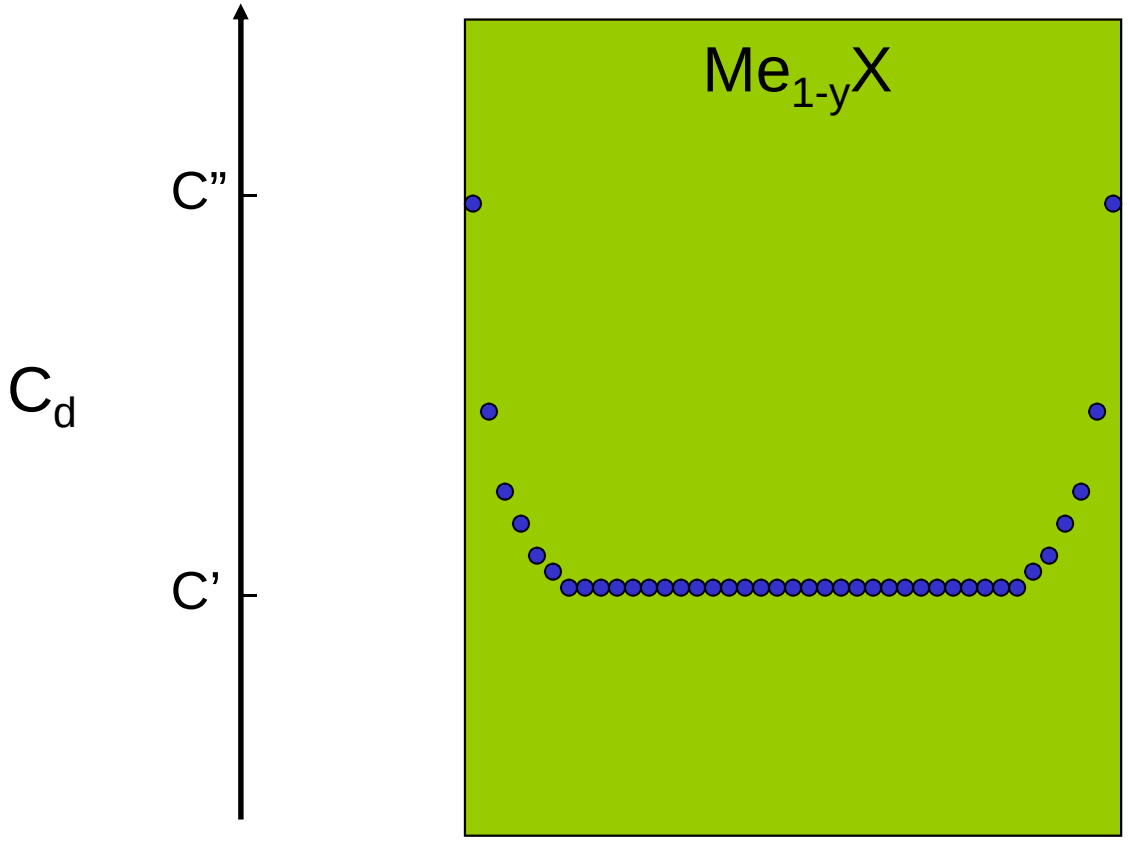

T = const; p” = const; p” > p’

Point defect concentration distribution during reequilibration of a $Me_{1-y}X$-type compound

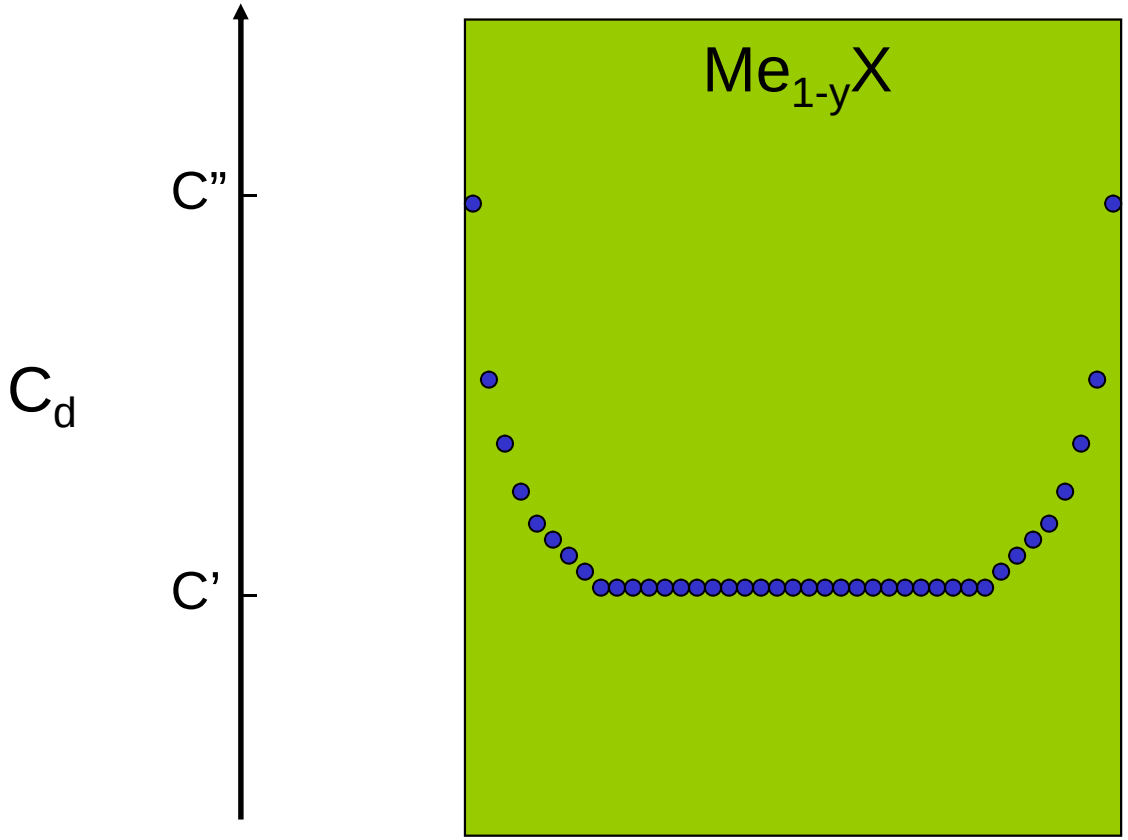

T = const; p” = const; p” > p’

Point defect concentration distribution during reequilibration of a $Me_{1-y}X$-type compound

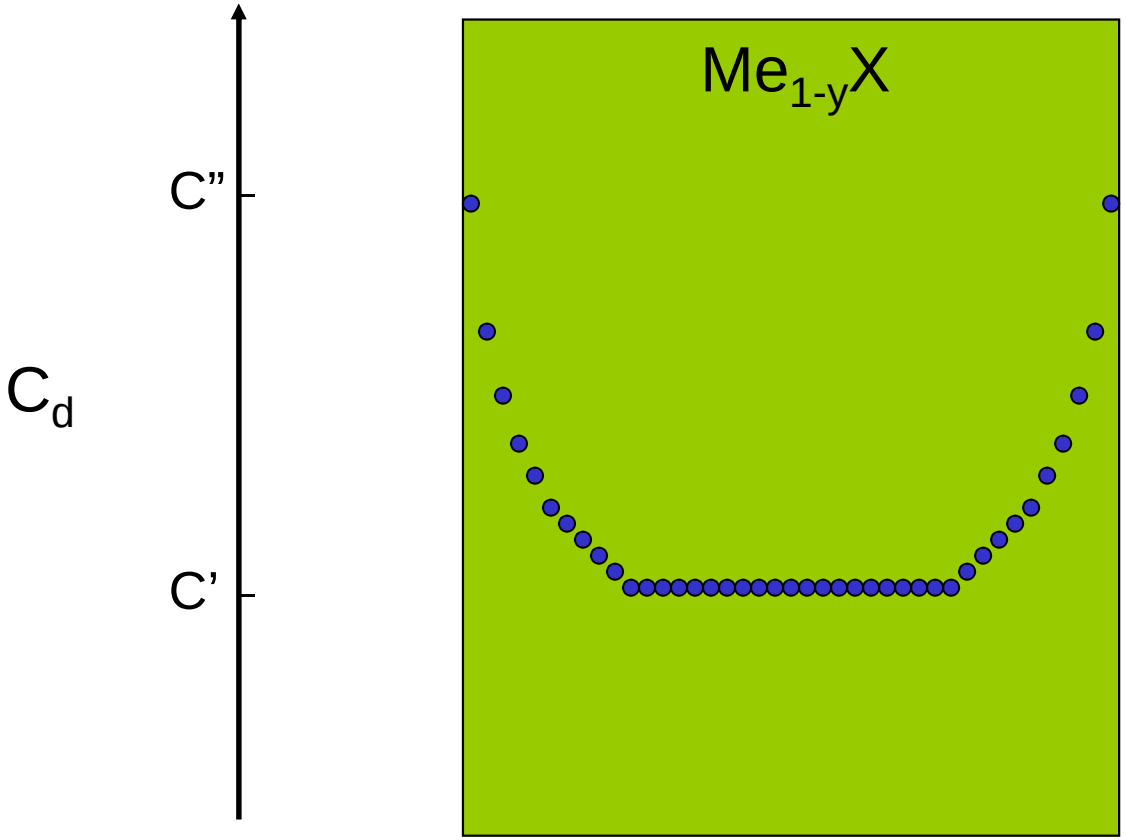

T = const; p” = const; p” > p’

Point defect concentration distribution during reequilibration of a $Me_{1-y}X$-type compound

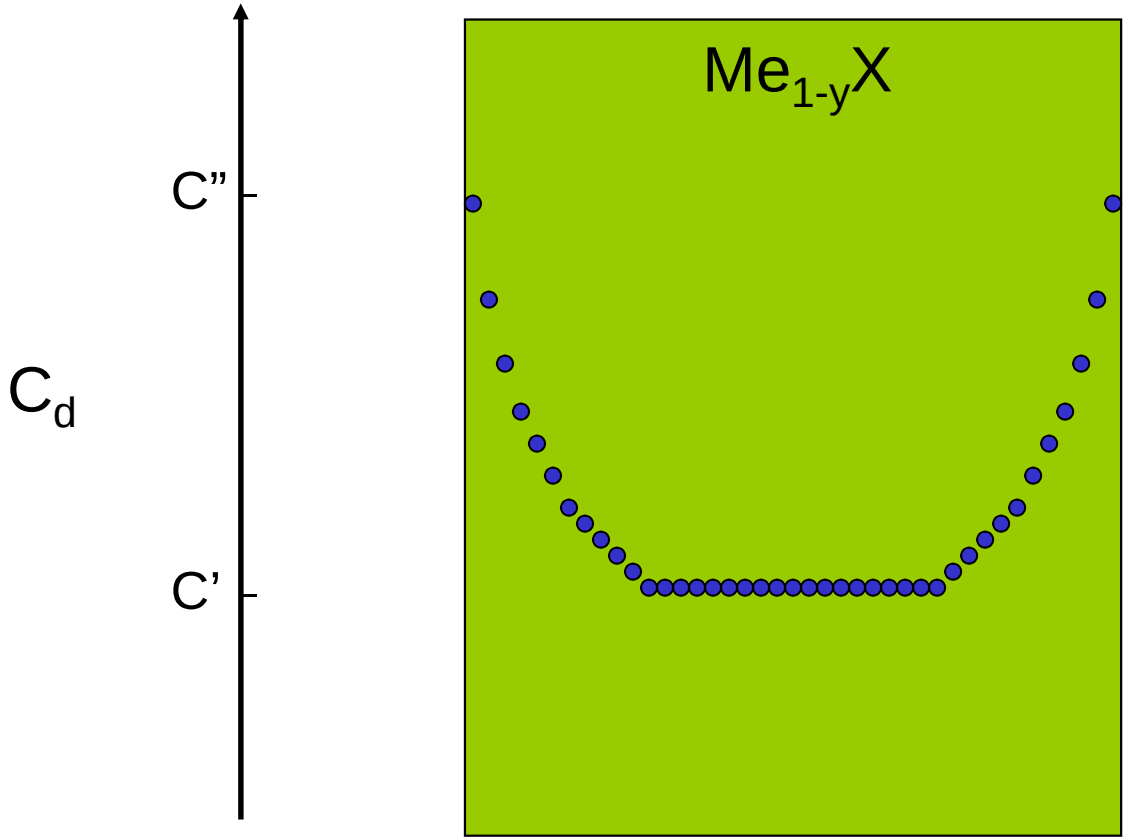

T = const; p” = const; p” > p’

Point defect concentration distribution during reequilibration of a $Me_{1-y}X$-type compound

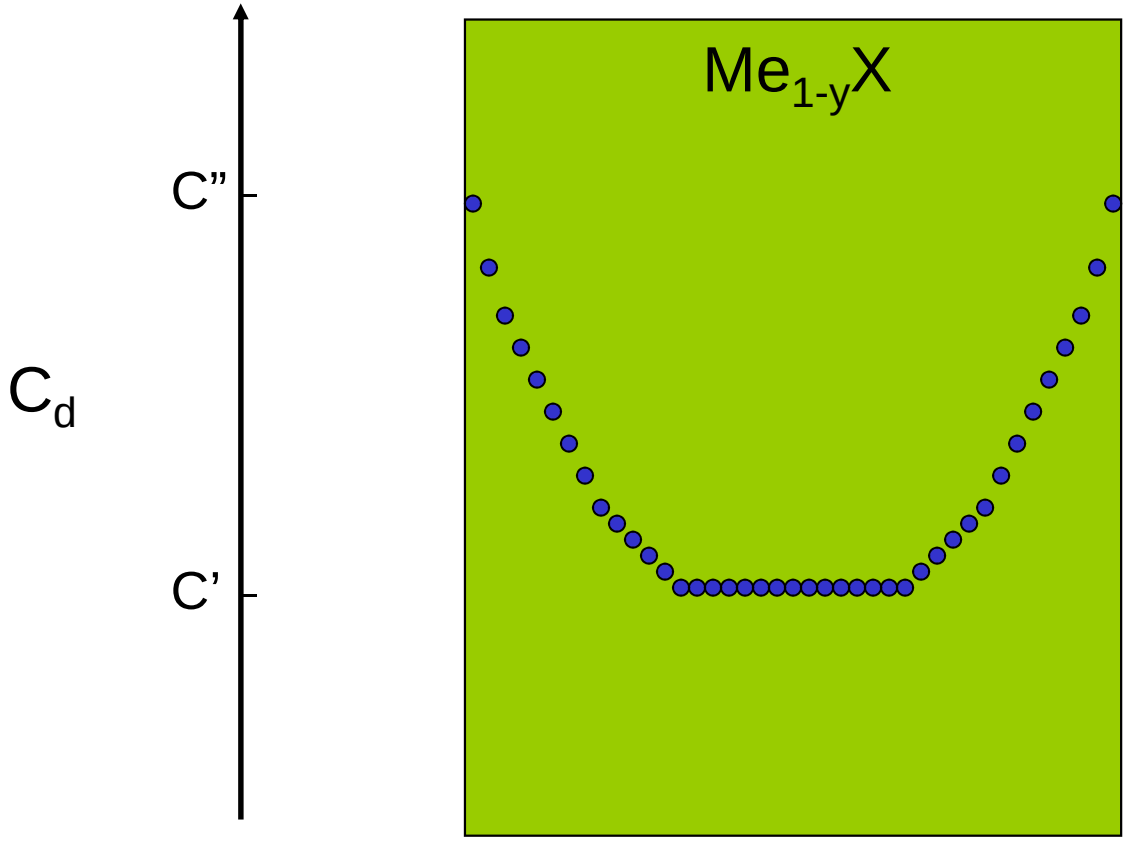

T = const; p” = const; p” > p’

Point defect concentration distribution during reequilibration of a $Me_{1-y}X$-type compound

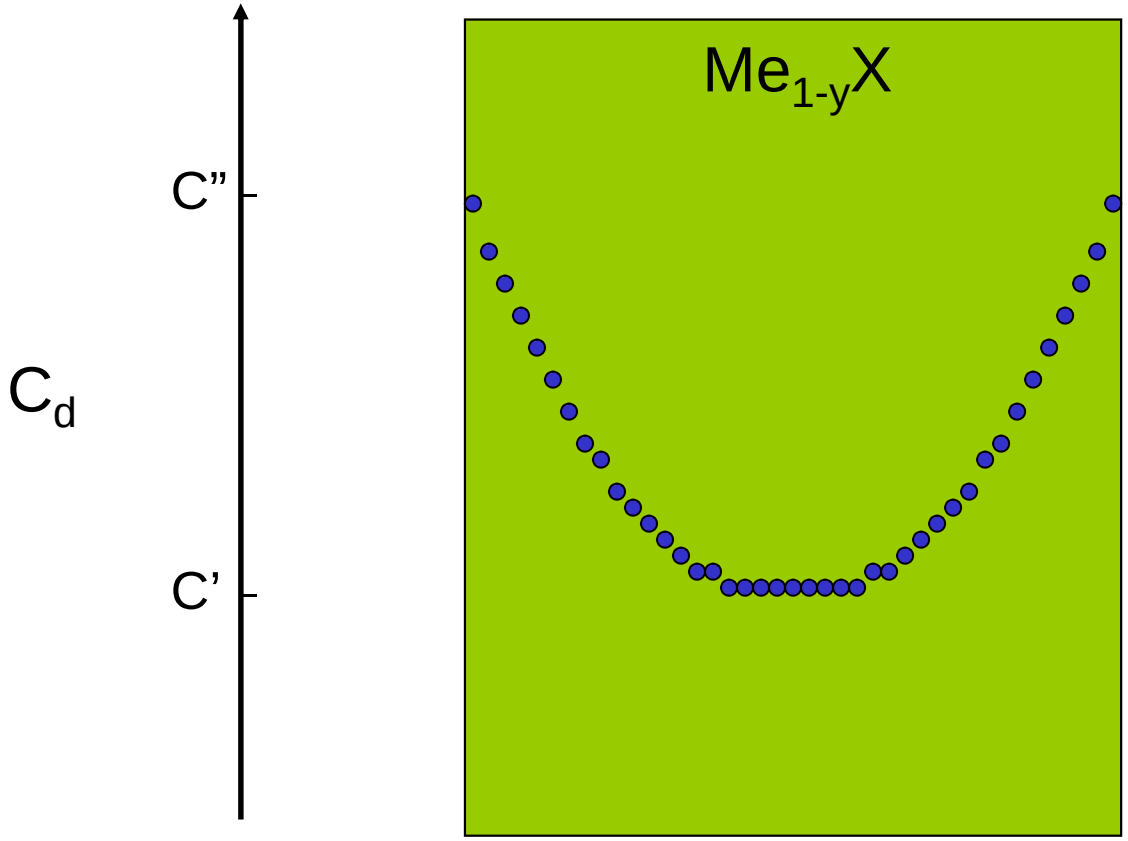

T = const; p” = const; p” > p’

Point defect concentration distribution during reequilibration of a $Me_{1-y}X$-type compound

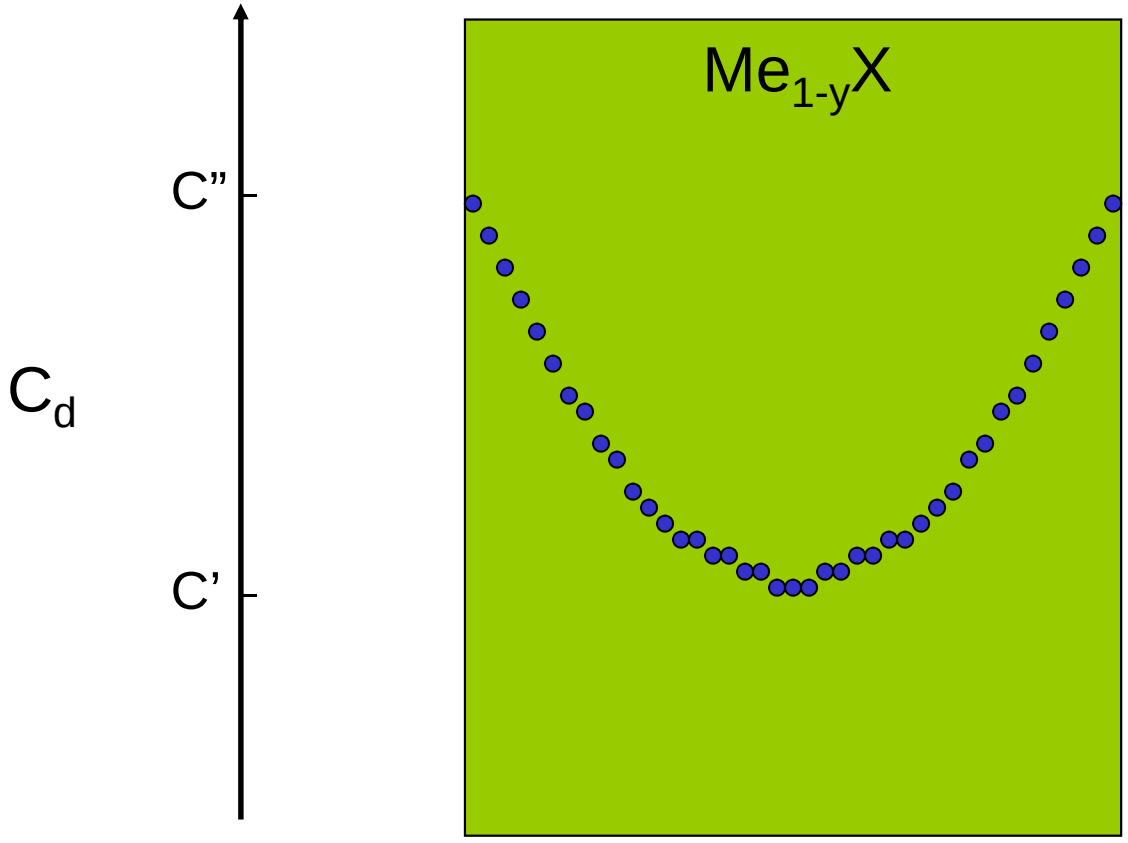

T = const; p” = const; p” > p’

Point defect concentration distribution during reequilibration of a $Me_{1-y}X$-type compound

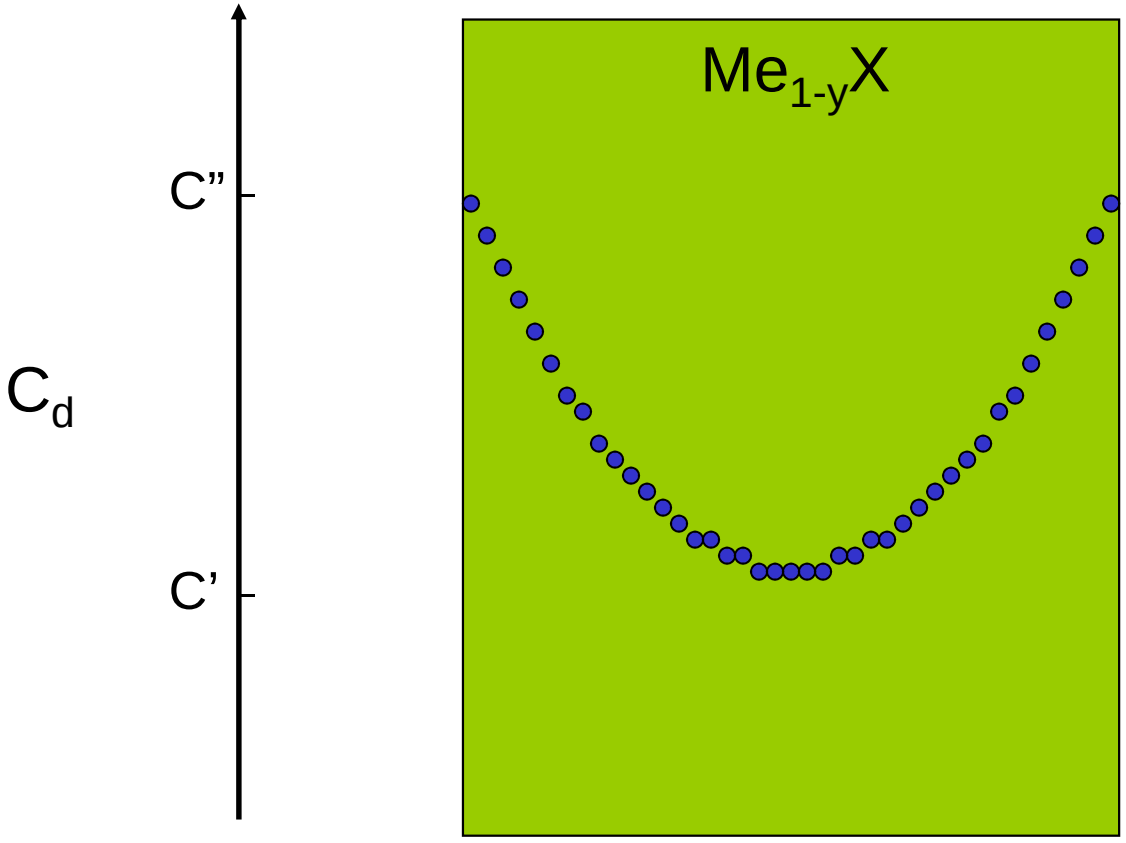

T = const; p” = const; p” > p’

Point defect concentration distribution during reequilibration of a $Me_{1-y}X$-type compound

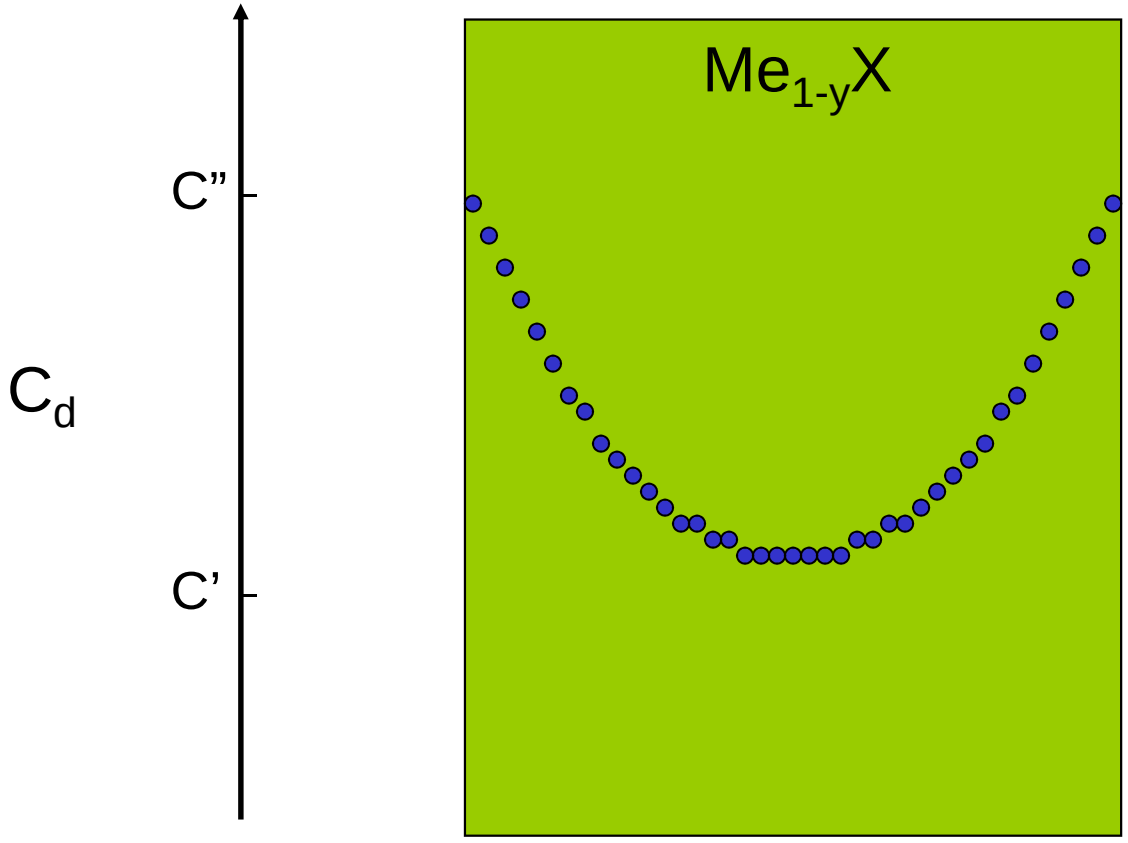

T = const; p” = const; p” > p’

Point defect concentration distribution during reequilibration of a $Me_{1-y}X$-type compound

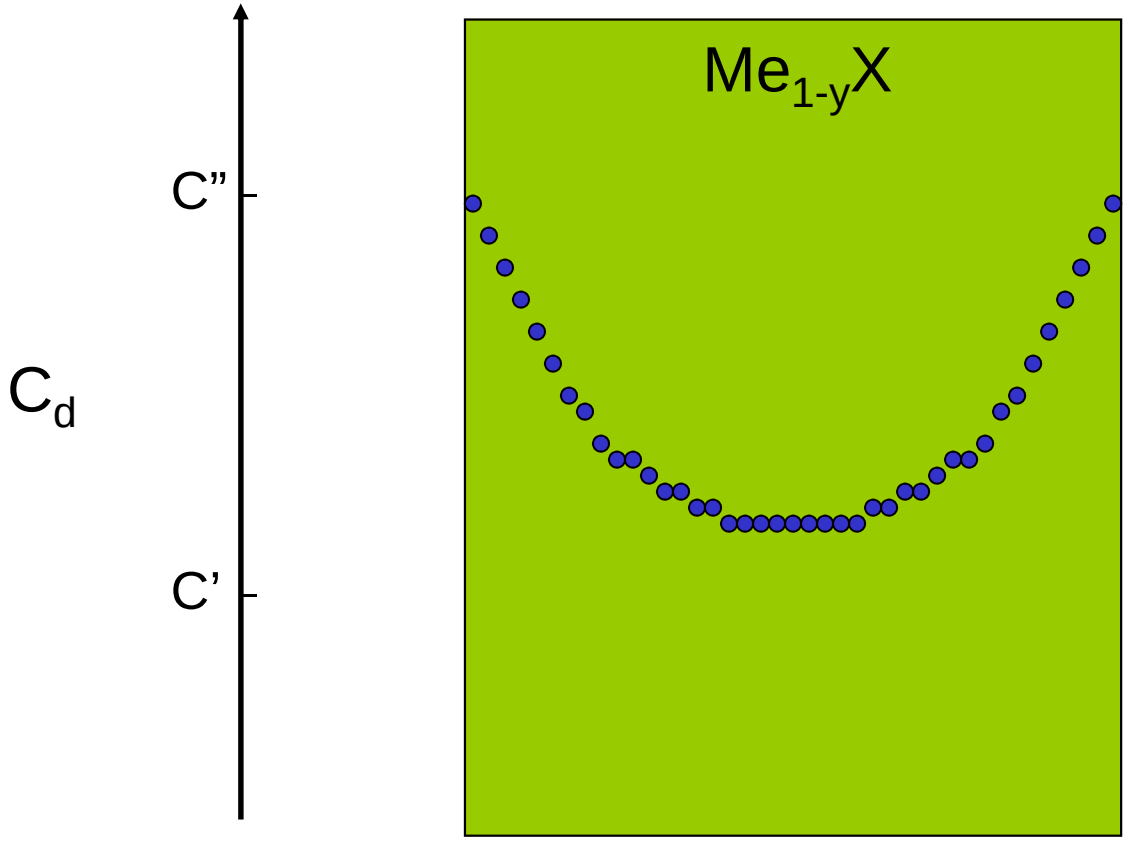

T = const; p” = const; p” > p’

Point defect concentration distribution during reequilibration of a $Me_{1-y}X$-type compound

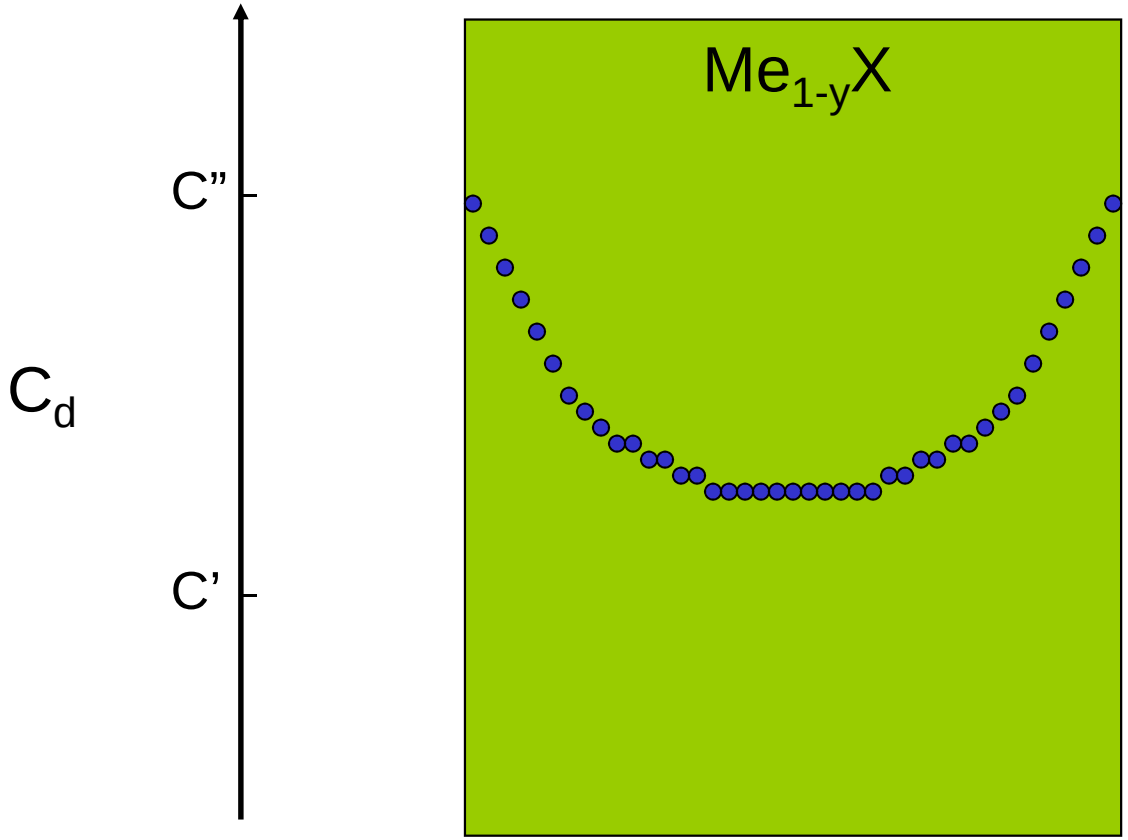

T = const; p” = const; p” > p’

Point defect concentration distribution during reequilibration of a $Me_{1-y}X$-type compound

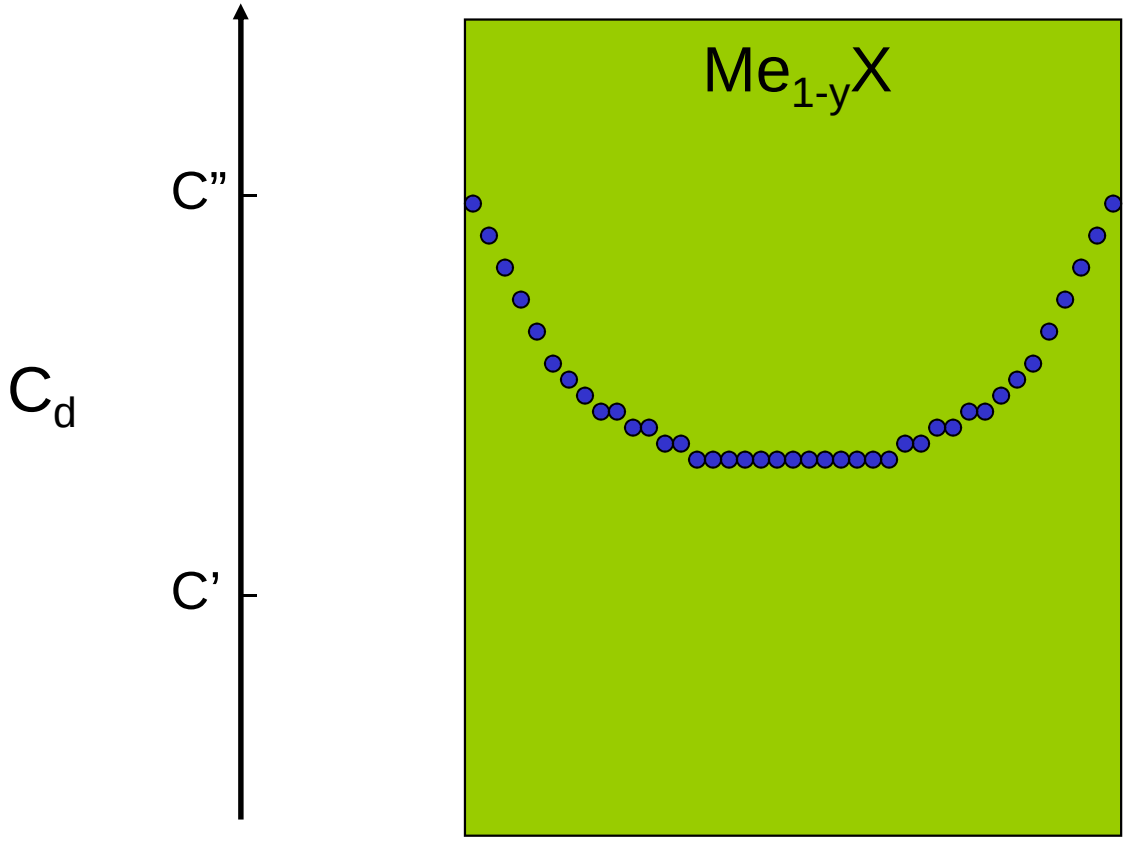

T = const; p” = const; p” > p’

Point defect concentration distribution during reequilibration of a $Me_{1-y}X$-type compound

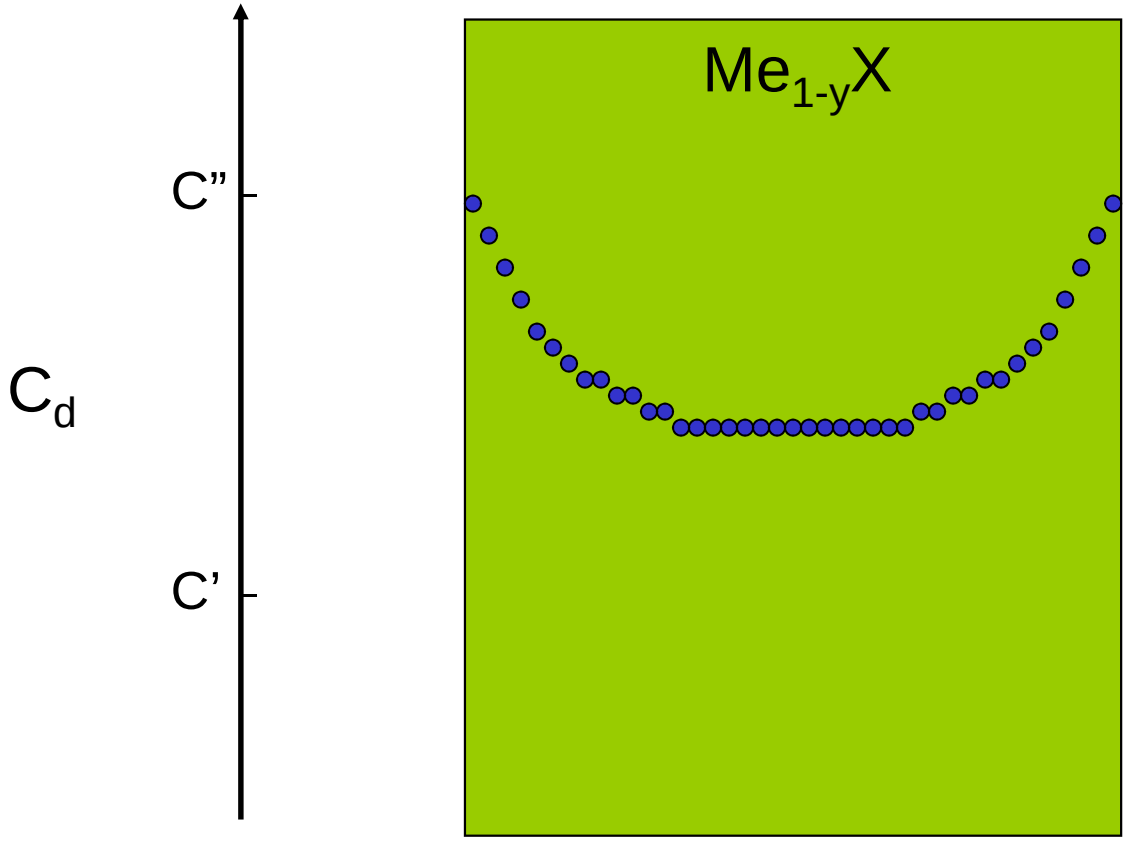

T = const; p” = const; p” > p’

Point defect concentration distribution during reequilibration of a $Me_{1-y}X$-type compound

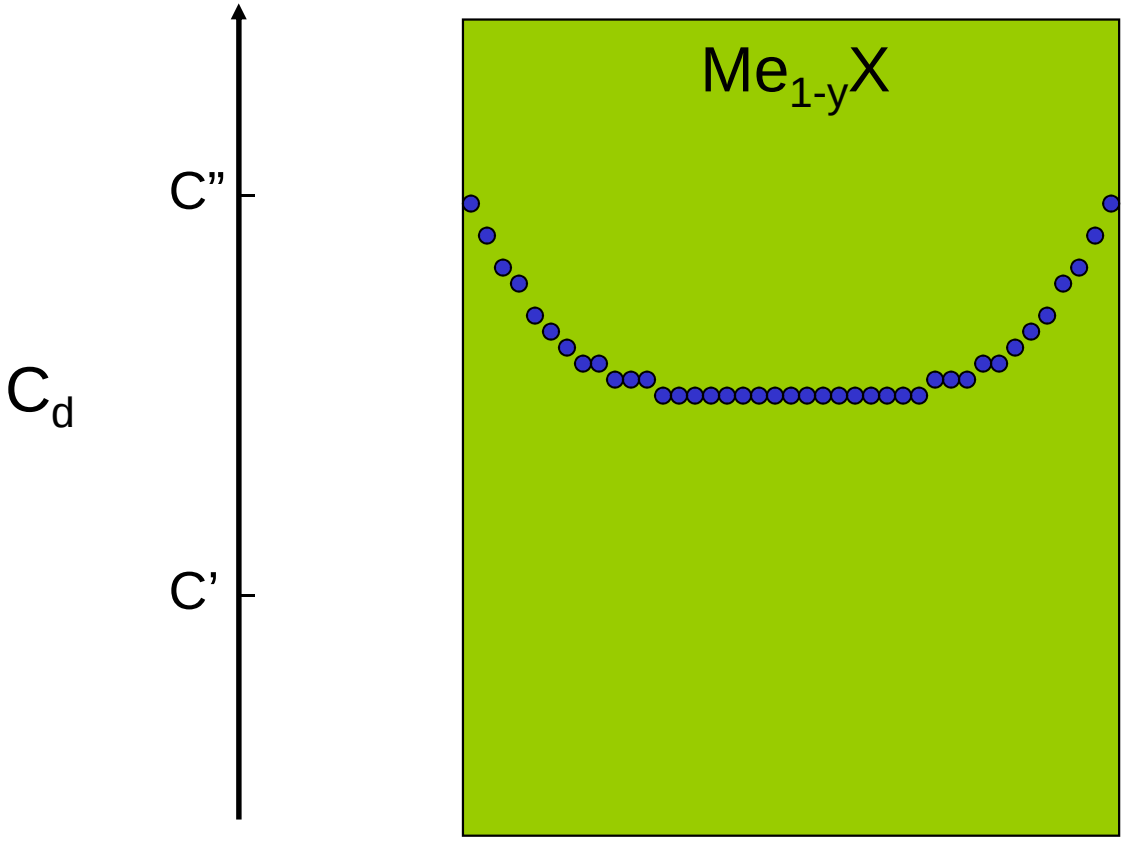

T = const; p” = const; p” > p’

Point defect concentration distribution during reequilibration of a $Me_{1-y}X$-type compound

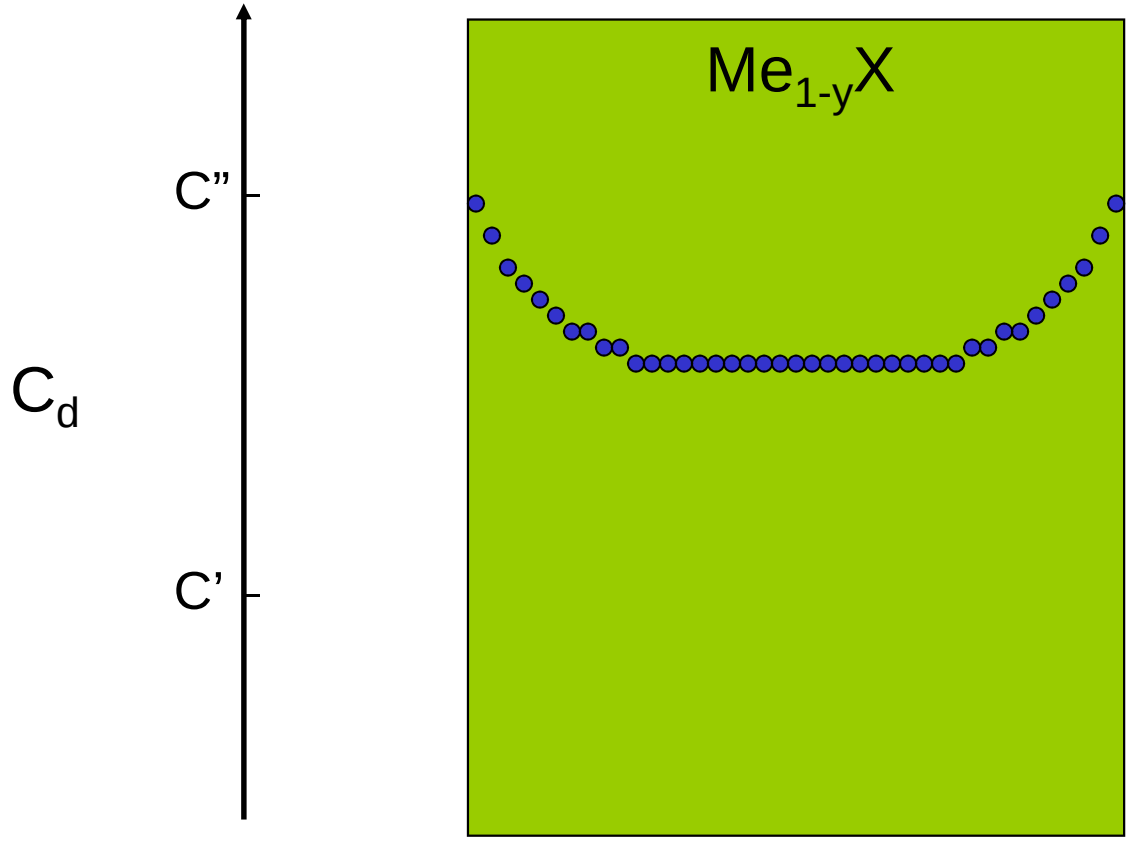

T = const; p” = const; p” > p’

Point defect concentration distribution during reequilibration of a $Me_{1-y}X$-type compound

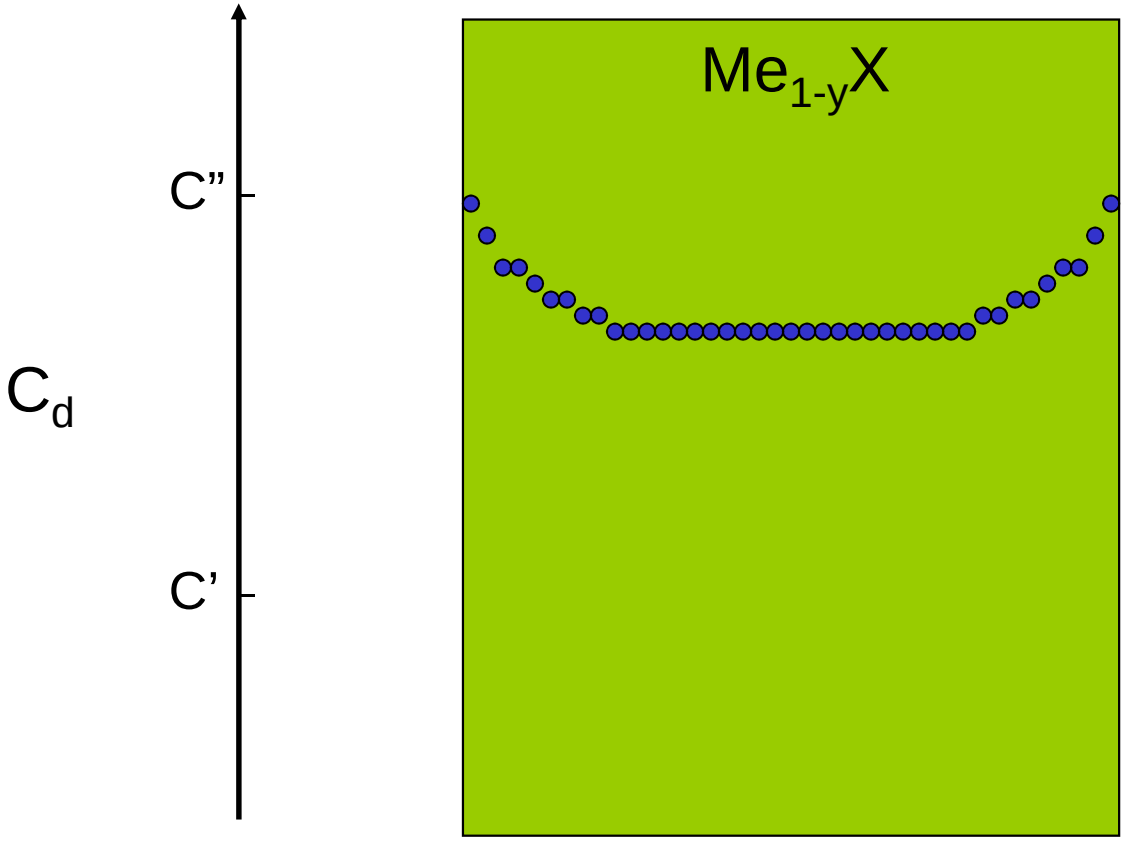

T = const; p” = const; p” > p’

Point defect concentration distribution during reequilibration of a $Me_{1-y}X$-type compound

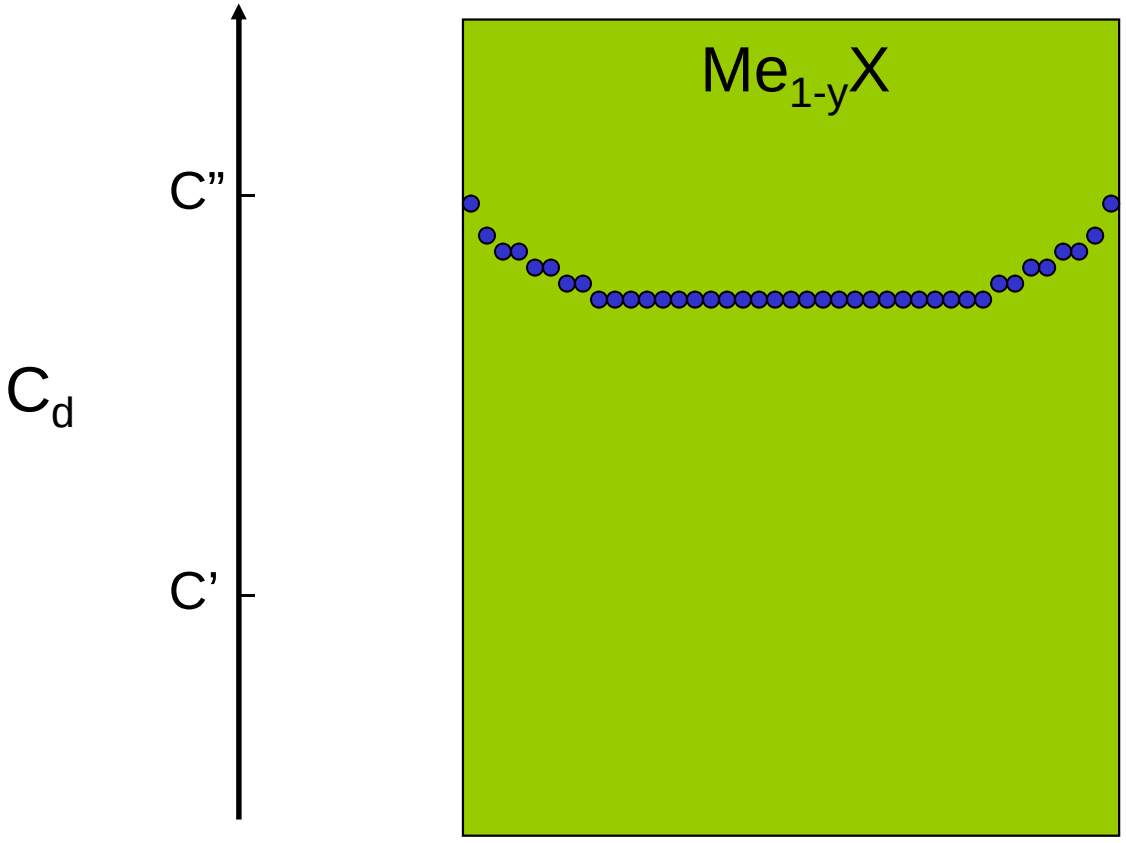

T = const; p” = const; p” > p’

Point defect concentration distribution during reequilibration of a $Me_{1-y}X$-type compound

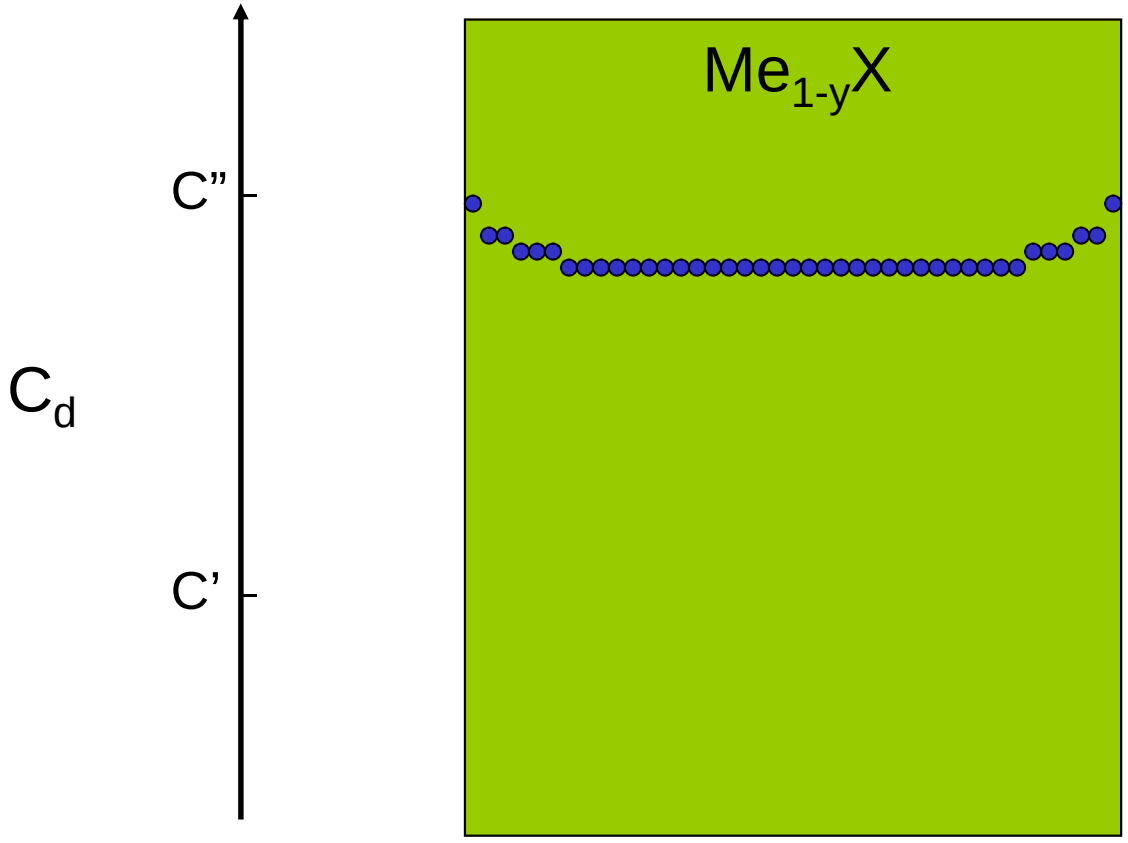

T = const; p” = const; p” > p’

Point defect concentration distribution during reequilibration of a $Me_{1-y}X$-type compound

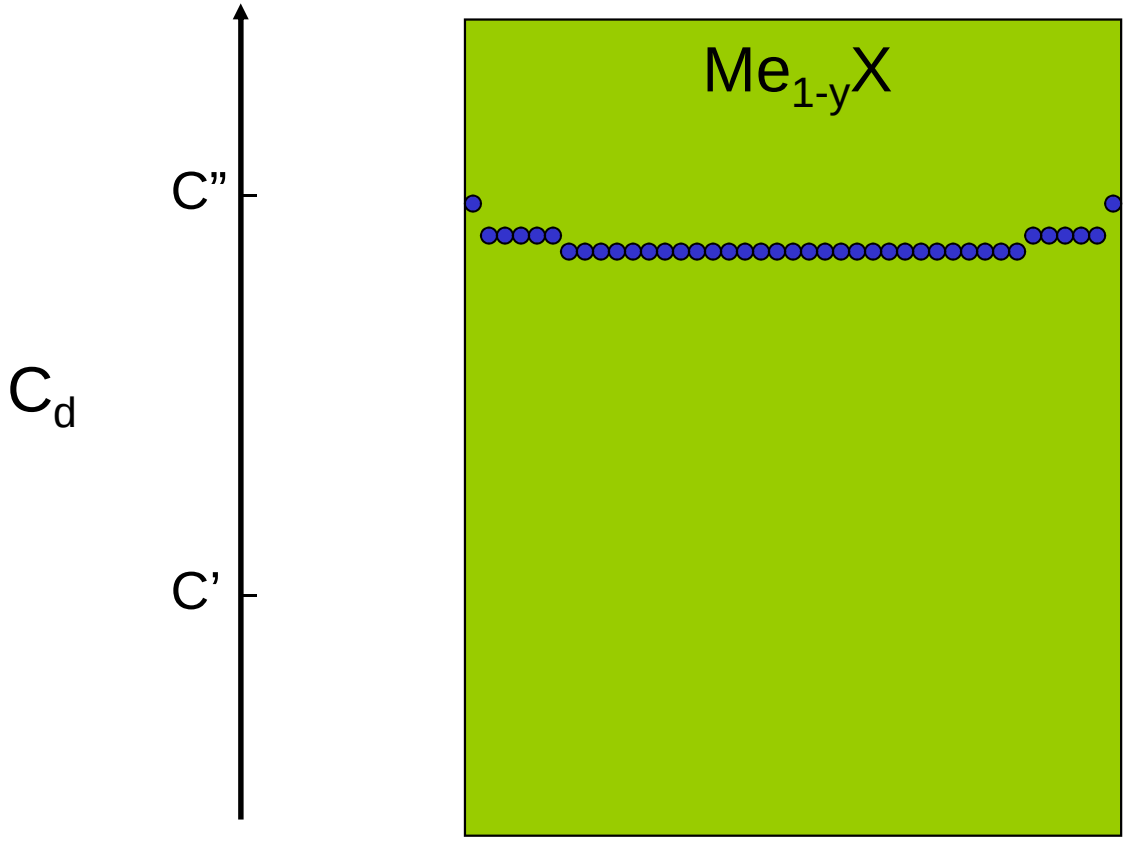

T = const; p” = const; p” > p’

Point defect concentration distribution during reequilibration of a $Me_{1-y}X$-type compound

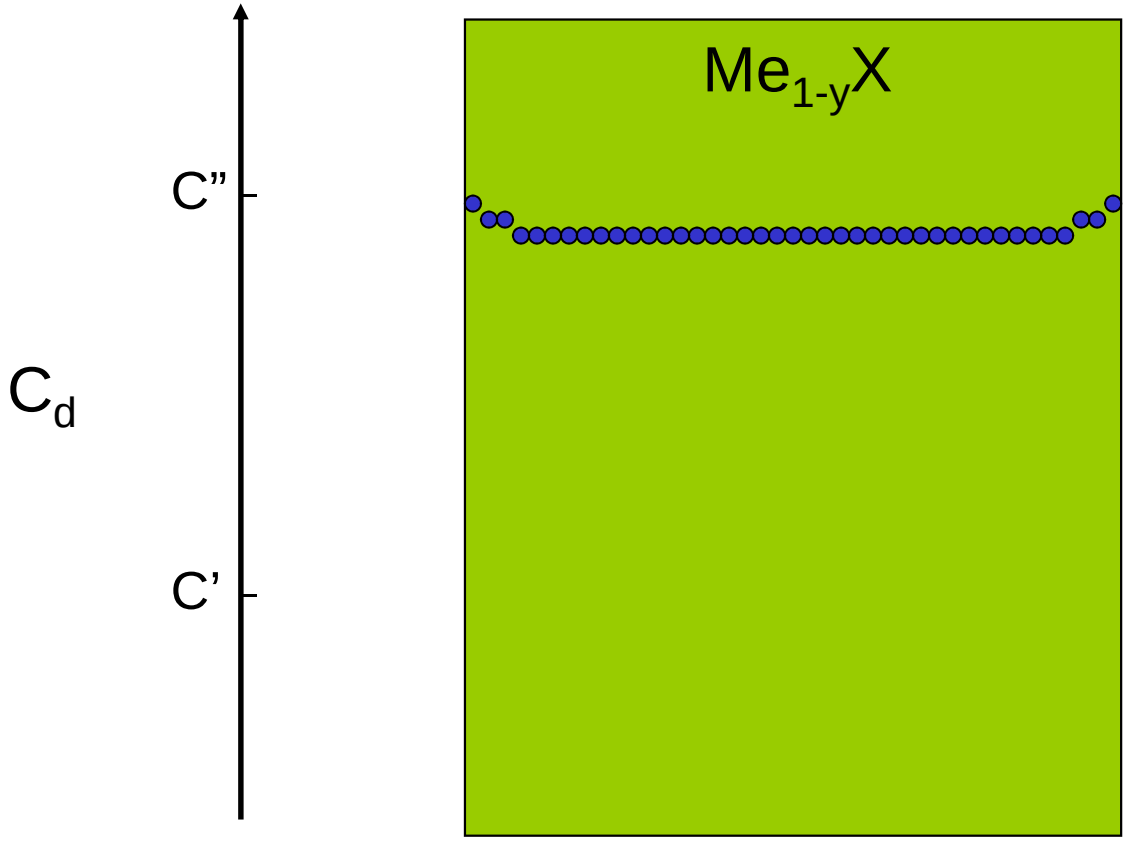

T = const; p” = const; p” > p’

Point defect concentration distribution during reequilibration of a $Me_{1-y}X$-type compound

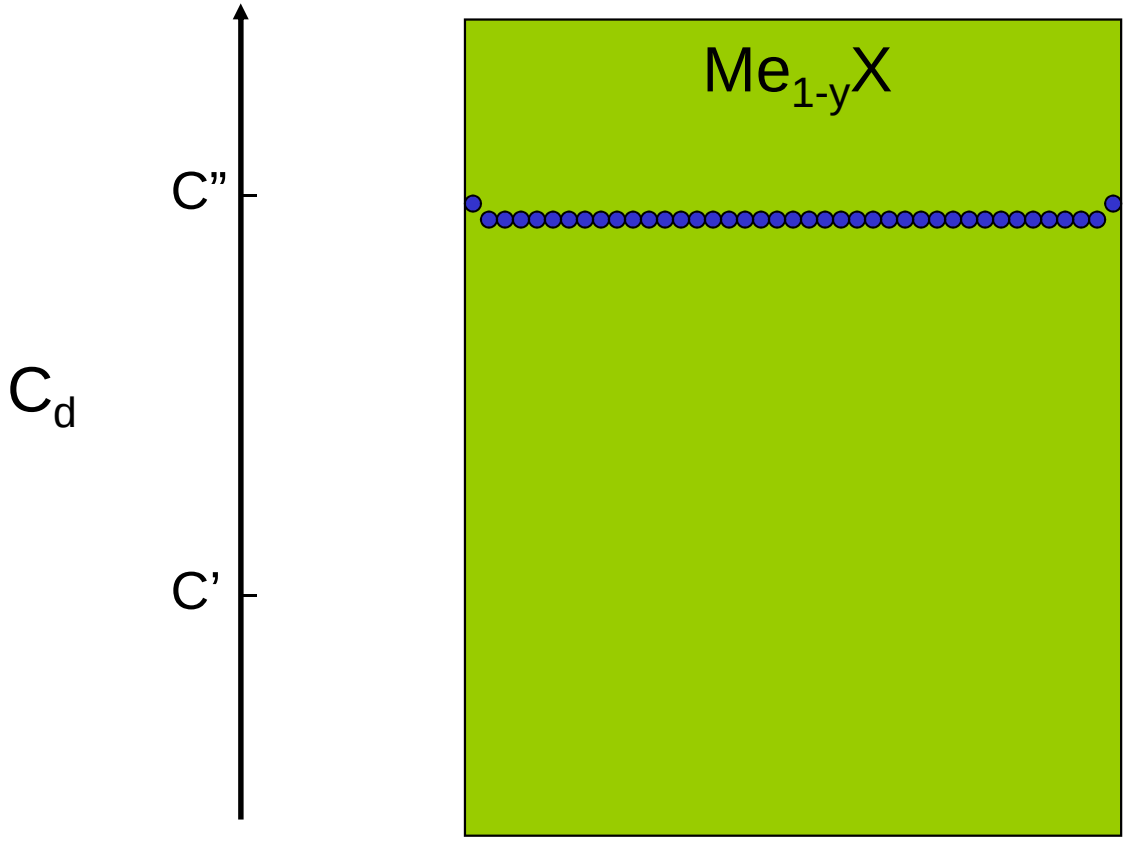

T = const; p” = const; p” > p’

Point defect concentration distribution during reequilibration of a $Me_{1-y}X$-type compound

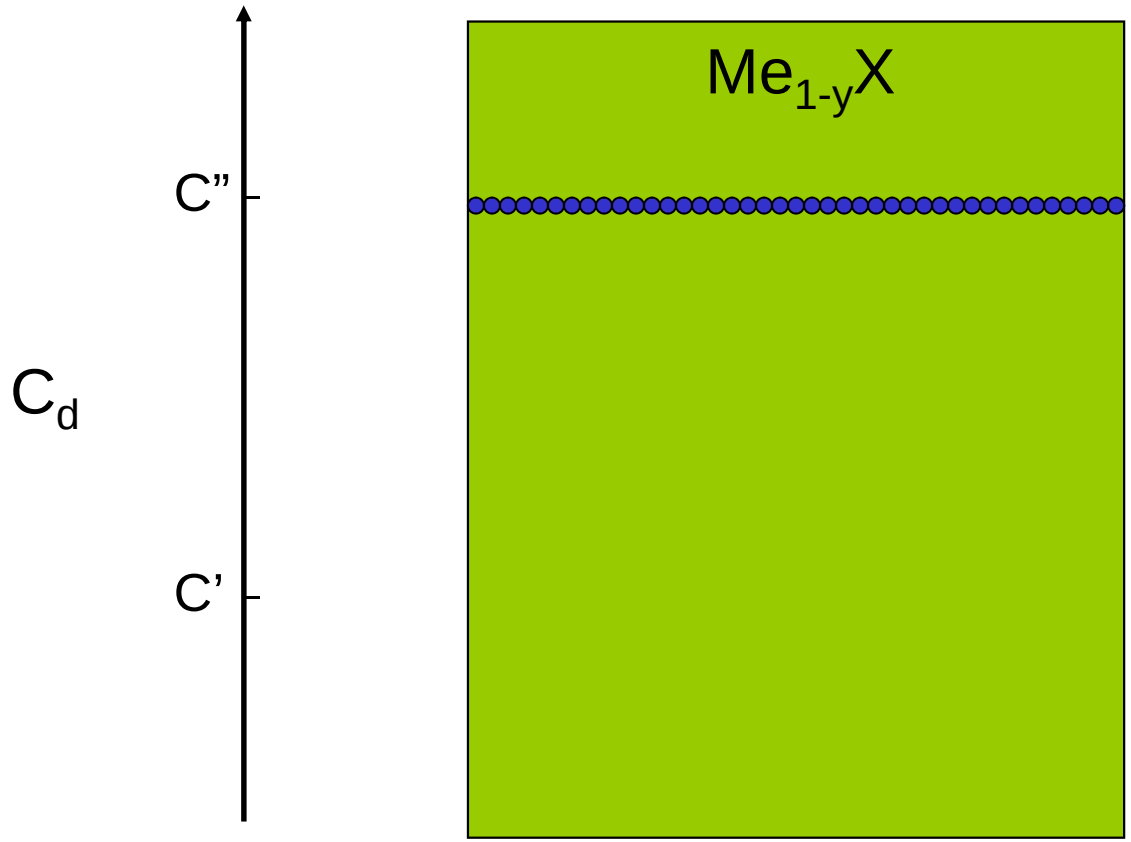

T = const; p” = const; p” > p’

Reequilibration method – result analysis

$$\frac{\Delta m_t}{\Delta m_k} = 1 - \frac{8}{\pi^2}\sum_{n=0}^{\infty}\frac{1}{(2n+1)^2}\exp\left(-\frac{(2n+1)^2\pi^2\tilde{D}t}{4a^2}\right)$$

$\tilde{D}$ **t/a² > 0,2:**

$$1 - \frac{\Delta m_t}{\Delta m_k} = \frac{8}{\pi^2}\exp\left(-\frac{\tilde{D}\pi^2 t}{4a^2}\right)$$

$$\ln\left(1 - \frac{\Delta m_t}{\Delta m_k}\right) = \ln\frac{8}{\pi^2} - \frac{\tilde{D}\pi^2 t}{4a^2}$$

where:

Δm_t – **sample mass change after a certain amount of time, t**

Δm_k – **total sample mass change**

a – **half of the sample thickness**

$\tilde{D}$ – **chemical diffusion coefficient.**

Theoretical reequlibration procedure

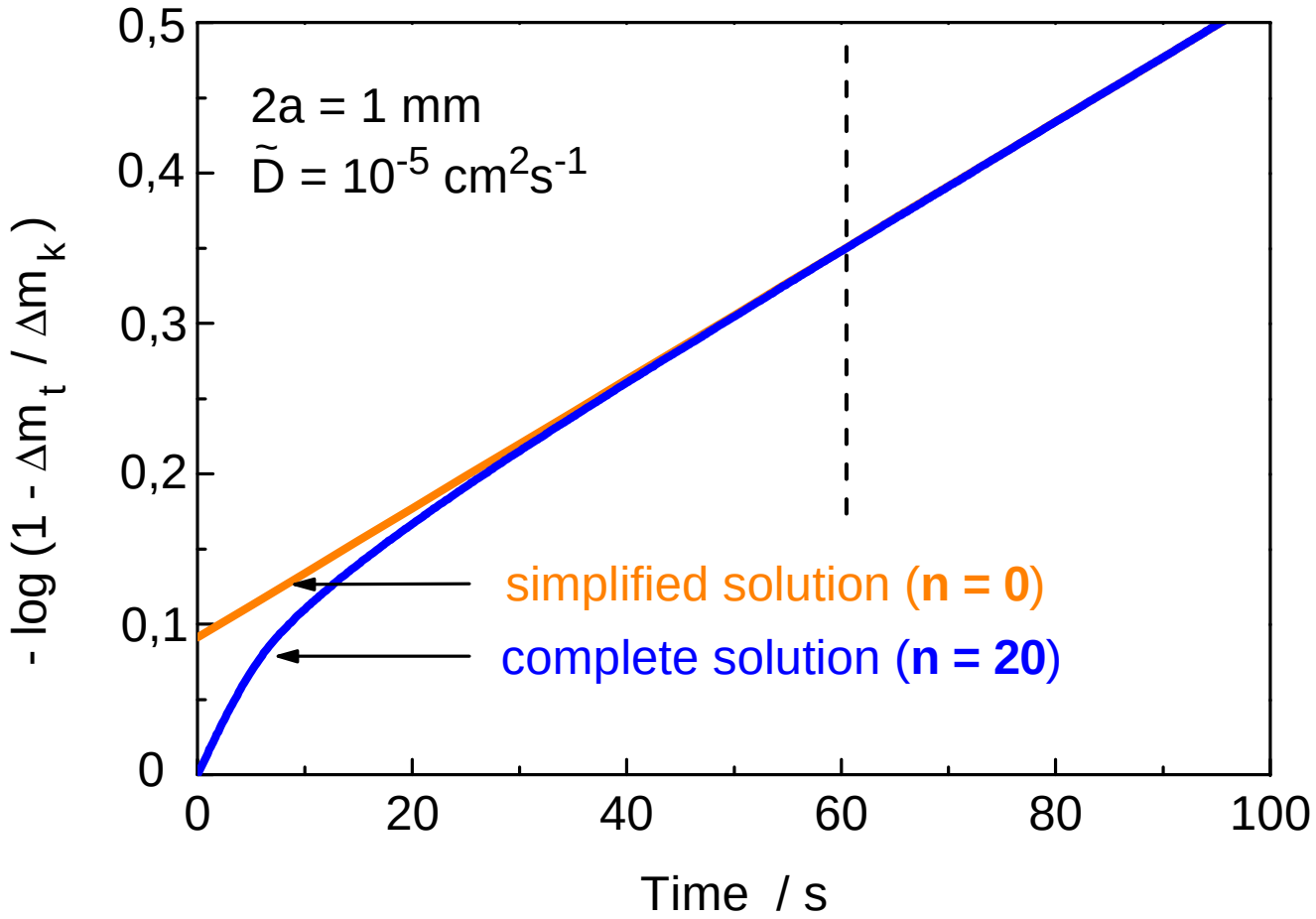

Two-stage oxidation method (Rosenburg)

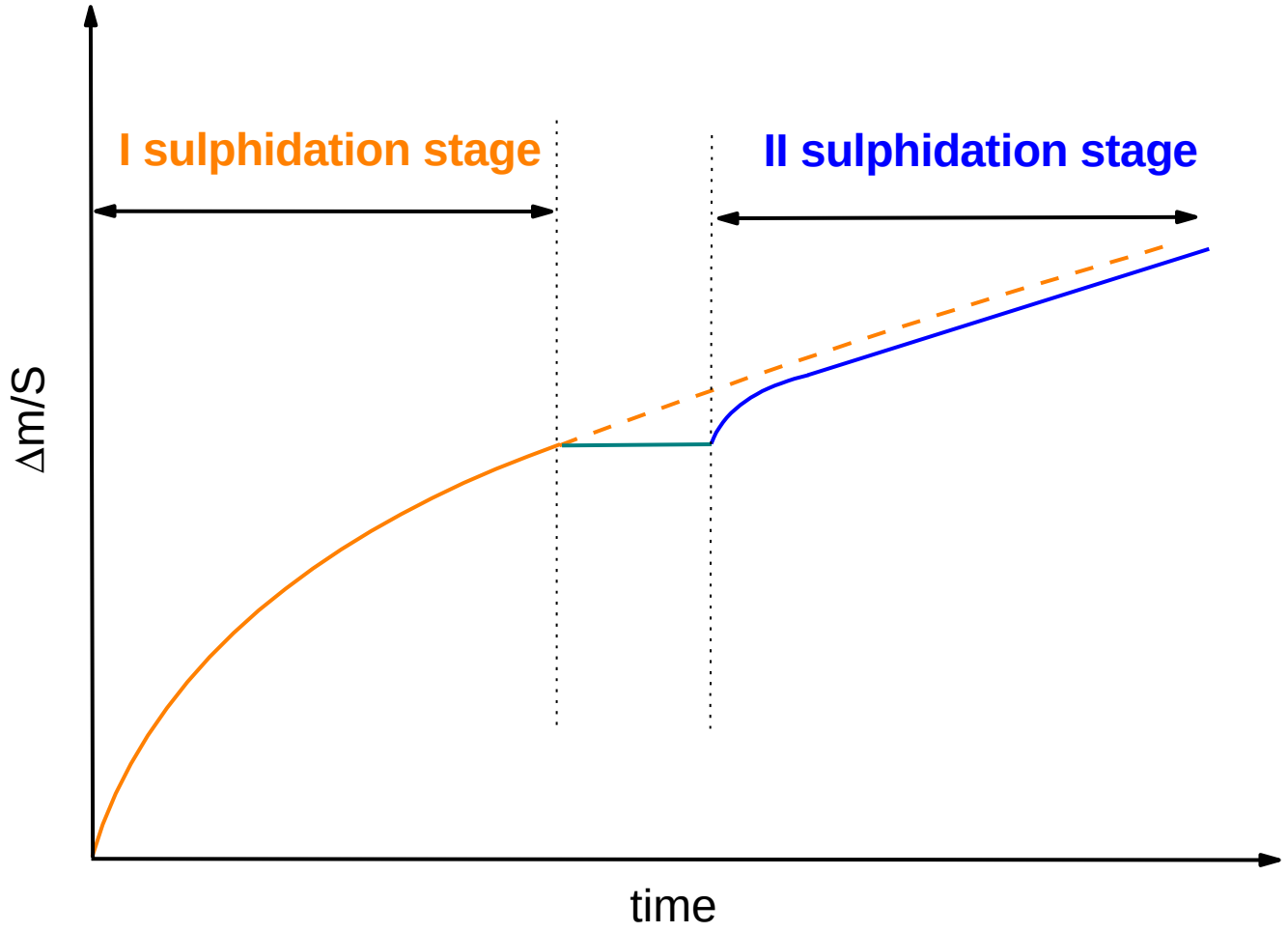

Two-stage oxidation method – point defect concentration distribution in a $Me_{1-y}X$-type scale

I sulphidation stage

T = const; p” = const

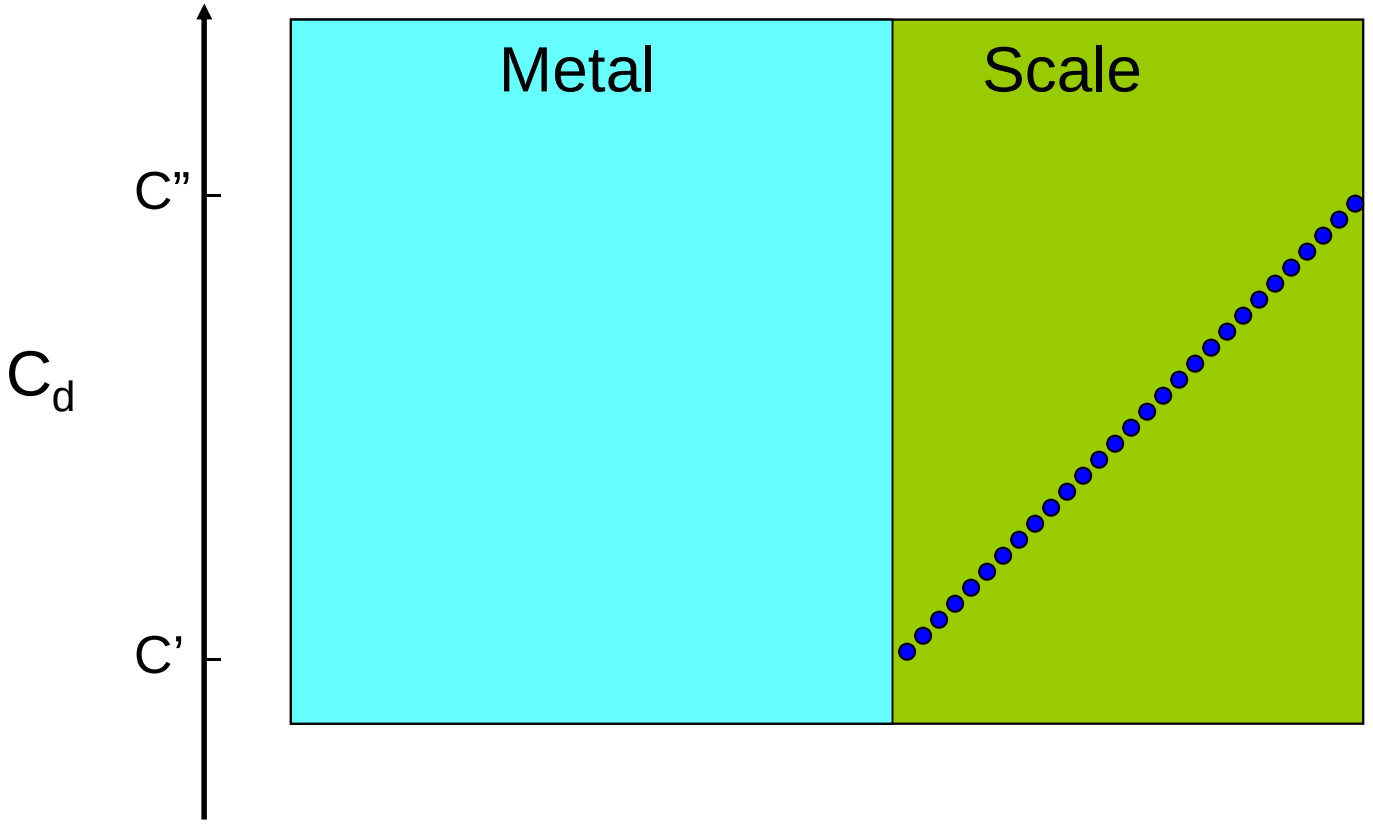

Two-stage oxidation method – point defect concentration distribution in a $Me_{1-y}X$-type scale

Thermodynamic equilibrium state

T = const; p’ = const

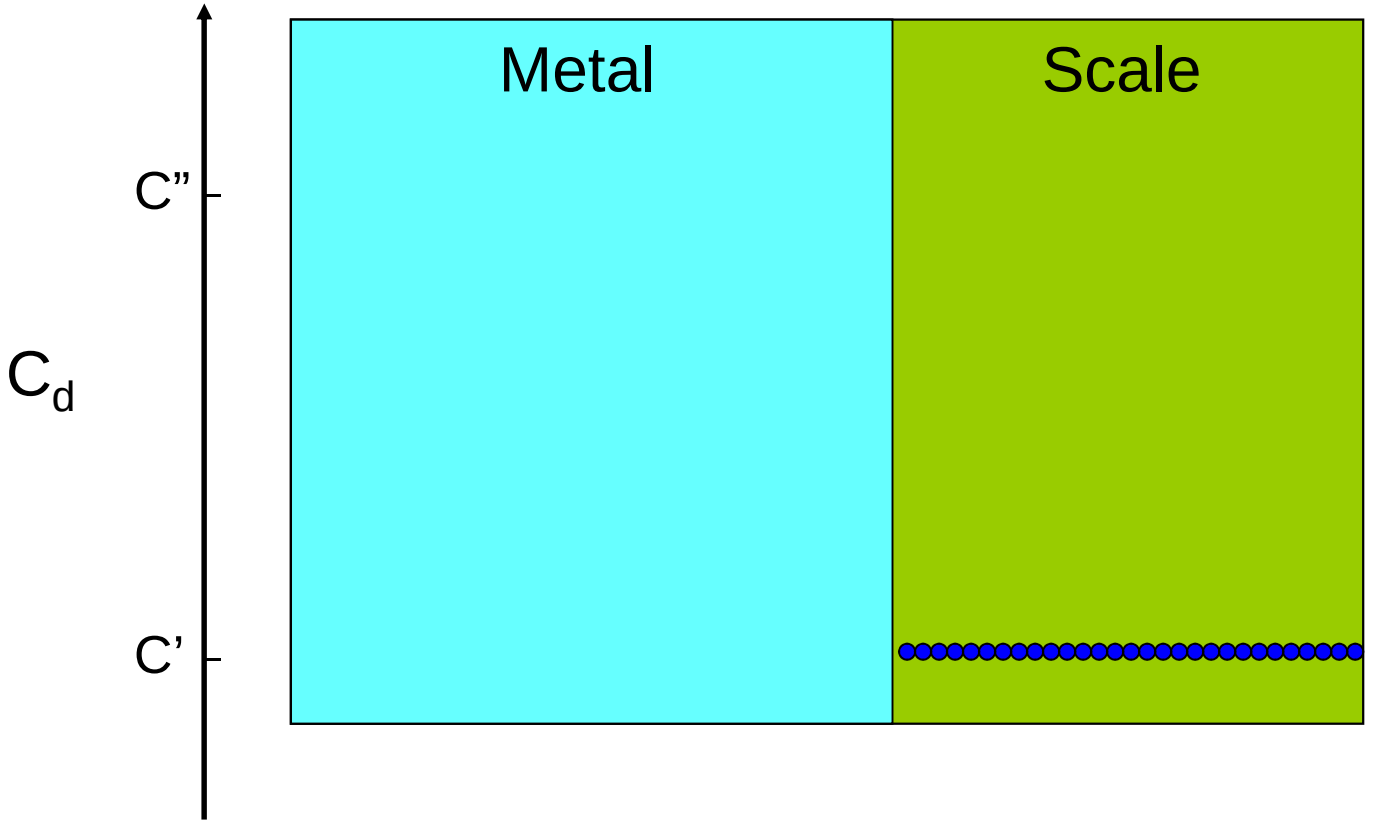

Two-stage oxidation method – point defect concentration distribution in a $Me_{1-y}X$-type scale

II sulphidation stage

T = const; p” = const

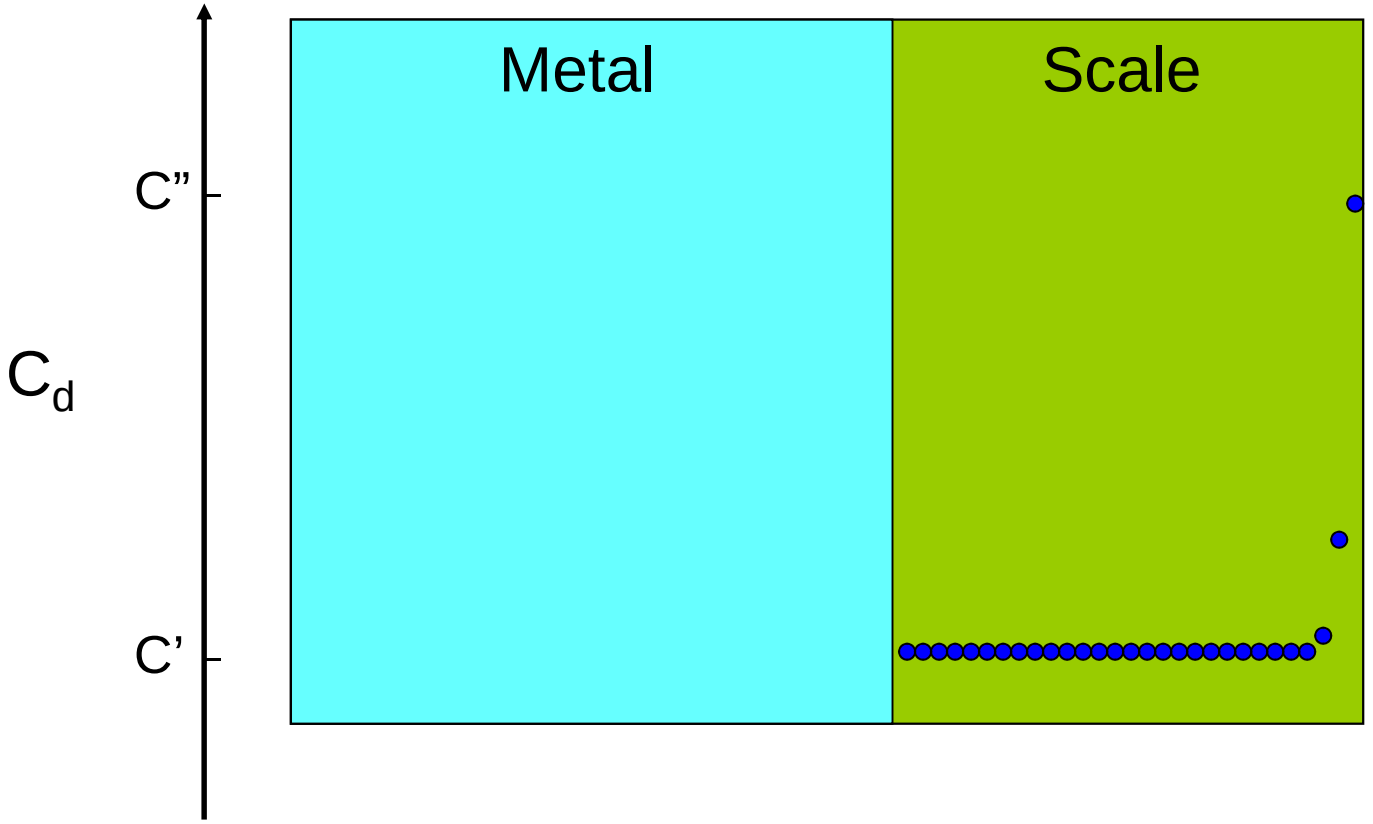

Two-stage oxidation method – point defect concentration distribution in a $Me_{1-y}X$-type scale

II sulphidation stage

T = const; p” = const

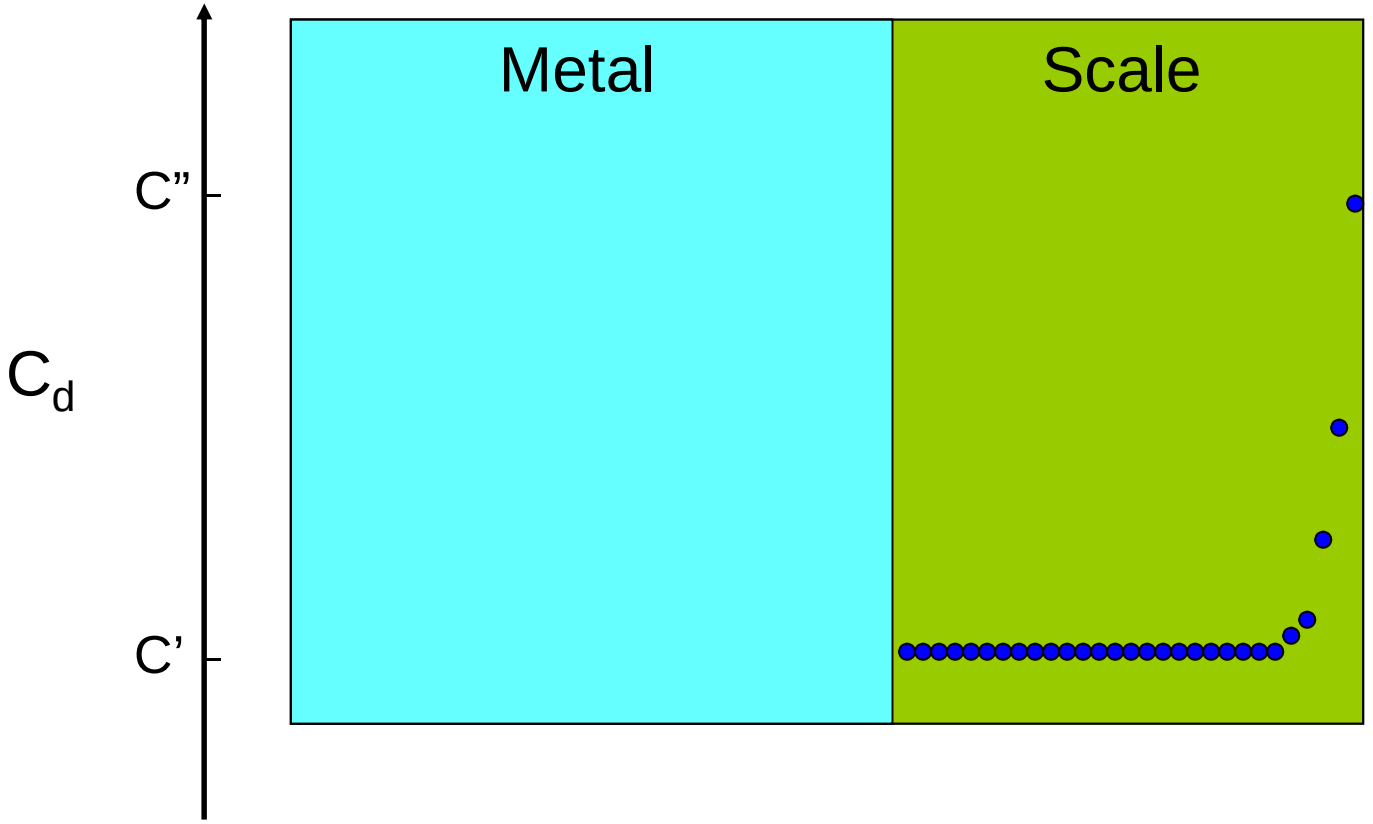

Two-stage oxidation method – point defect concentration distribution in a $Me_{1-y}X$-type scale

II sulphidation stage

T = const; p” = const

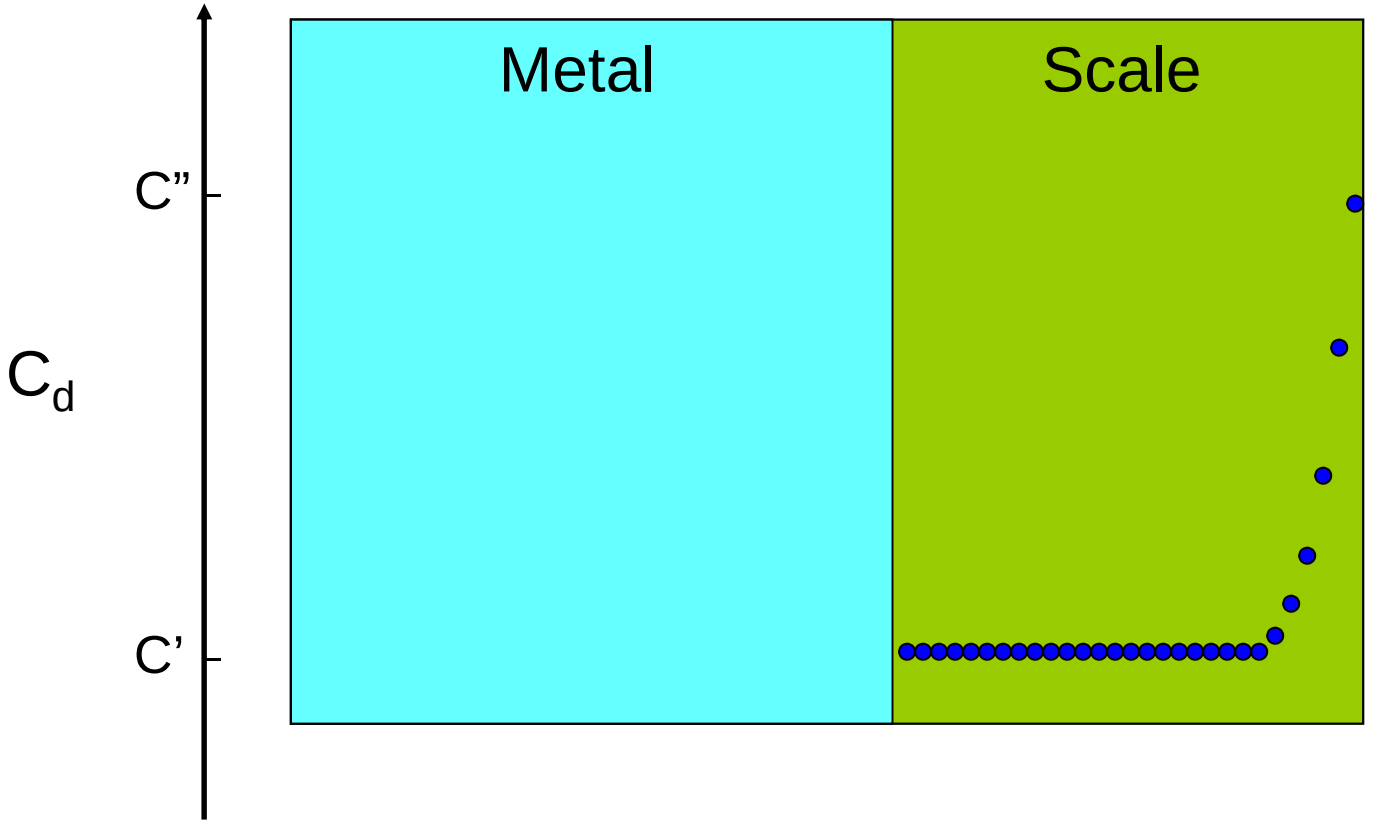

Two-stage oxidation method – point defect concentration distribution in a $Me_{1-y}X$-type scale

II sulphidation stage

T = const; p” = const

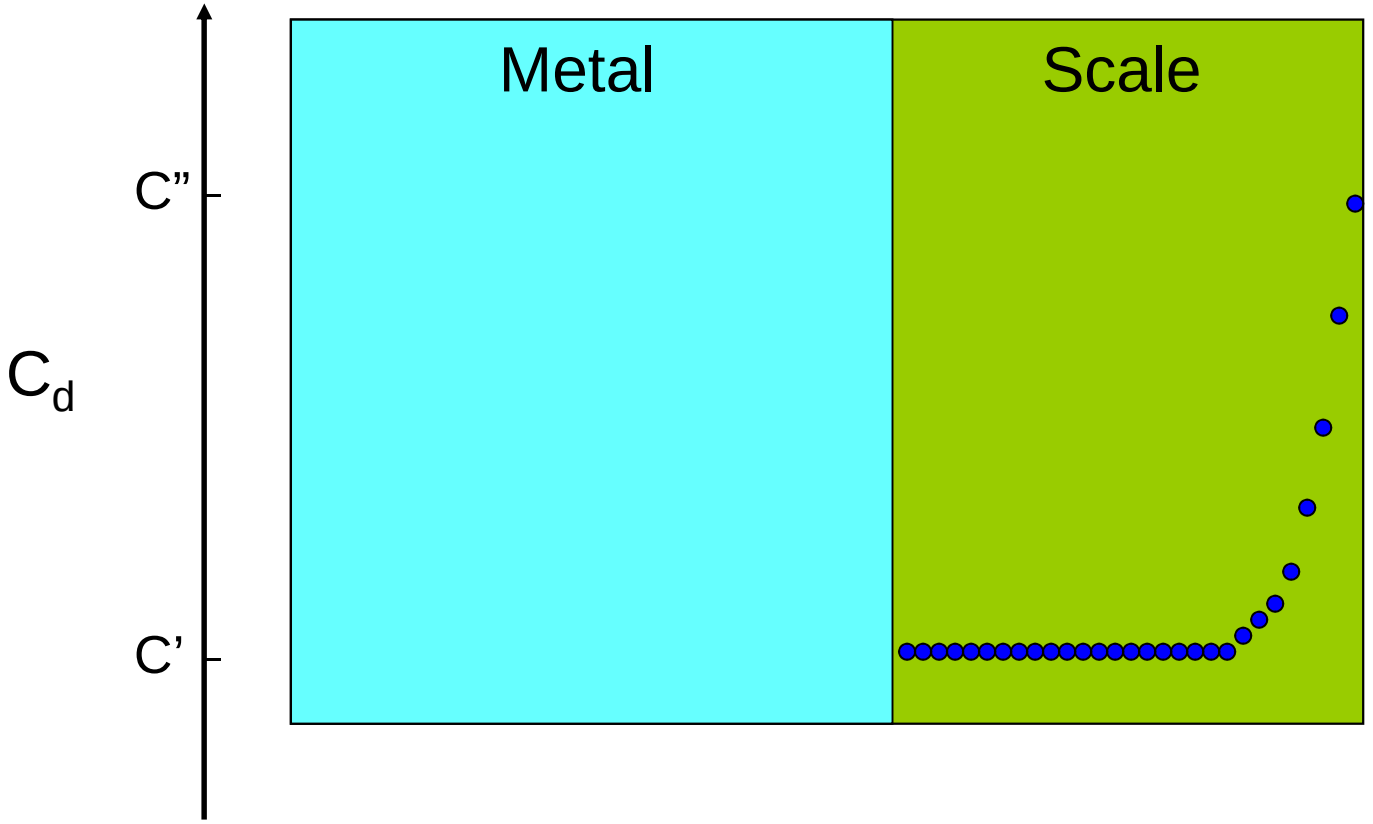

Two-stage oxidation method – point defect concentration distribution in a $Me_{1-y}X$-type scale

II sulphidation stage

T = const; p” = const

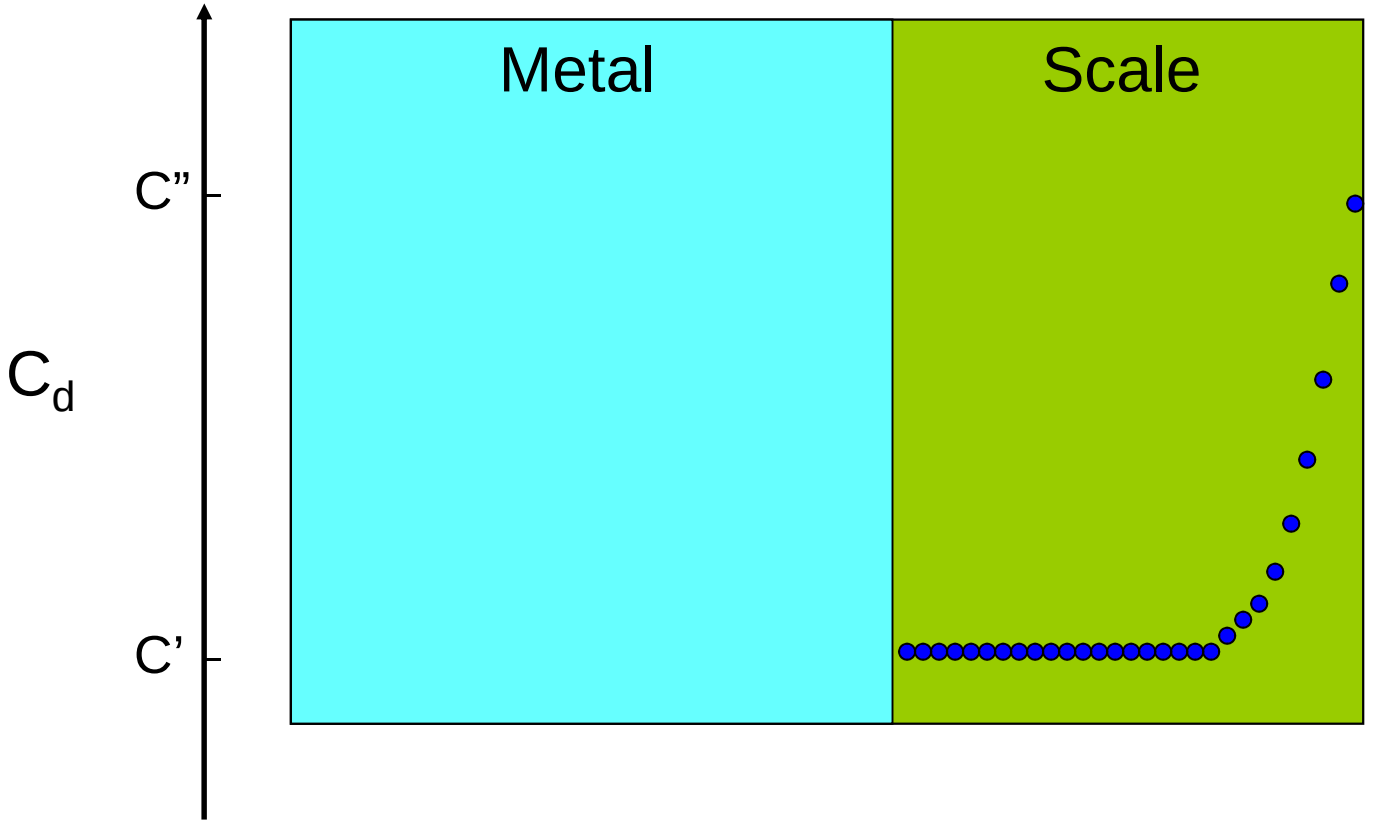

Two-stage oxidation method – point defect concentration distribution in a $Me_{1-y}X$-type scale

II sulphidation stage

T = const; p” = const

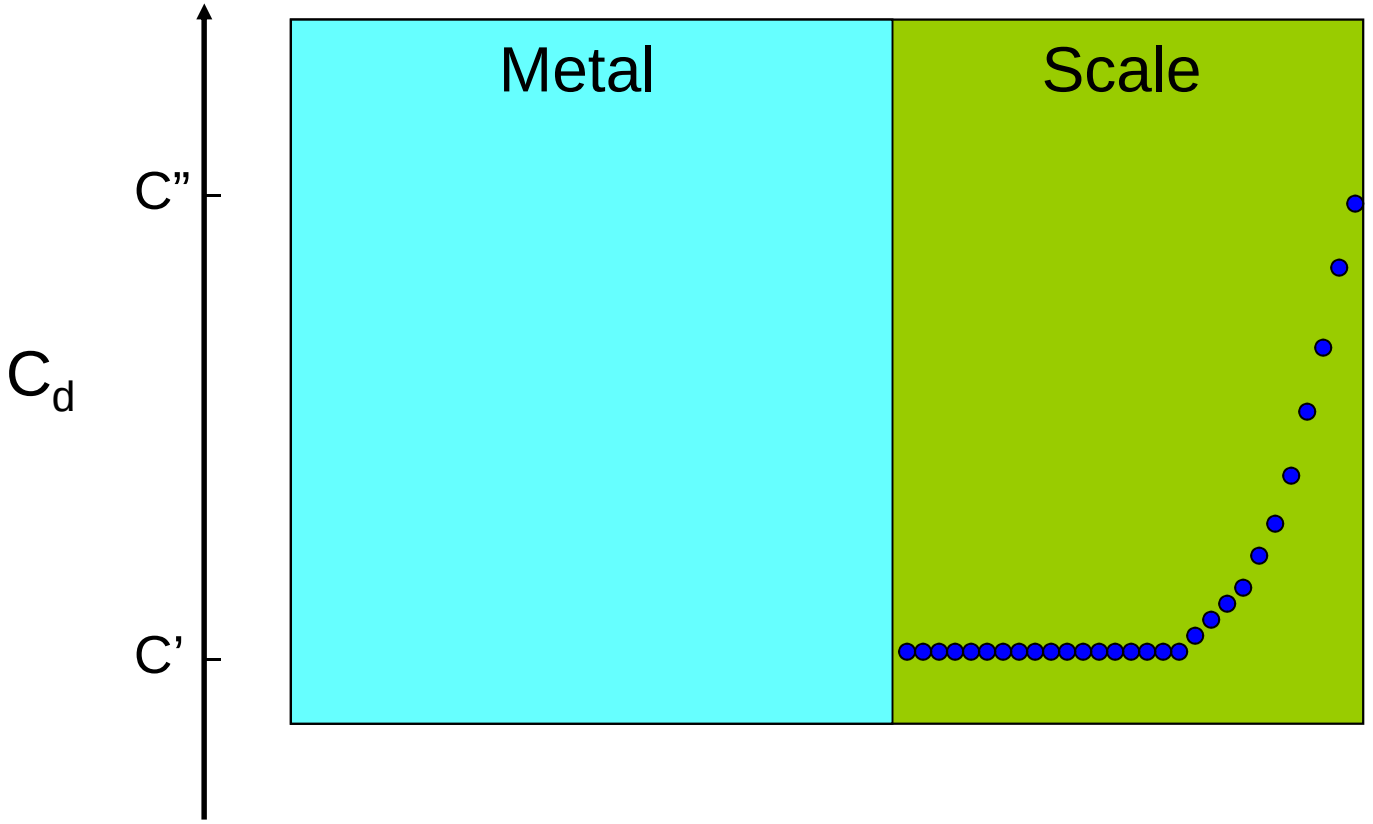

Two-stage oxidation method – point defect concentration distribution in a $Me_{1-y}X$-type scale

II sulphidation stage

T = const; p” = const

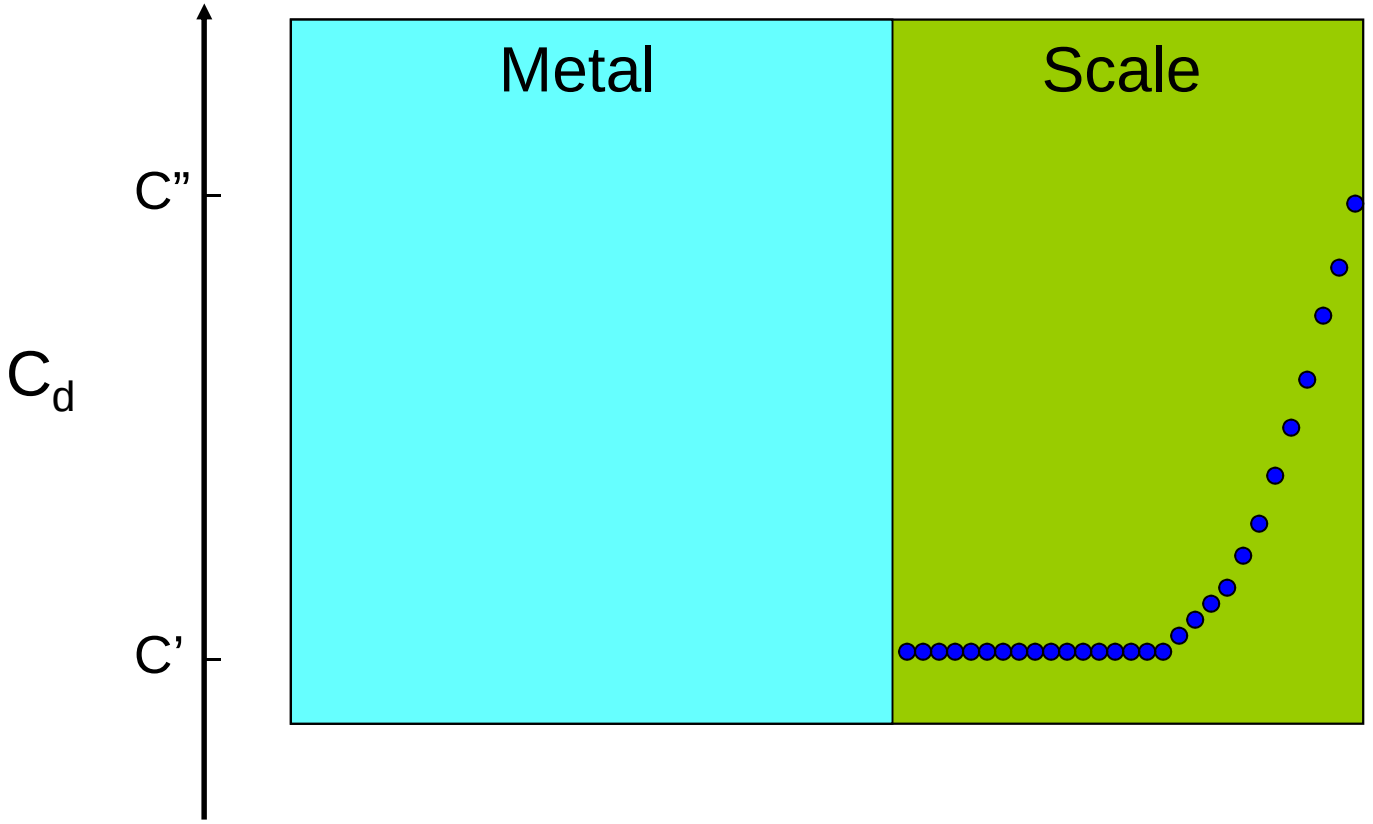

Two-stage oxidation method – point defect concentration distribution in a $Me_{1-y}X$-type scale

II sulphidation stage

T = const; p” = const

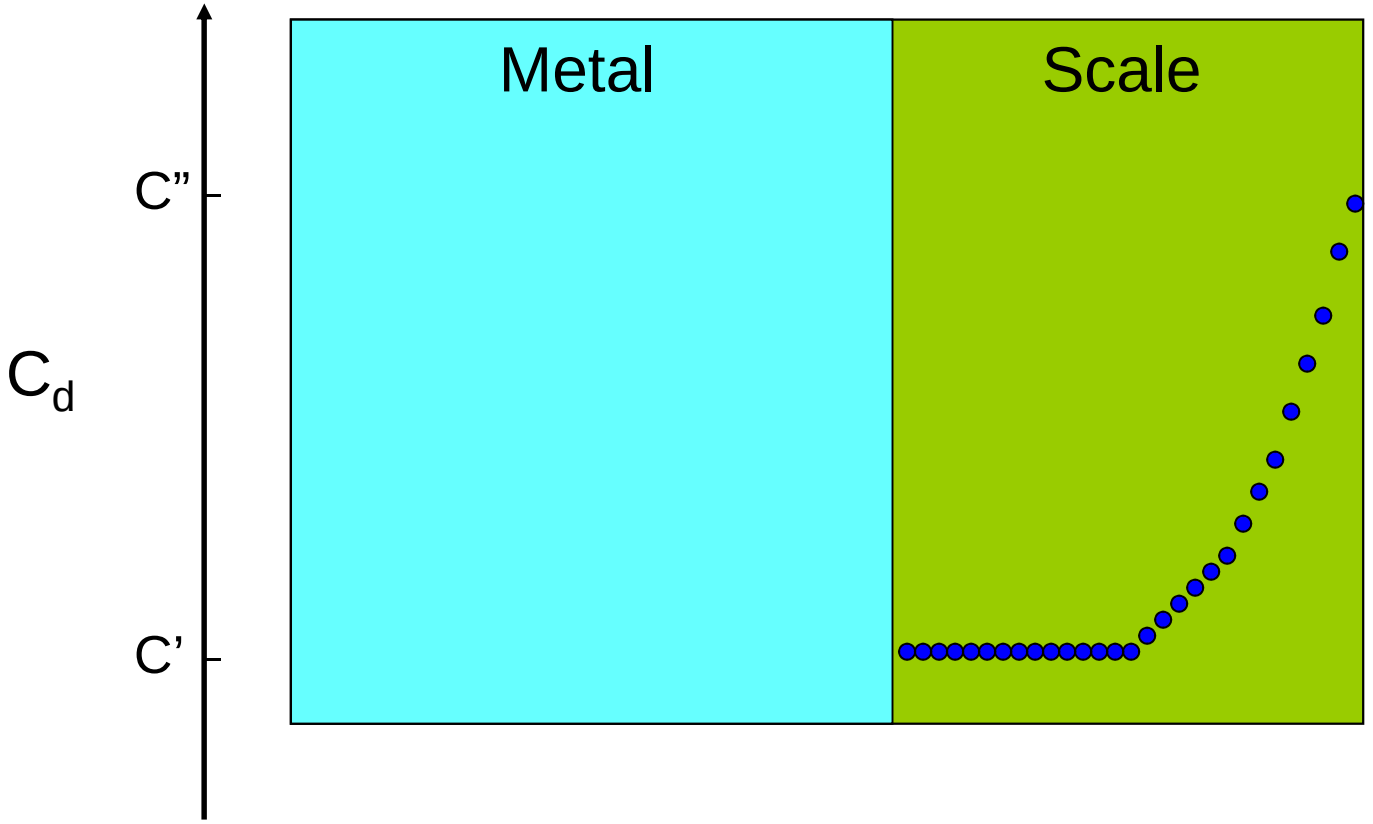

Two-stage oxidation method – point defect concentration distribution in a $Me_{1-y}X$-type scale

II sulphidation stage

T = const; p” = const

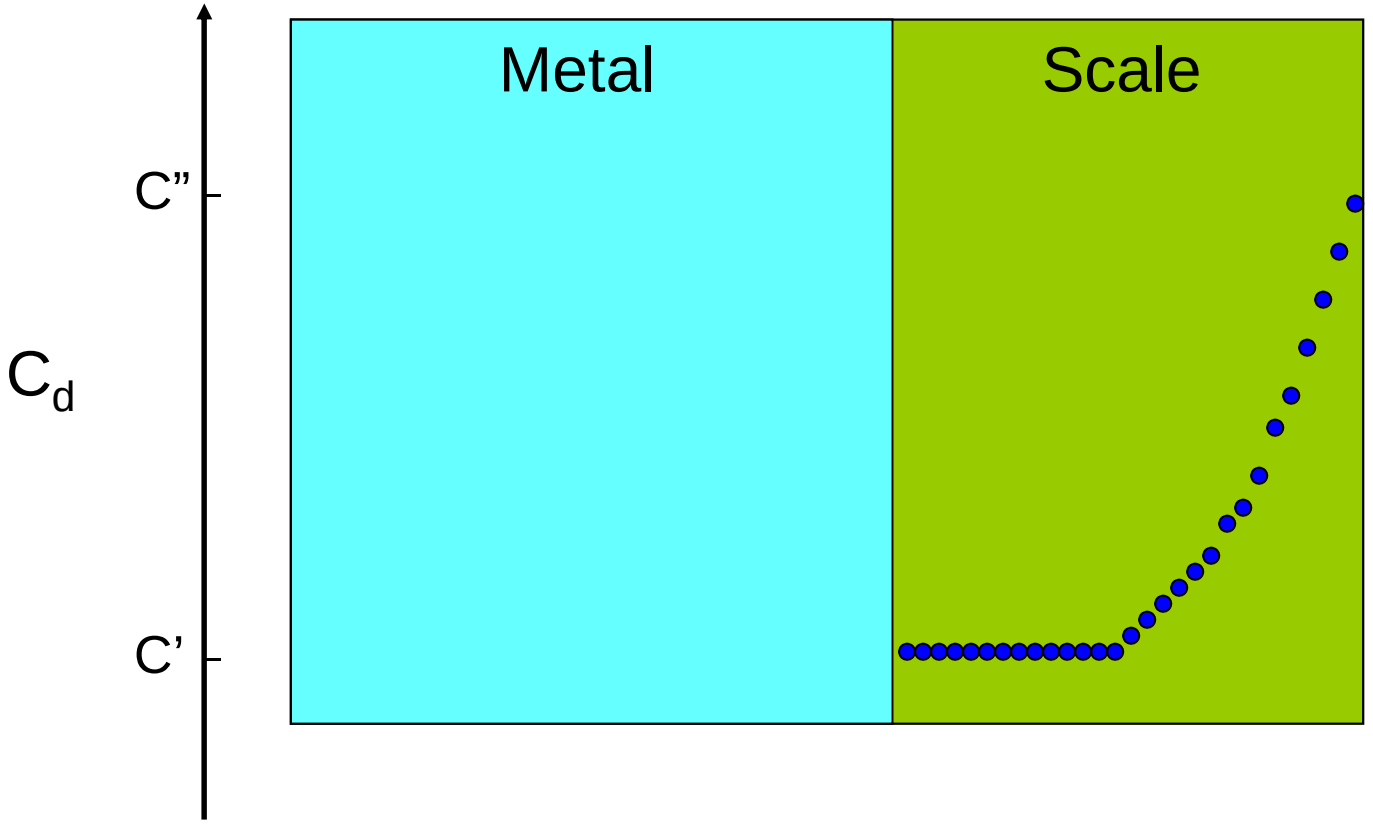

Two-stage oxidation method – point defect concentration distribution in a $Me_{1-y}X$-type scale

II sulphidation stage

T = const; p” = const

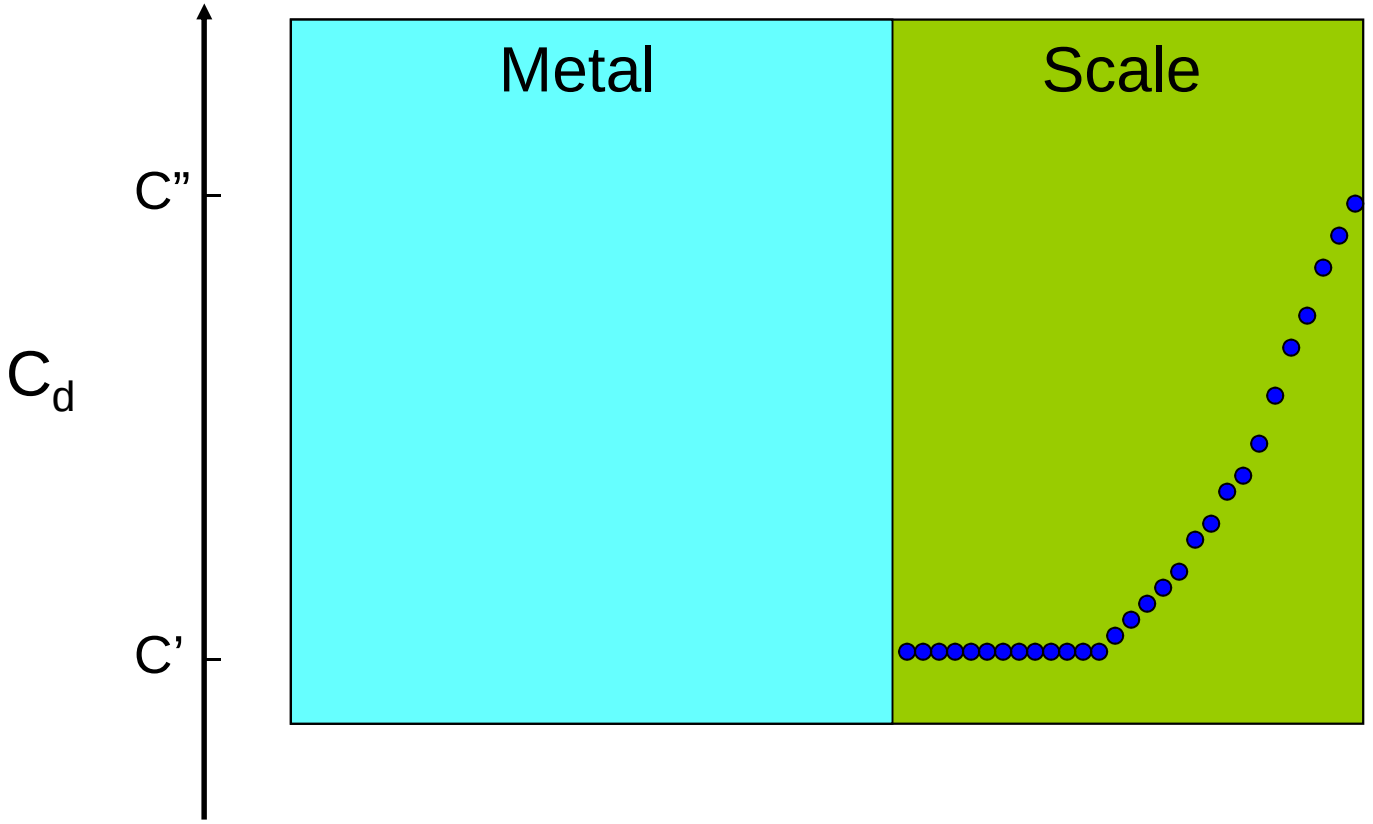

Two-stage oxidation method – point defect concentration distribution in a $Me_{1-y}X$-type scale

II sulphidation stage

T = const; p” = const

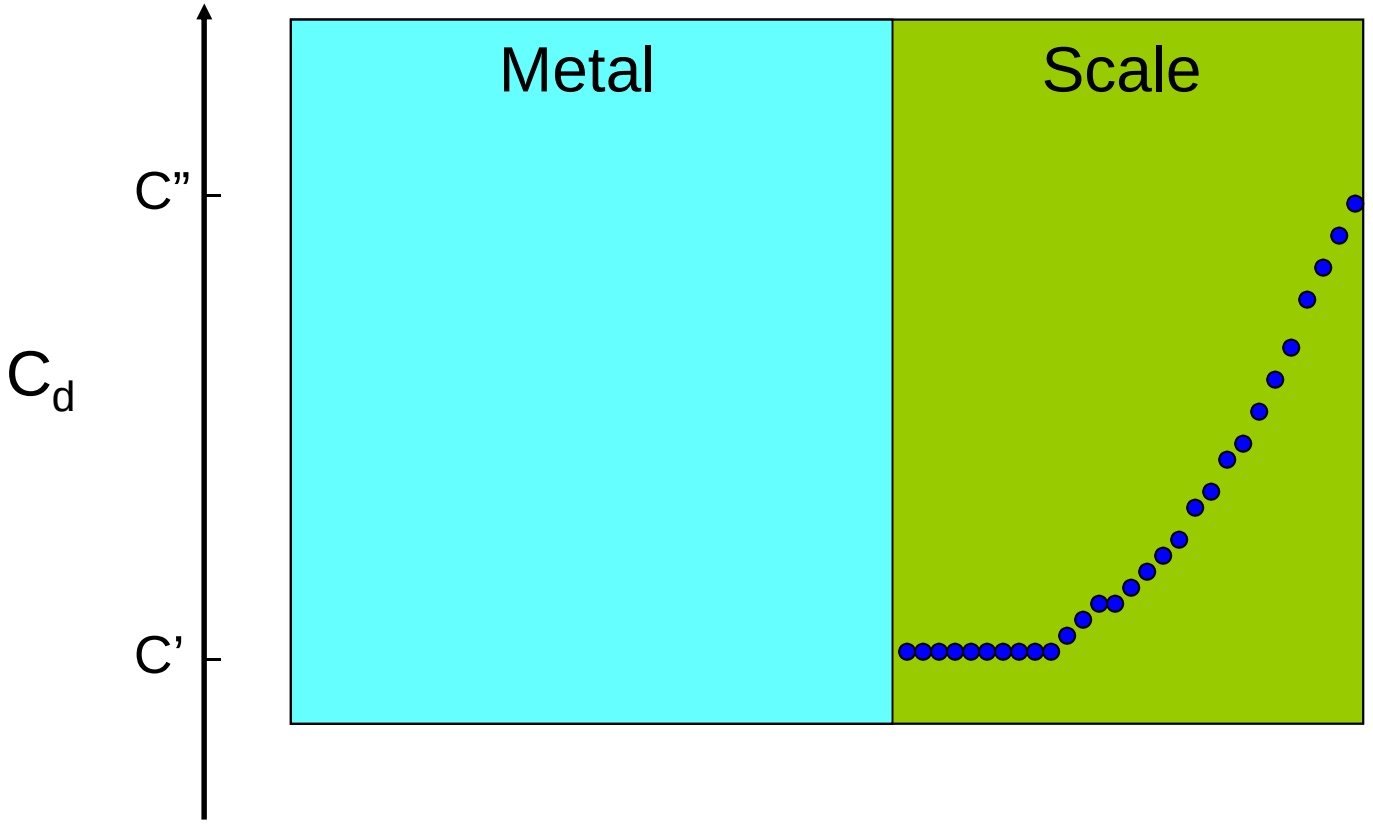

Two-stage oxidation method – point defect concentration distribution in a $Me_{1-y}X$-type scale

II sulphidation stage

T = const; p” = const

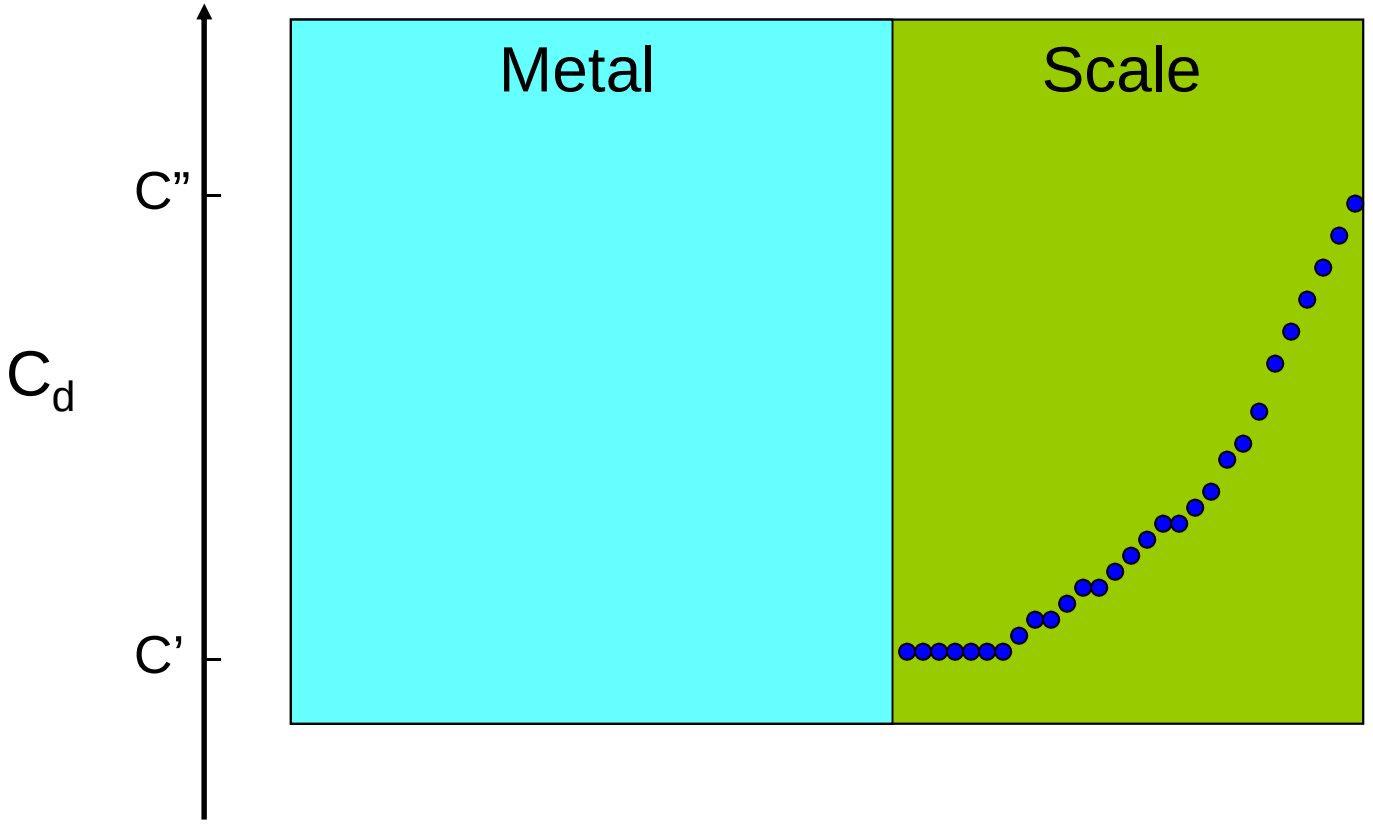

Two-stage oxidation method – point defect concentration distribution in a $Me_{1-y}X$-type scale

II sulphidation stage

T = const; p” = const

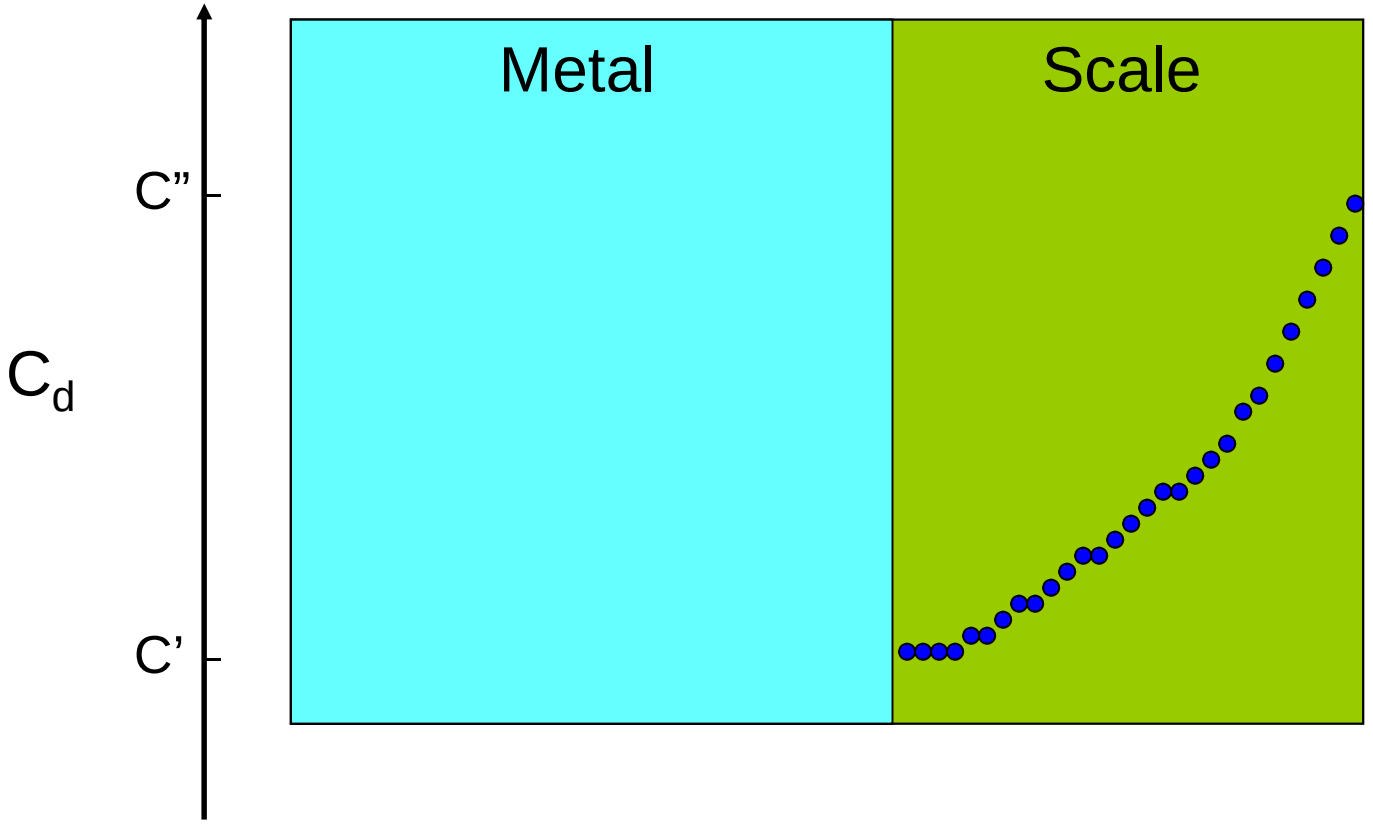

Two-stage oxidation method – point defect concentration distribution in a $Me_{1-y}X$-type scale

II sulphidation stage

T = const; p” = const

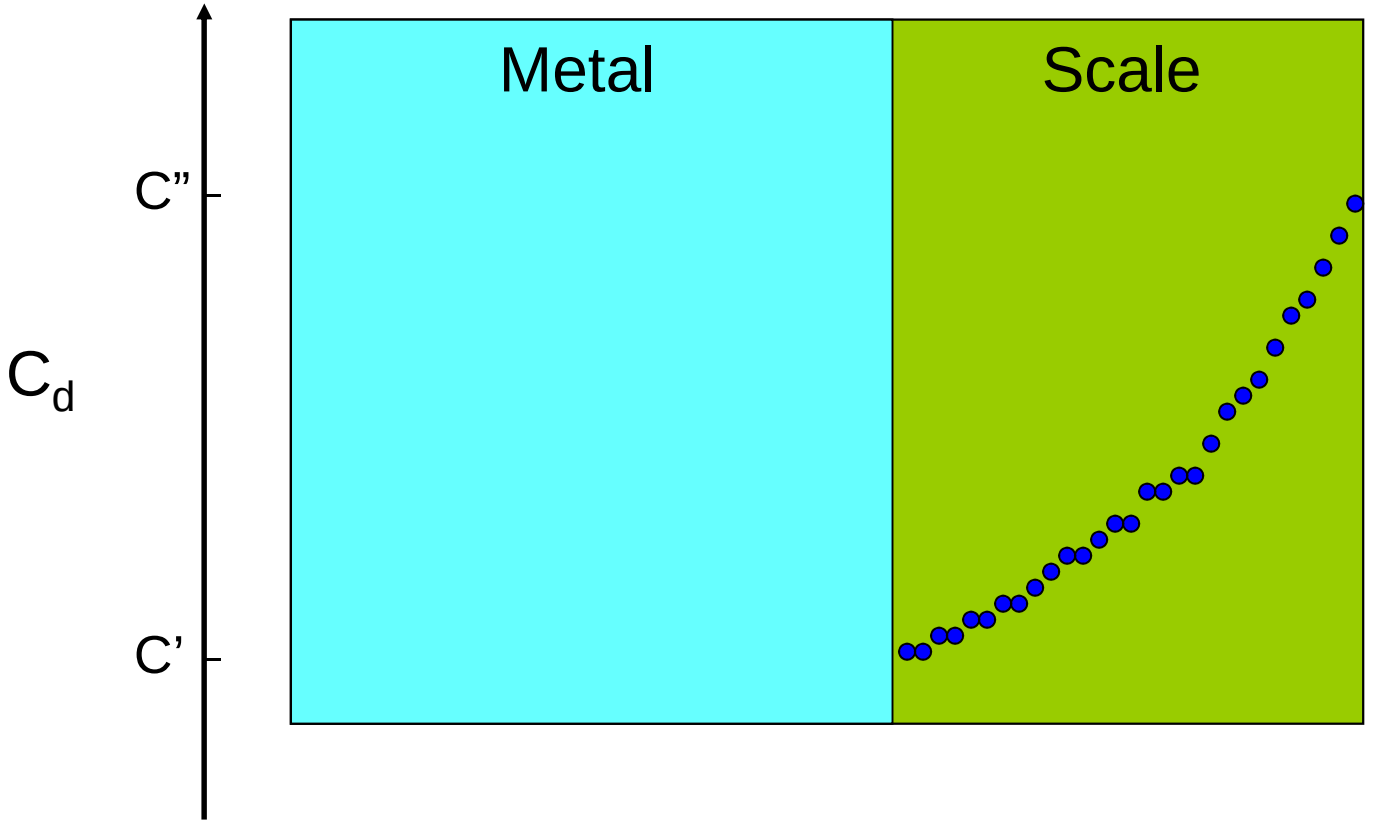

Two-stage oxidation method – point defect concentration distribution in a $Me_{1-y}X$-type scale

II sulphidation stage

T = const; p” = const

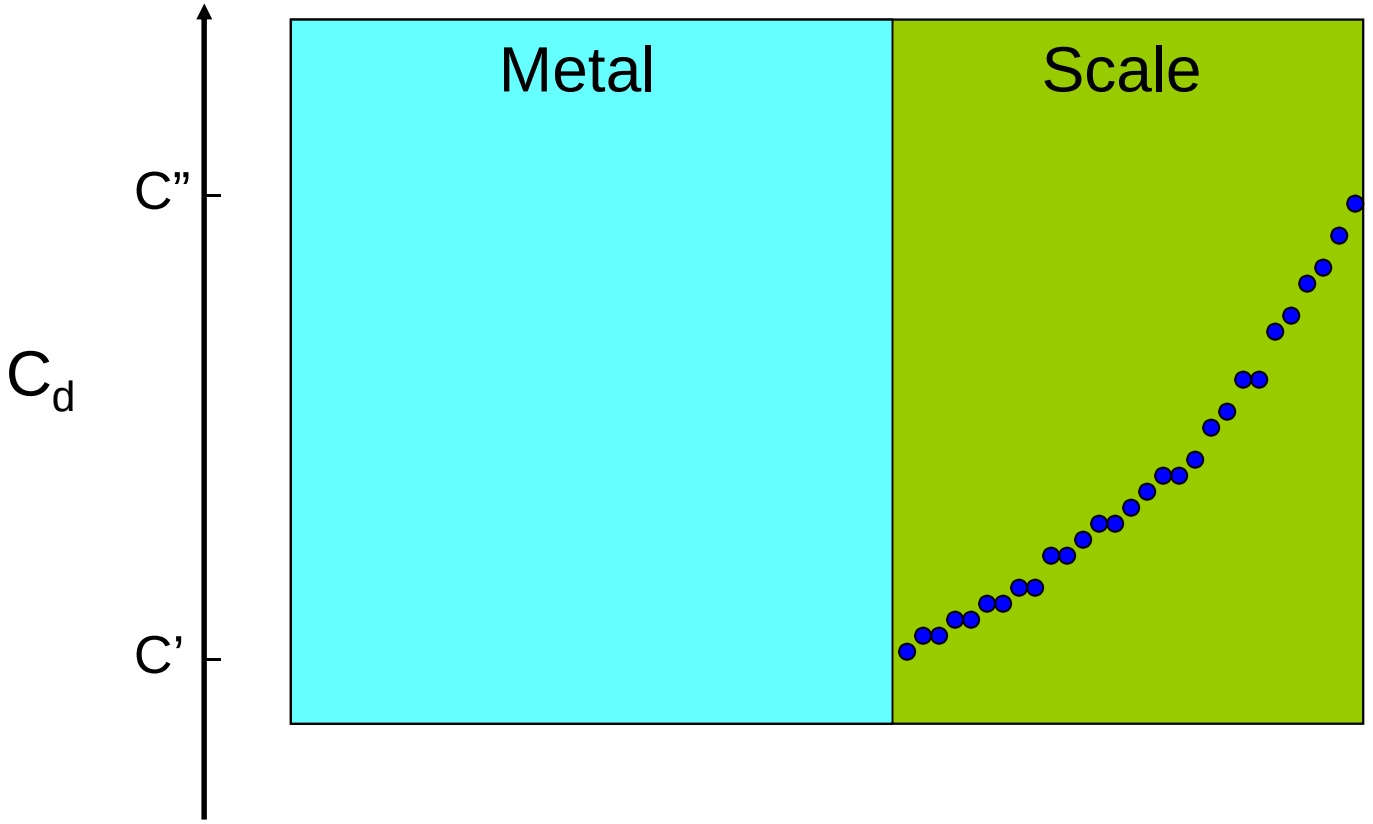

Two-stage oxidation method – point defect concentration distribution in a $Me_{1-y}X$-type scale

II sulphidation stage

T = const; p” = const

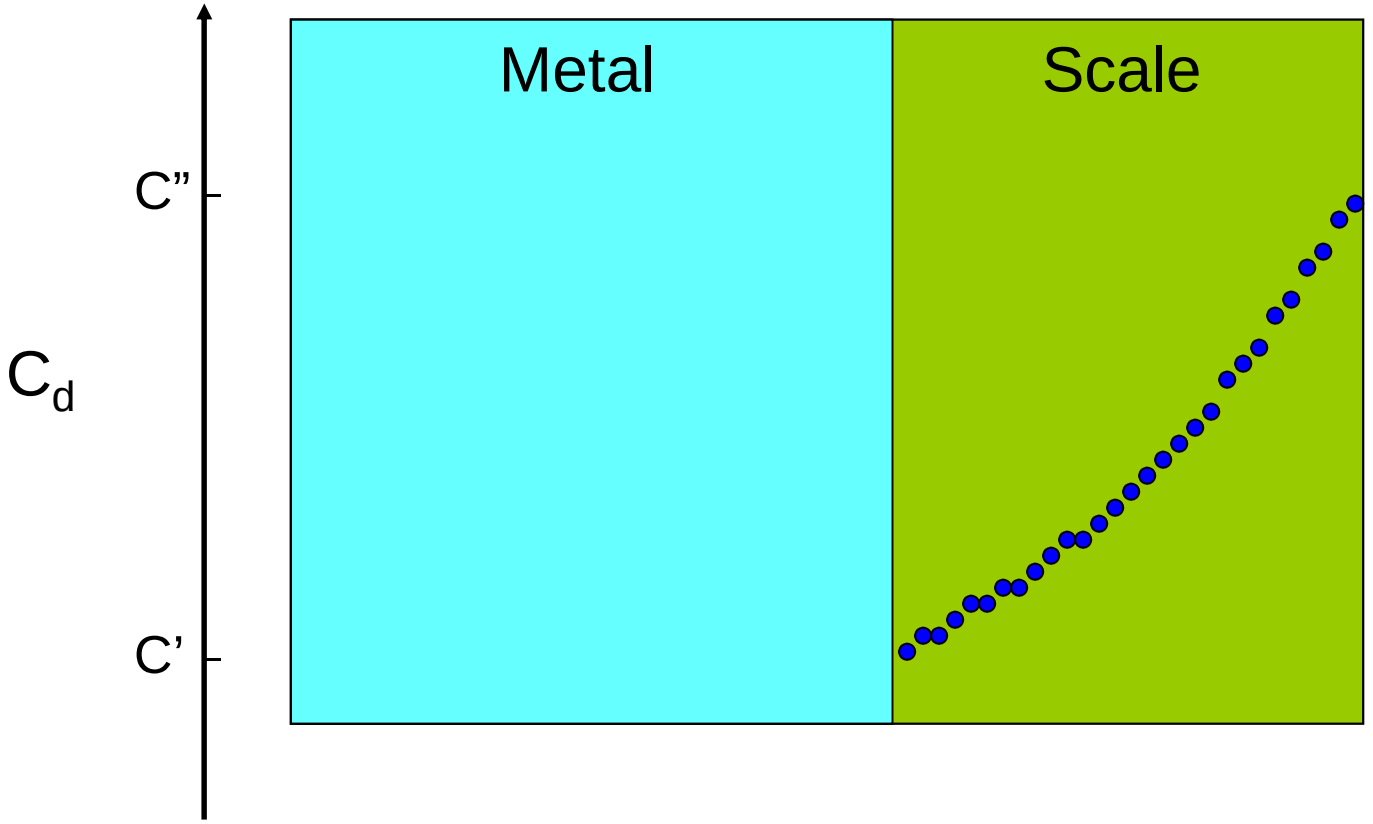

Two-stage oxidation method – point defect concentration distribution in a $Me_{1-y}X$-type scale

II sulphidation stage

T = const; p” = const

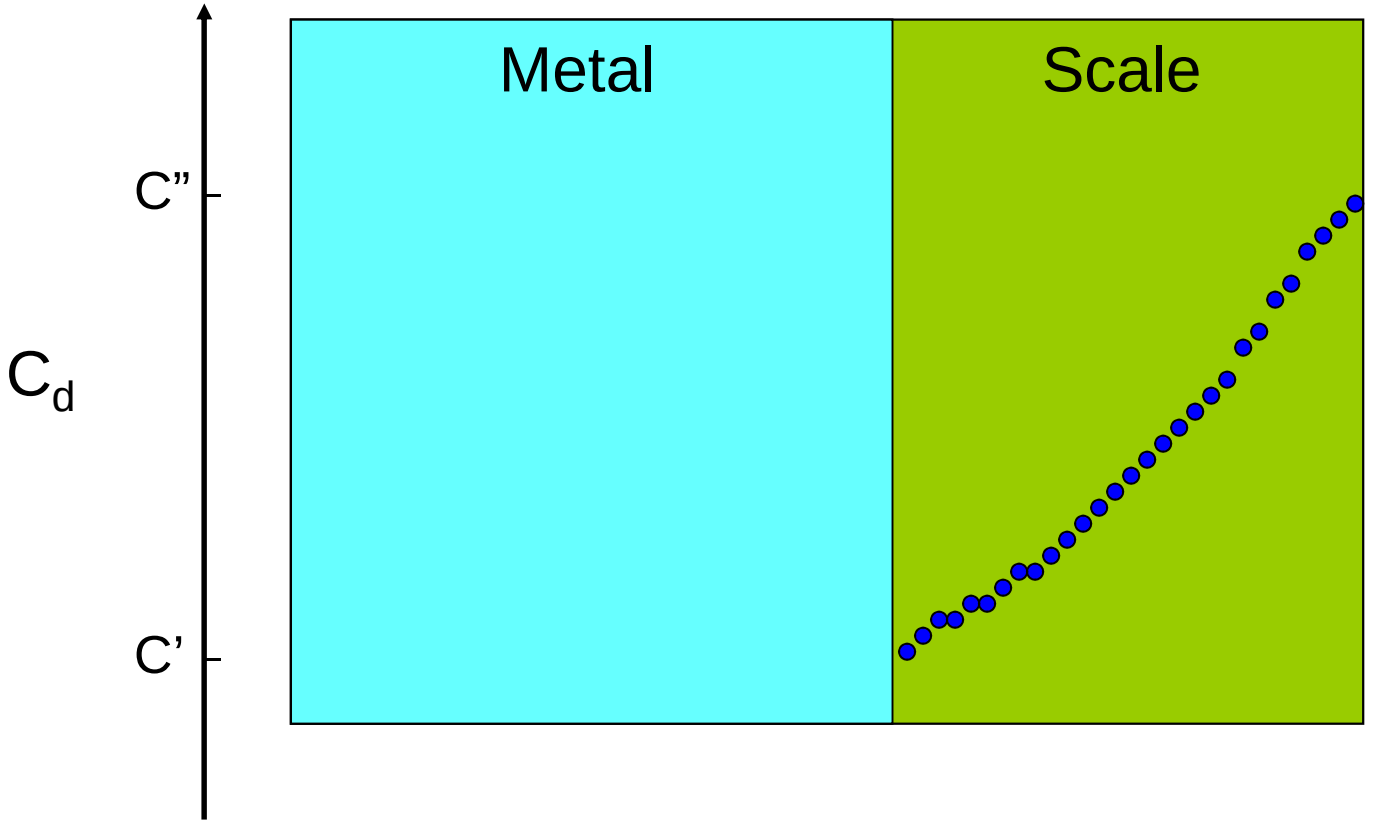

Two-stage oxidation method – point defect concentration distribution in a $Me_{1-y}X$-type scale

II sulphidation stage

T = const; p” = const

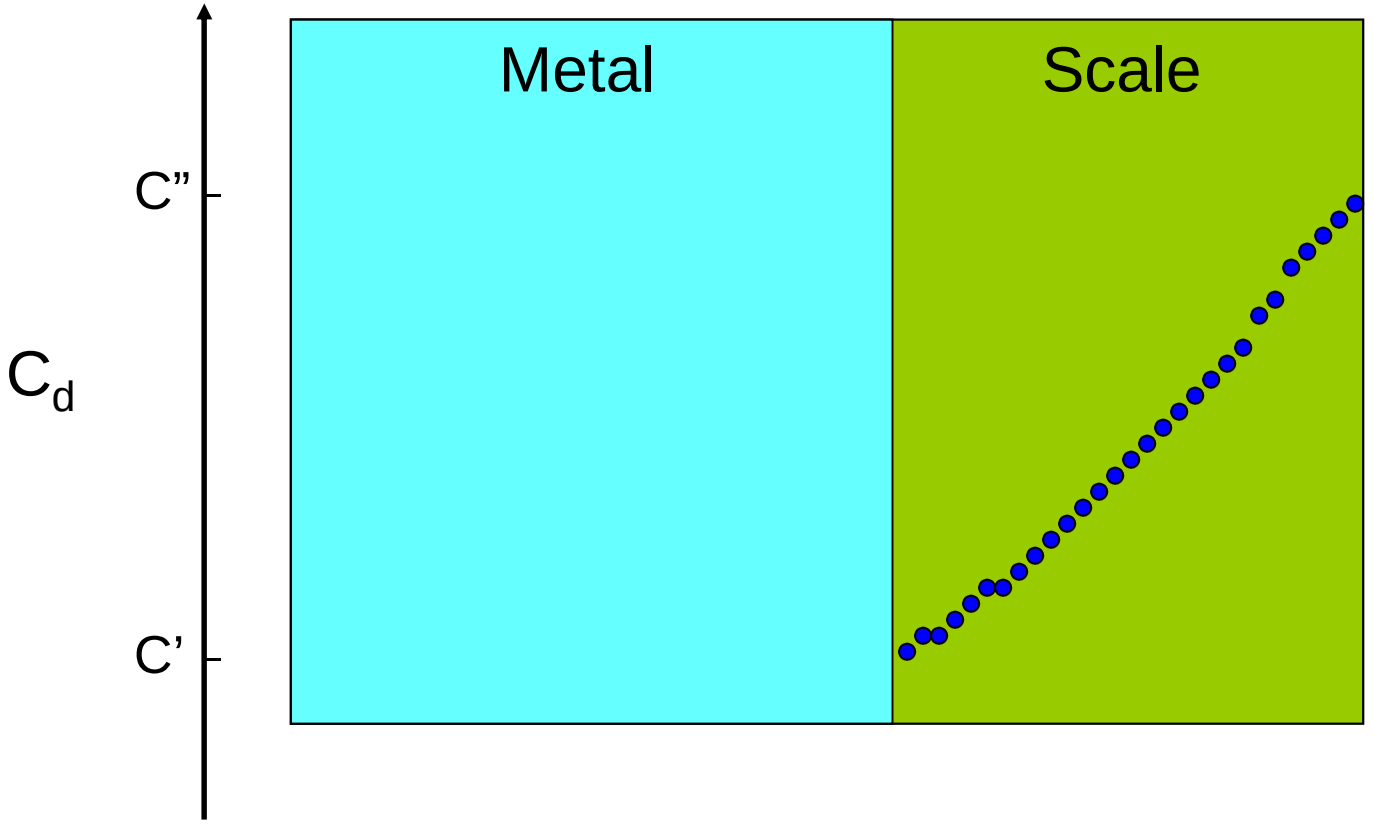

Two-stage oxidation method – point defect concentration distribution in a $Me_{1-y}X$-type scale

II sulphidation stage

T = const; p” = const

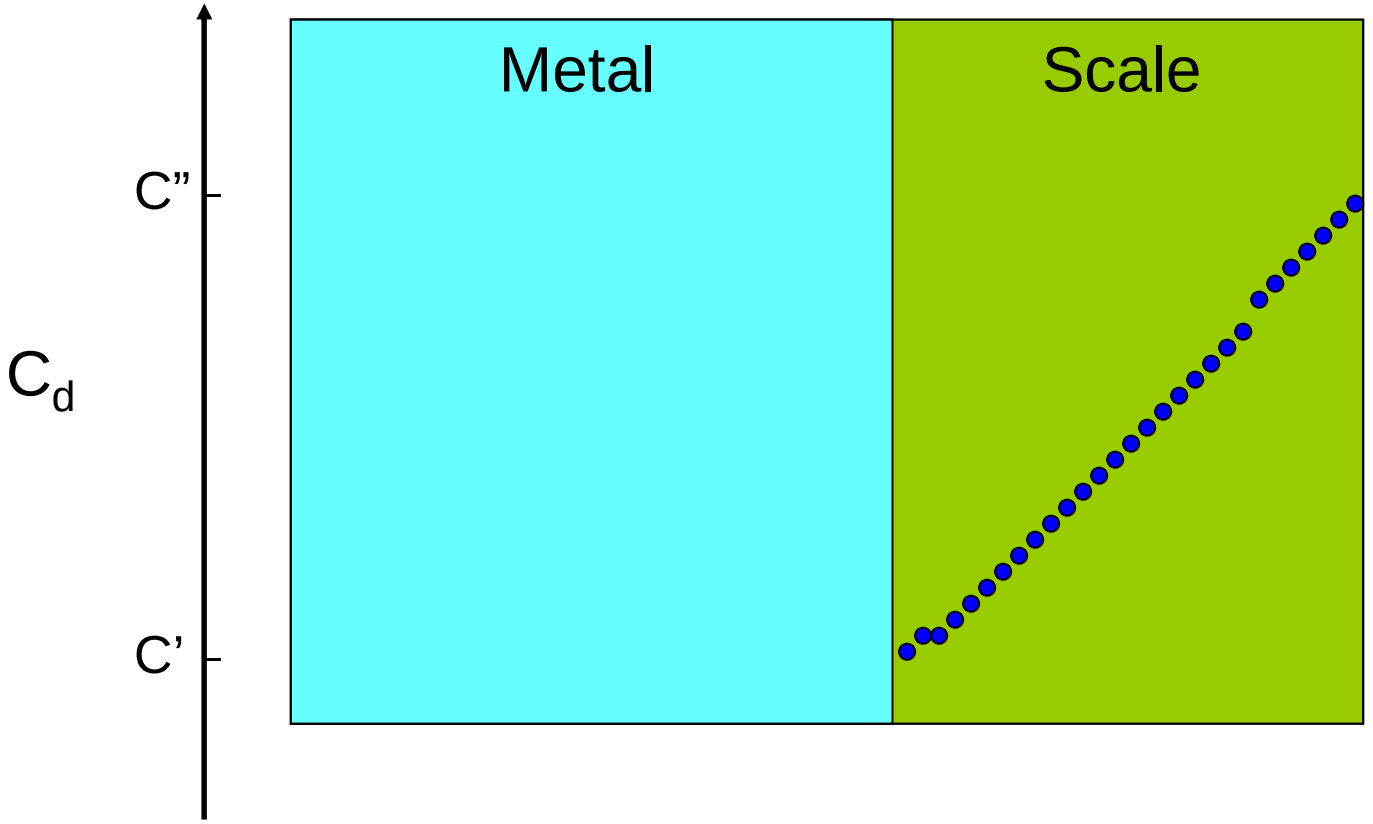

Two-stage oxidation method – point defect concentration distribution in a $Me_{1-y}X$-type scale

II sulphidation stage

T = const; p” = const

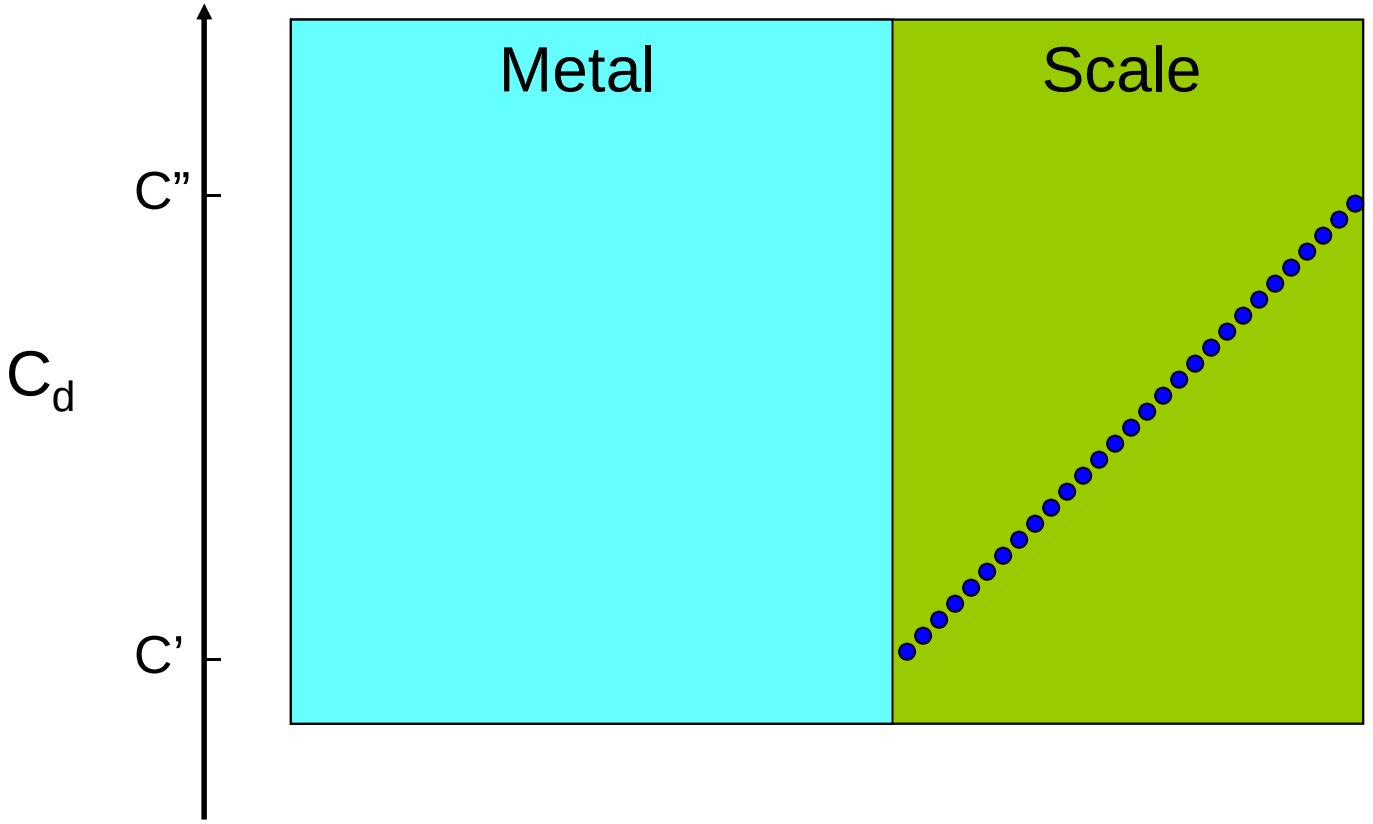

Two-stage oxidation method – results analysis

$$C(x) = C_0 + (C_k - C_0)\frac{x}{X_0} + \frac{2}{\pi}\sum_{n=1}^{\infty}\frac{C_k\cos(n\pi) - C_0}{n}\sin\left(\frac{n\pi x}{X_0}\right)\exp\left(-\frac{n^2\pi^2\tilde{D}t}{X_0^2}\right) +$$

$$+\frac{4C_0}{\pi}\sum_{m=0}^{\infty}\frac{1}{2m+1}\sin\frac{(2m+1)\pi x}{X_0}\exp\left(-\frac{(2m+1)^2\pi^2\tilde{D}t}{X_0^2}\right)$$

$$N_d = \tilde{D}\int_0^t\left(\frac{\partial c(x)}{\partial x}\right)\Bigg|_{x=X_0}dt = -\frac{2C_kX_0}{\pi^2}\sum_{n=1}^{\infty}\frac{1}{n^2}\cdot\left[\exp\left(-\frac{\tilde{D}\pi^2n^2t}{X_0^2}\right) - 1\right] +$$

$$\frac{\tilde{D}C_kt}{X_0} + \frac{4C_kX_0}{\pi^2}\sum_{m=0}\frac{1}{(2m+1)^2}\cdot\left[\exp\left(-\frac{\tilde{D}\pi^2(2m+1)^2t}{X_0^2}\right) - 1\right]$$

$$N_d = \frac{\tilde{D}C_kt}{X_0} + \frac{X_0C_k}{3} \qquad \text{dla} \quad t > X_0^2/2\tilde{D}$$

$$N_d = \frac{2C_k\sqrt{\tilde{D}t}}{\sqrt{\pi}} \qquad \text{dla} \quad t << X_0^2/\tilde{D}$$

Two-stage oxidation method – results analysis

$$\tilde{D} = \left(\frac{1{,}128 k_l X_0}{k_p} \right)^2$$

$$C_d = \frac{\left(\frac{k_p}{1{,}128} \right)^2}{k_l X_0}$$

where:

$\tilde{D}$ **– chemical diffusion coefficient, C_d – defect concentration, X_0 – scale thickness in the I stage of oxidation, k_p ($gcm^{-2}s^{-0,5}$) i k_l ($gcm^{-2}s^{-1}$) – straight line coefficients plotted in the parabolic and linear system, respectively.**

Description of scale transport property studies on the example of manganese sulfide

$Mn_{1-y}S$ – deviation from stoichiometry measurement

Rau, 1978 – indirect method

$$y = [V''_{Mn}] = 4{,}77 \cdot 10^{-2}\, p_{S_2}^{1/6} \exp\left(-\frac{41{,}5\ kJ/mol}{RT}\right)$$

H. Rau, J. Phys. Chem. Solids, **39**, 339 (1978).

Own research – direct method

I. Microthermogravimetry

$$y = 1 - \frac{m_{Mn} \cdot M_S}{m_S \cdot M_{Mn}}$$

$$y = [V''_{Mn}] = 4{,}43 \cdot 10^{-2}\, p_{S_2}^{1/6} \exp\left(-\frac{41{,}0\ kJ/mol}{RT}\right)$$

II. Two-stage sulphidation

$$y = [V''_{Mn}] = 5{,}41 \cdot 10^{-2}\, p_{S_2}^{1/6} \exp\left(-\frac{42{,}0\ kJ/mol}{RT}\right)$$

Z. Grzesik and S. Mrowec, "Kinetics and thermodynamics of point defects in nonstoichiometric metal oxides and sulphides. Microthermogravimetric study", J. Therm. Anal. Cal., **90**, 269-282 (2007).

Temperature dependence of the self-diffusion coefficient

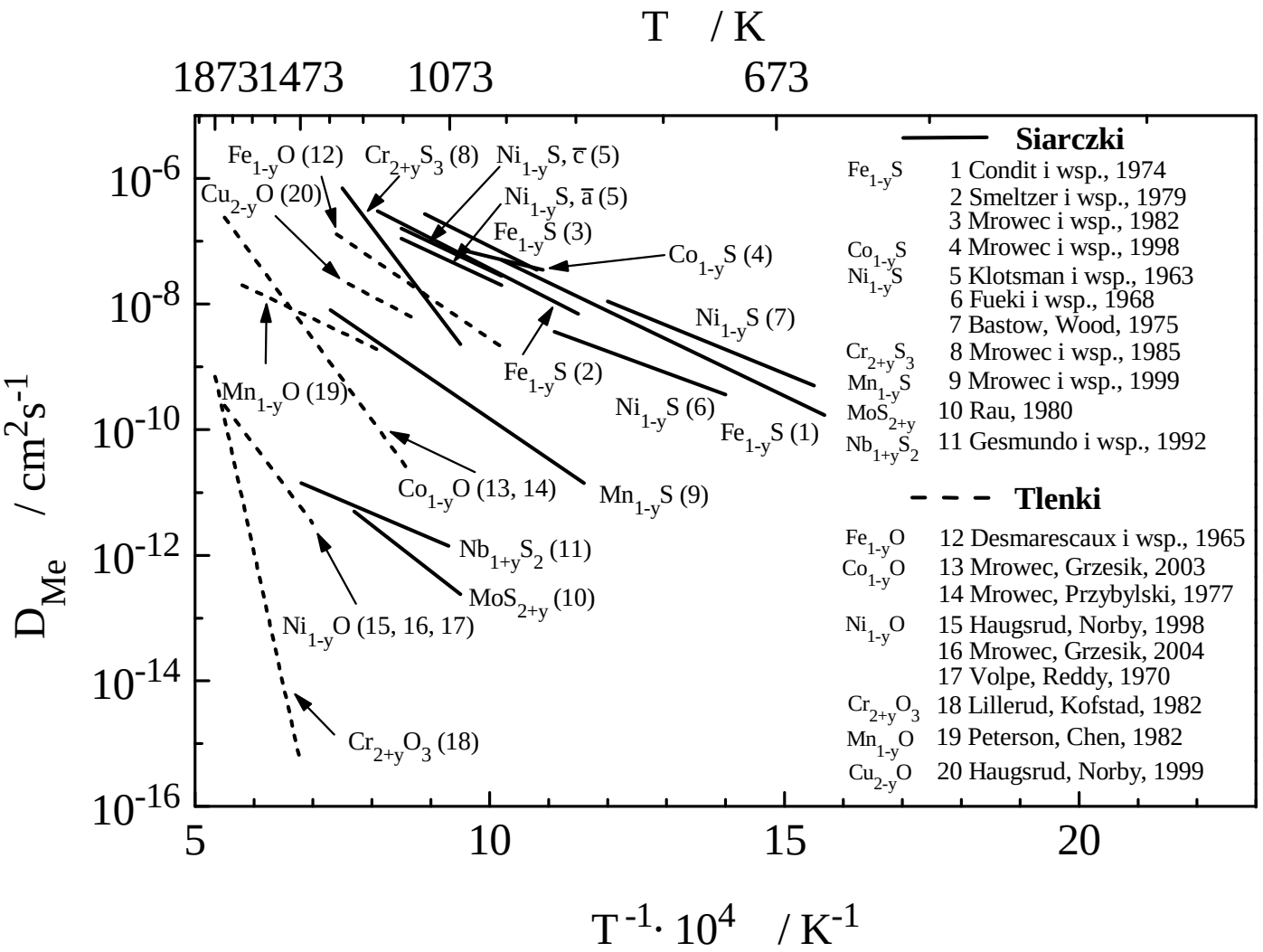

Z. Grzesik, "Własności transportowe zgorzelin siarczkowych powstających w procesie wysokotemperaturowej korozji metali", Ceramika, **87**, 1-124 (2005).

$Mn_{1-y}S$ – reequilibration kinetics

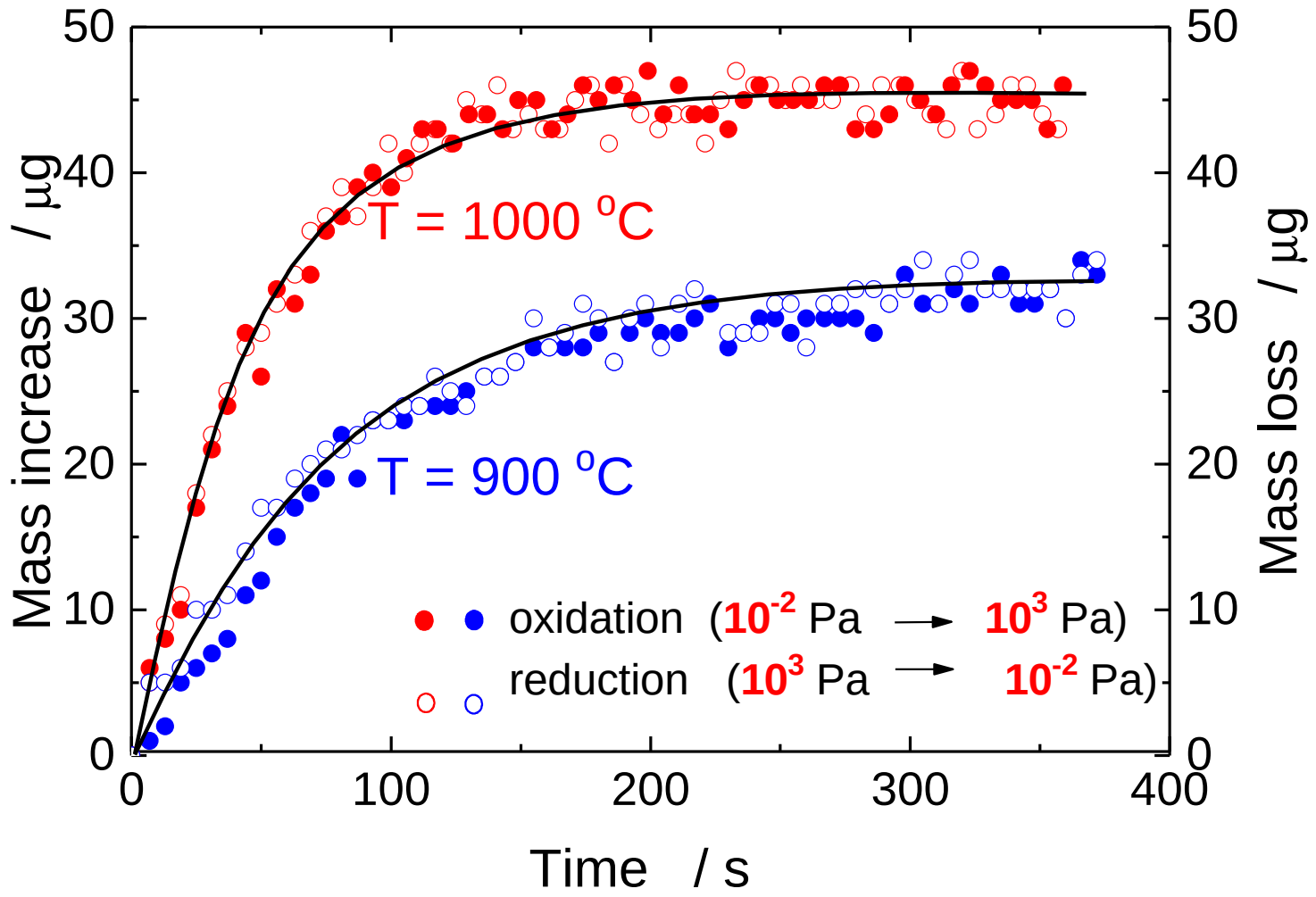

$Mn_{1-y}S$ – dependence of $\tilde{D}$ on pressure

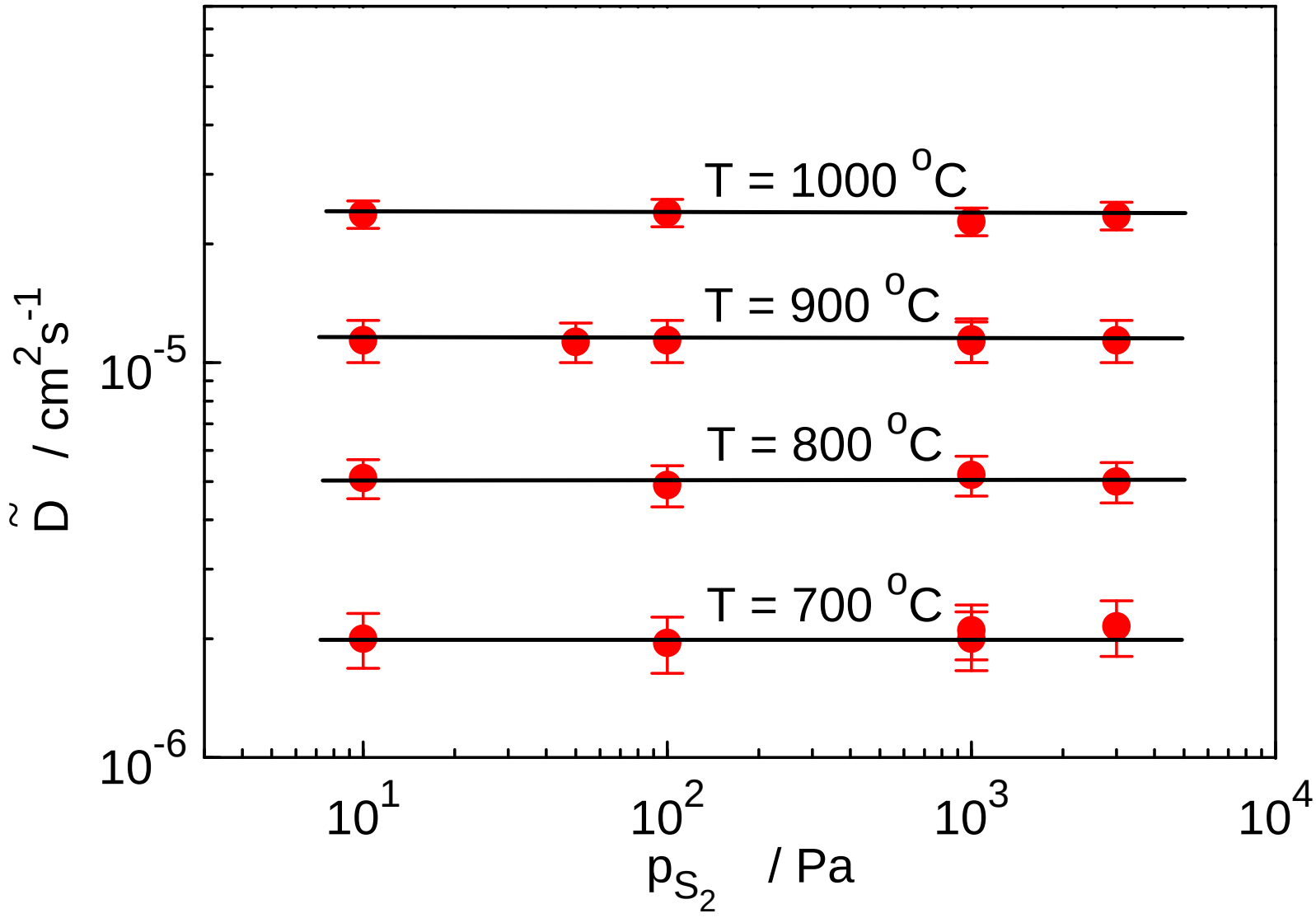

Comparison between experimentally determined and calculated k'_p values of manganese sulfide

$$k'_p = \tilde{D} \cdot y$$

I. Kinetics of Mn sulphidation *(experiment)*

$$k'_p = 3{,}49 \cdot 10^{-3} \cdot p_{S_2}^{1/6} \exp\left(-\frac{127{,}0\ \mathrm{kJ/mol}}{RT}\right) \quad \mathrm{cm^2 s^{-1}}$$

II. Reequilibration and deviation from stoichiometry *(calculations)*

$$k'_p = 2{,}09 \cdot 10^{-3} \cdot p_{S_2}^{1/6} \exp\left(-\frac{123{,}5\ \mathrm{kJ/mol}}{RT}\right) \quad \mathrm{cm^2 s^{-1}}$$

III. Two-stage sulphidation *(calculations)*

$$k'_p = 2{,}62 \cdot 10^{-3} \cdot p_{S_2}^{1/6} \exp\left(-\frac{124{,}4\ \mathrm{kJ/mol}}{RT}\right) \quad \mathrm{cm^2 s^{-1}}$$

Image of the surface and cross-section of a sulfide scale on manganese

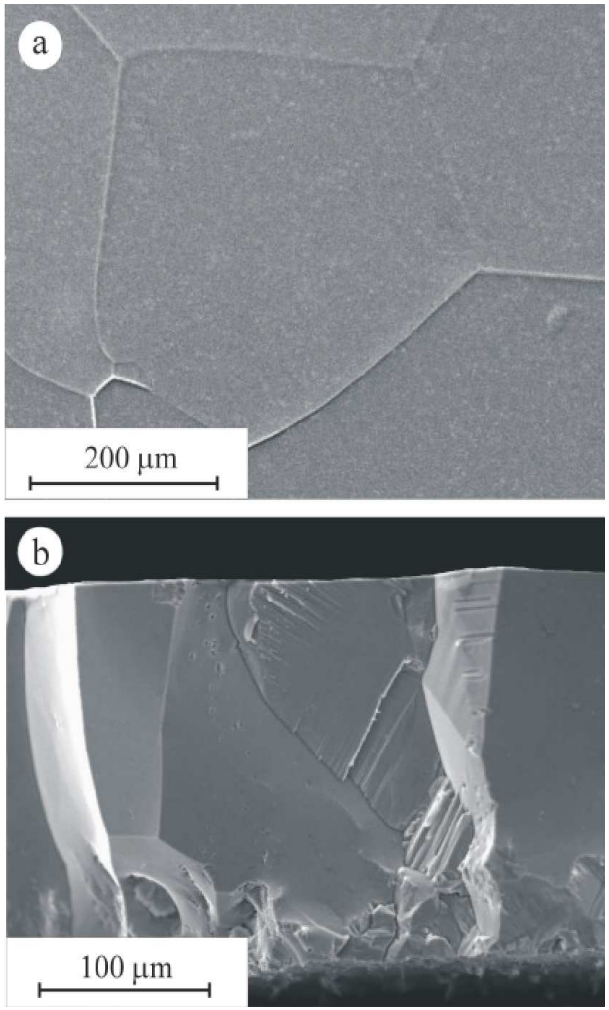

T = 1000 °C,
$p(S_2) = 10^3$ Pa,
t = 240 h

surface

fracture

Z. Grzesik, "Własności transportowe zgorzelin siarczkowych powstających w procesie wysokotemperaturowej korozji metali", Ceramika, **87**, 1-124 (2005).

Projection of the MnS crystallographic structure in the ⟨100⟩ direction

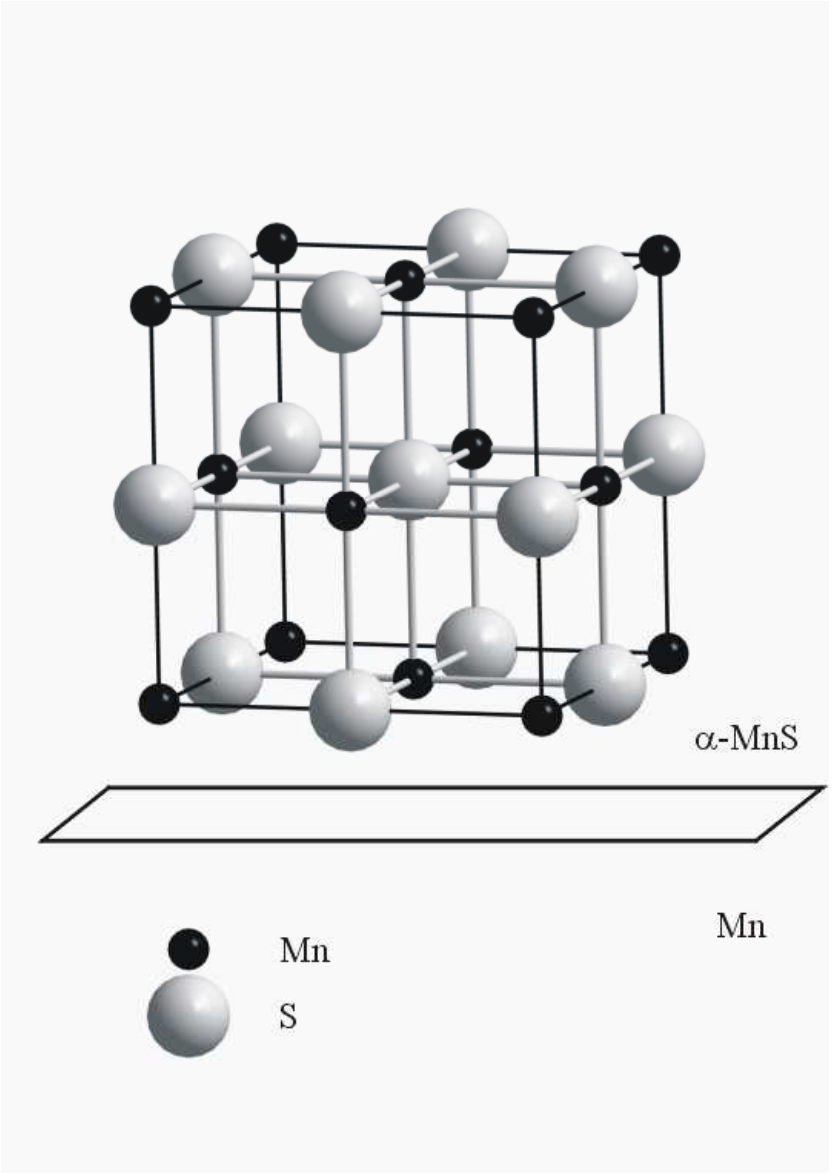

Comparison between the sulphidation and oxidation rates of metals

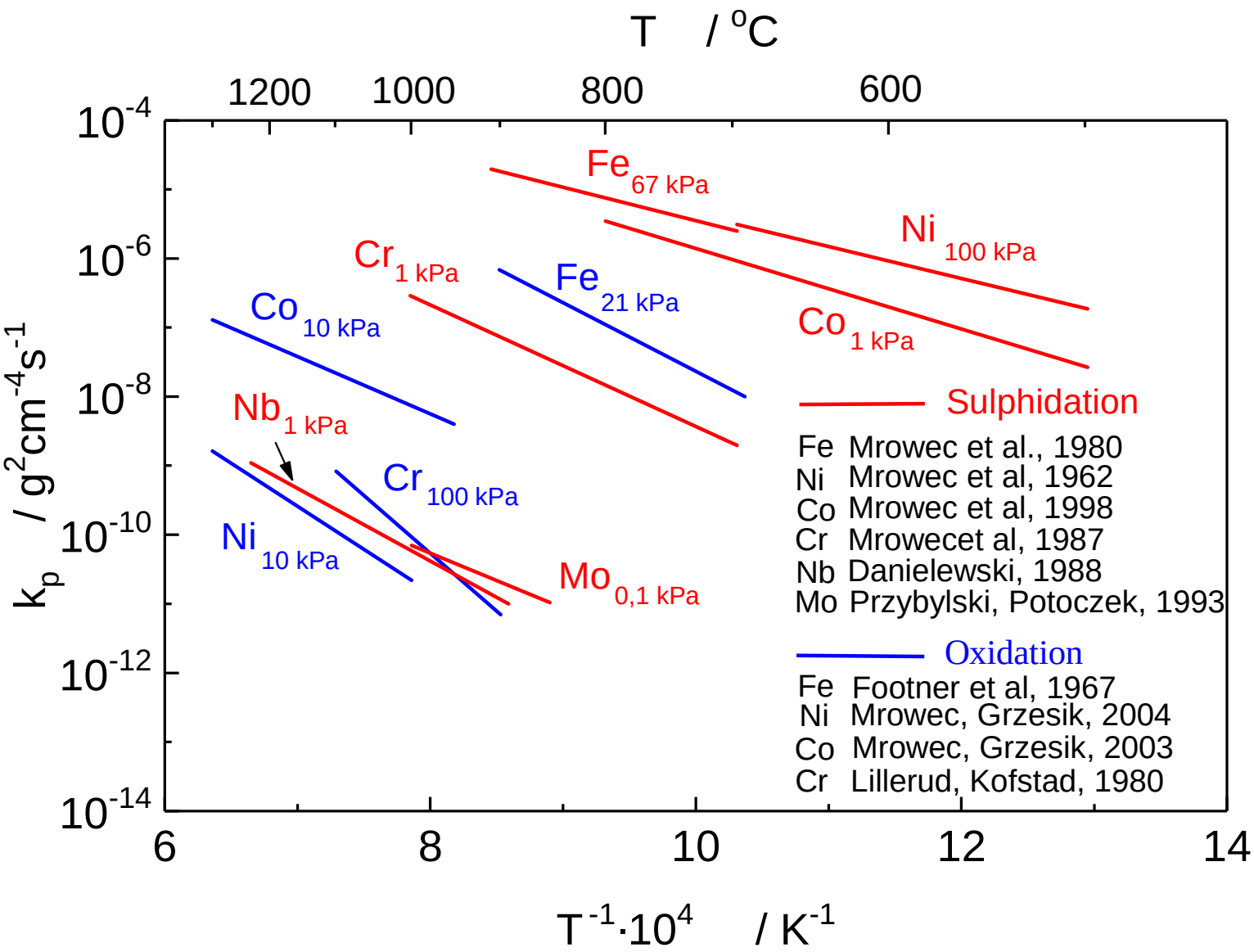

Pressure dependence of deviation from stoichiometry in $Nb_{1+y}S_2$

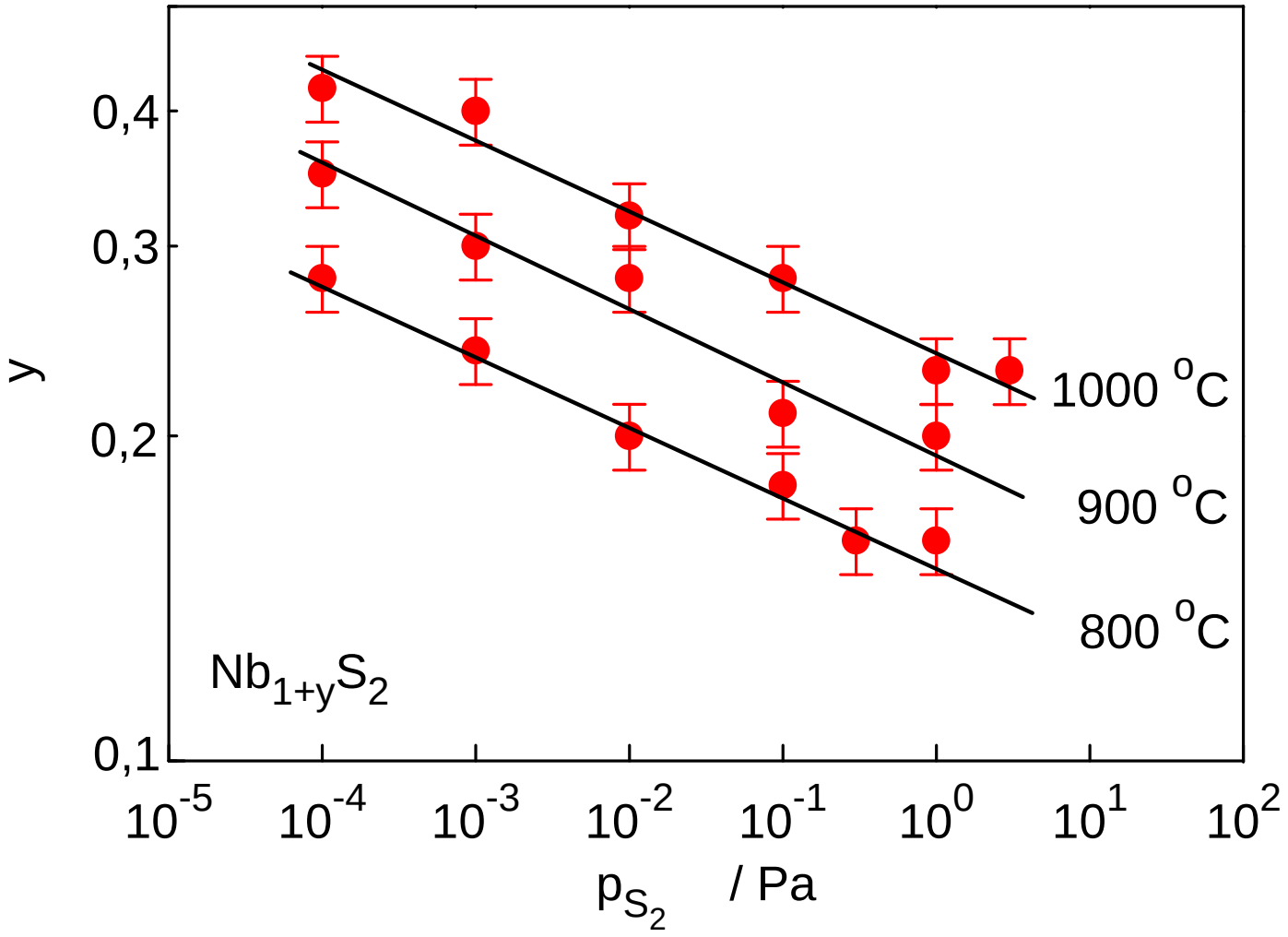

Temperature dependence of $\tilde{D}$ for selected metal sulfides and oxides

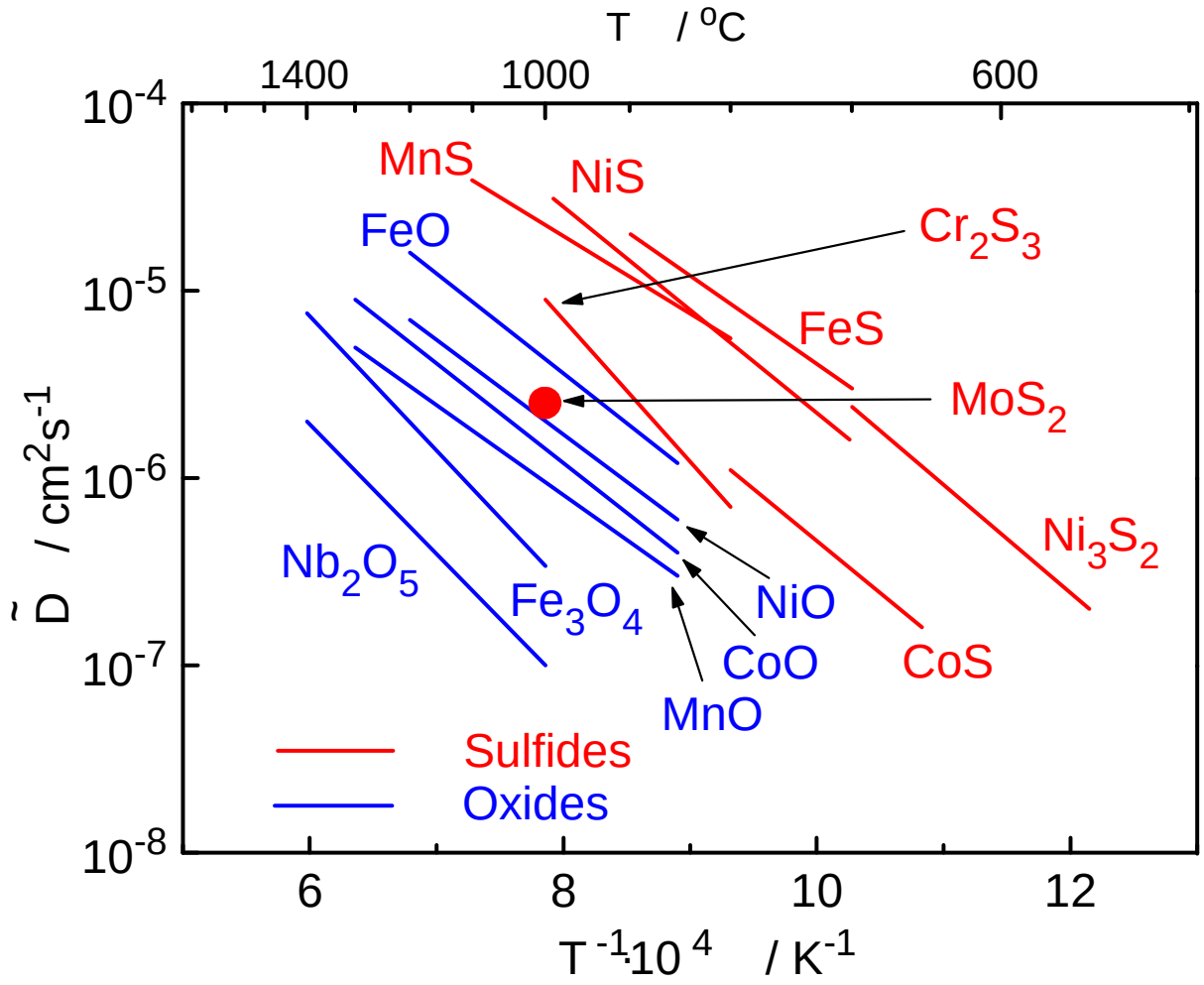

$Nb_{1+y}S_2$ – temperature dependence of $\tilde{D}$

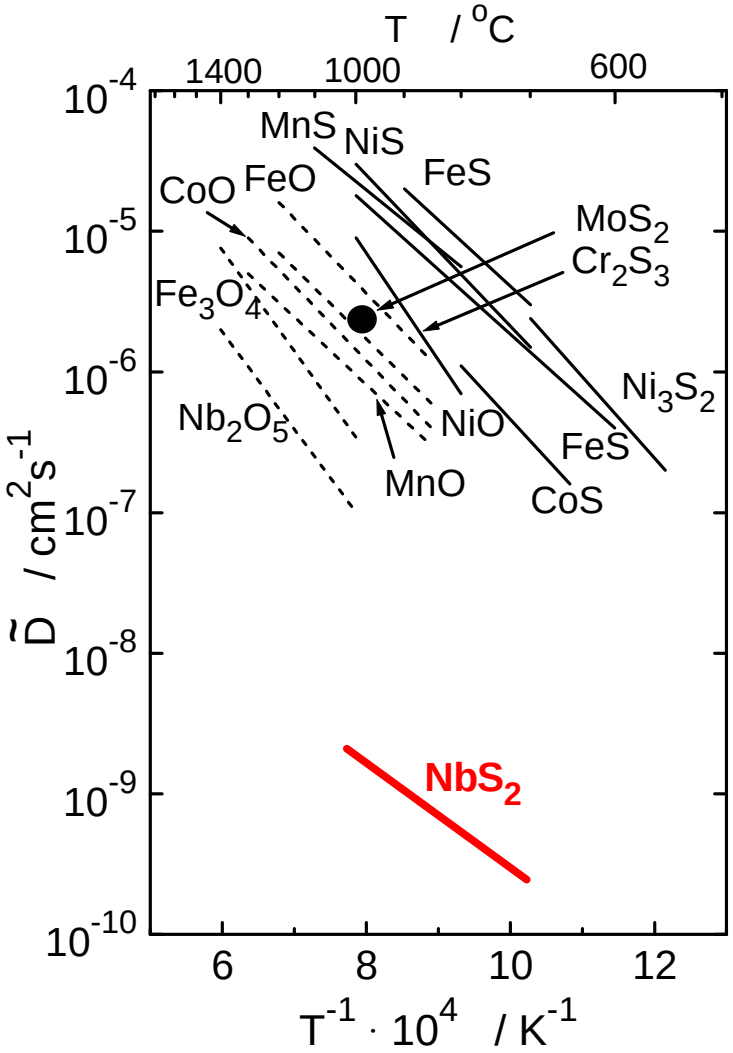

Z. Grzesik, S. Mrowec, ”On the sulphidation mechanism of niobium and some Nb-alloys at high temperatures”, Corrosion Science, **50**, 605-613 (2008).

Image of the surface and cross-section of a sulfide scale on niobium

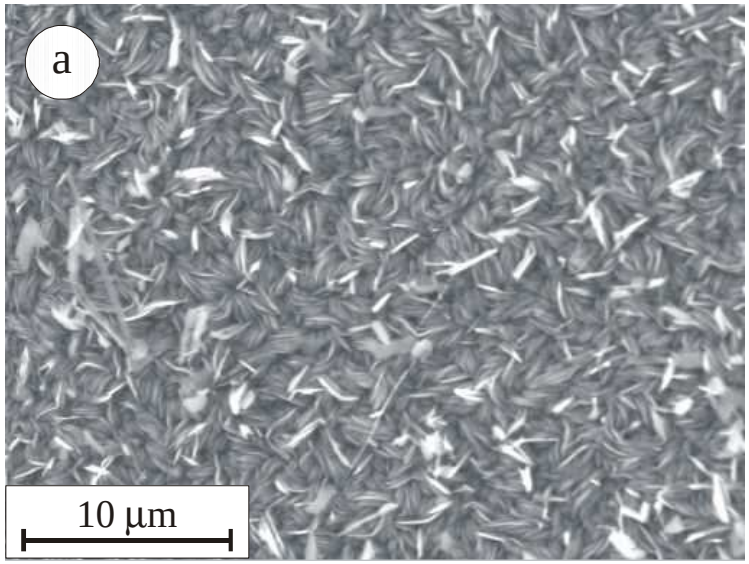

T = 1000 °C,
$p(S_2)$ = 1 Pa,
t = 120 h

surface

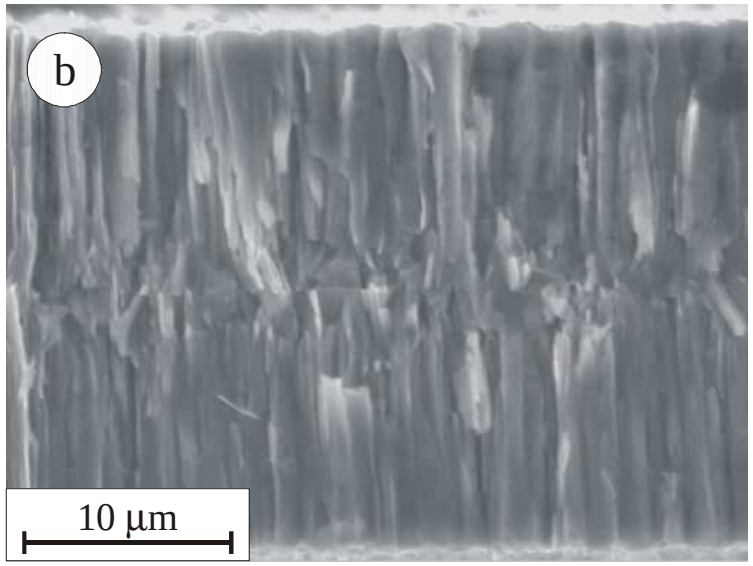

fracture

Perspective projection of 2H-NbS_2 crystallographic structure in the ⟨100 direction ⟩

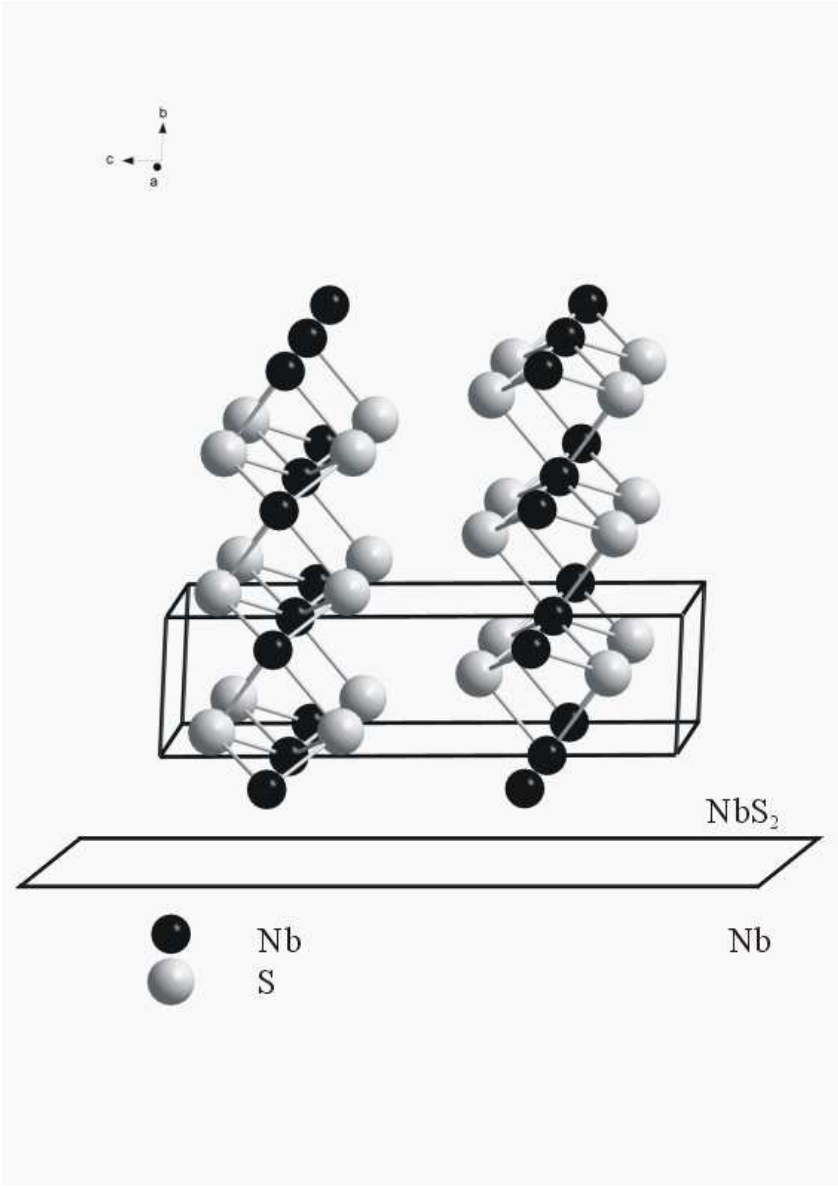

Perspective projection of $Nb_{1+y}S_2$ crystallographic structure (for y = 1/3) in the ⟨100 direction⟩

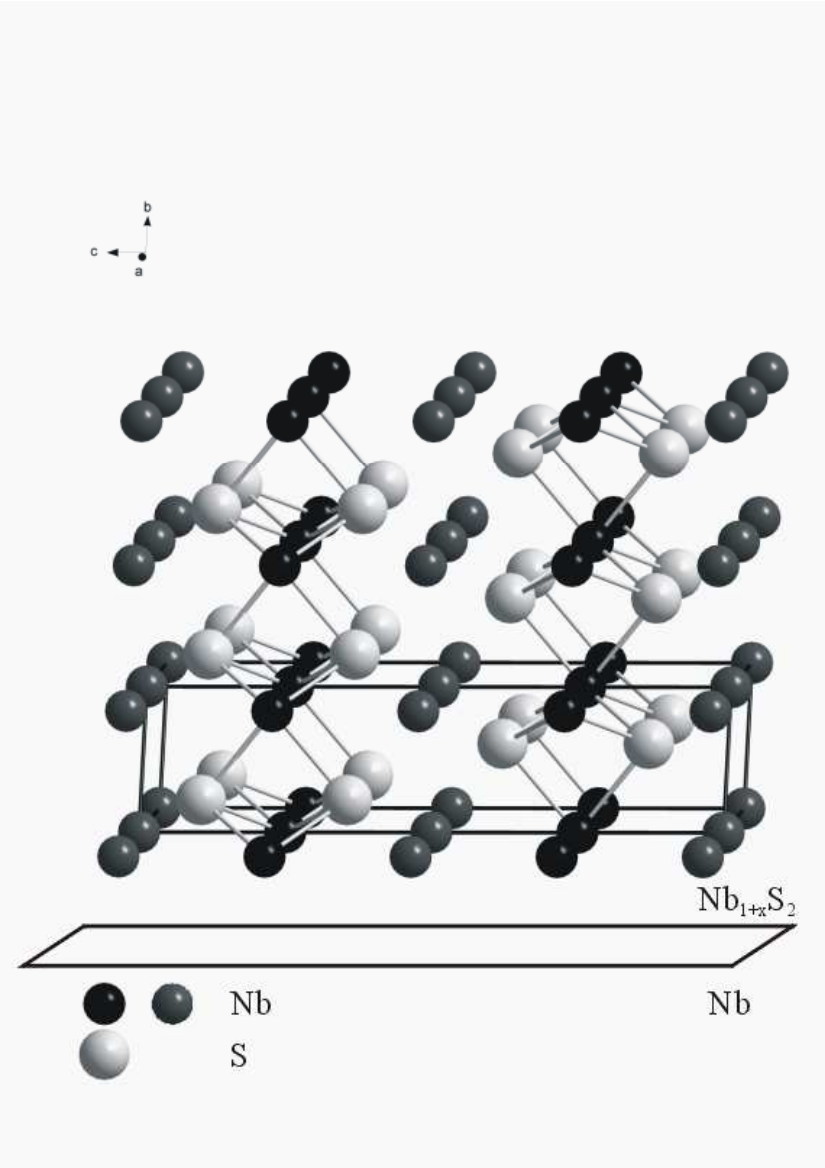

Temperature dependence of $\tilde{D}$ for nickel and cobalt sulfides

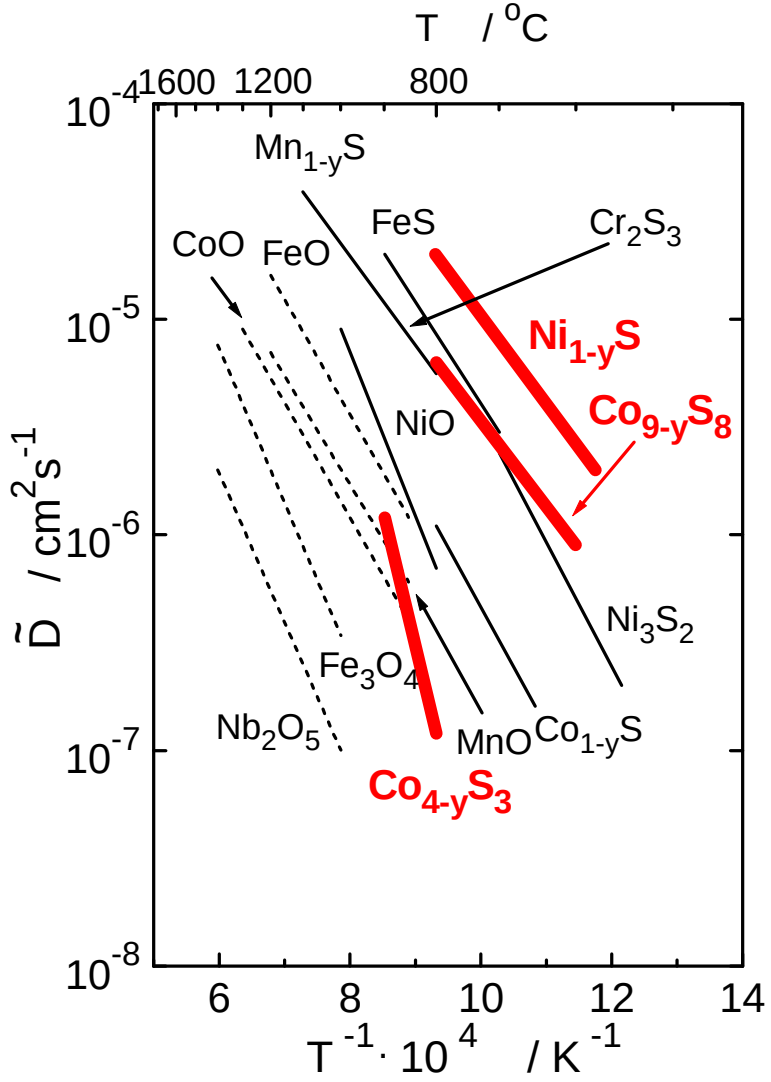

Comparison between experimental and calculated k'_p values for $Co_{4-y}S_3$

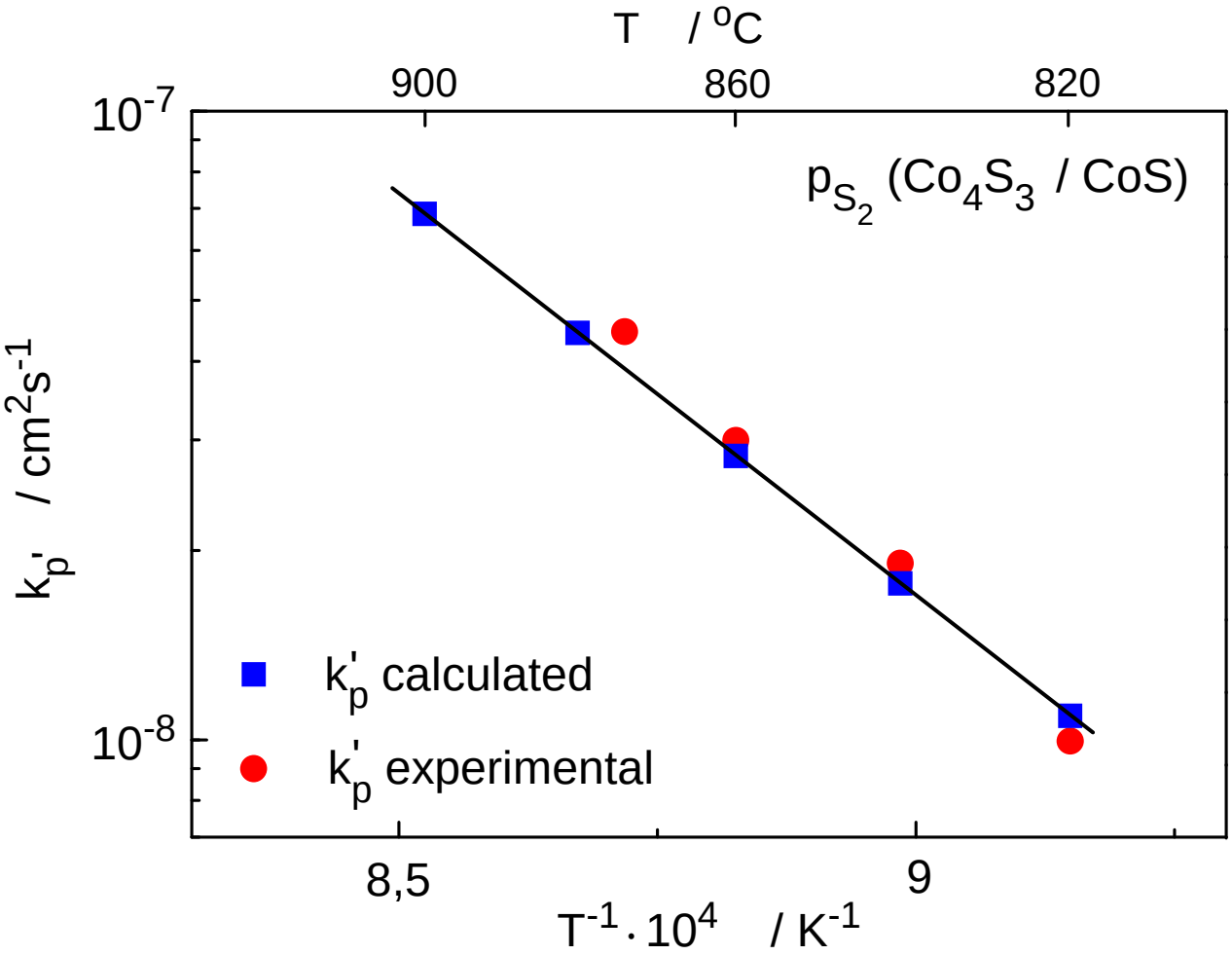

Comparison between experimental and calculated k'_p values for Co_9S_8

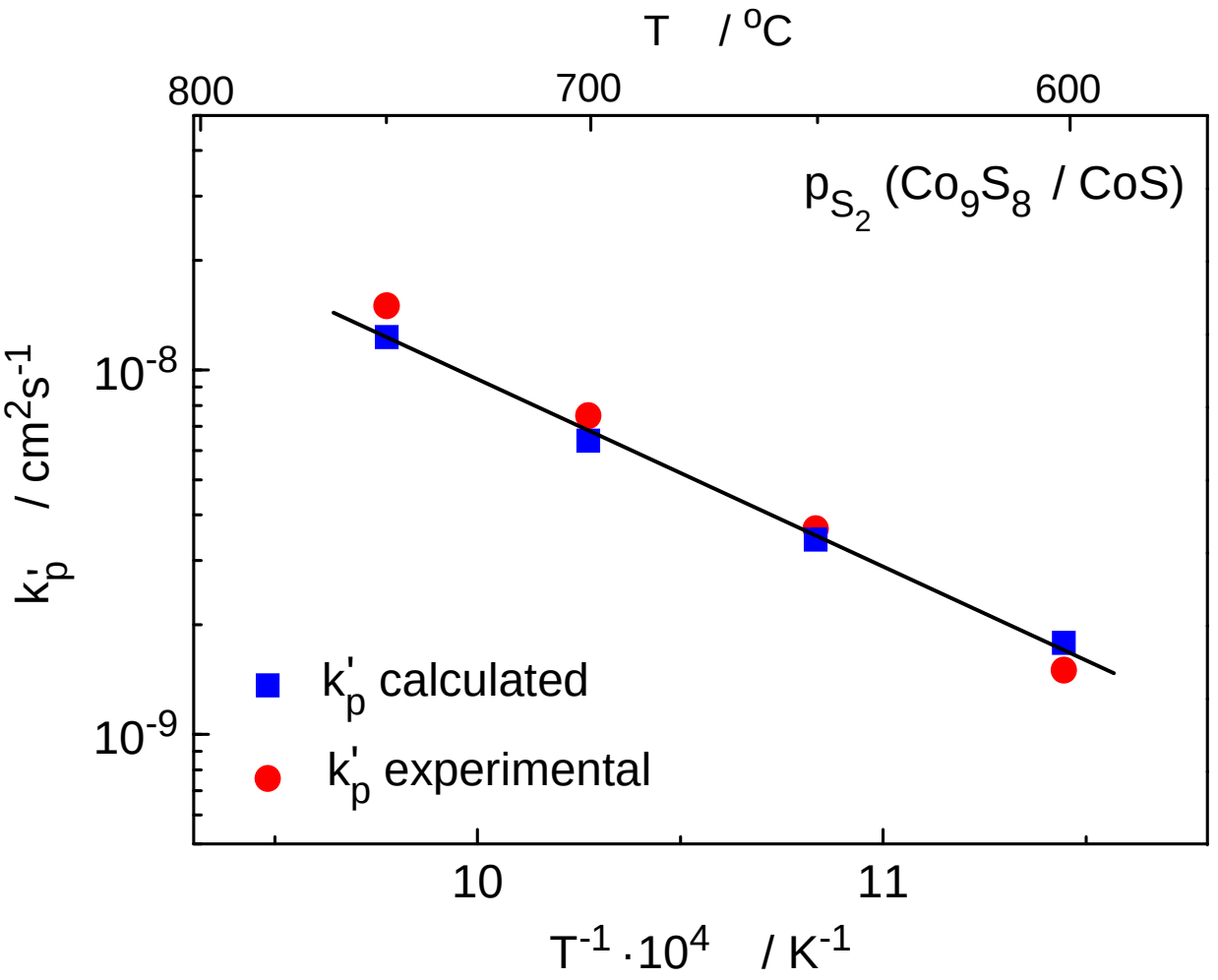

Comparison between experimental and calculated k'_p values for $Ni_{1-y}S$

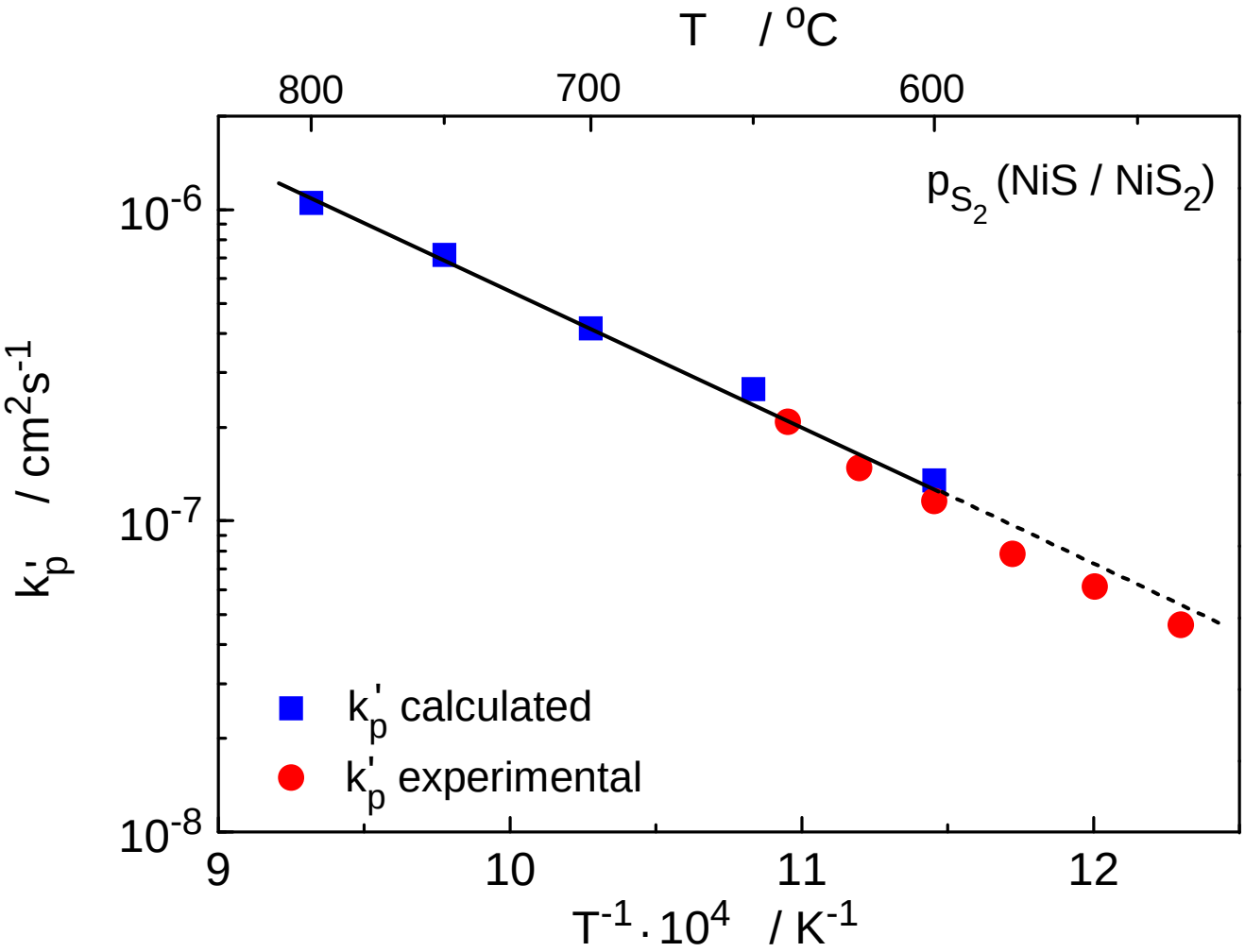

SEM images of sulfide scales formed on cobalt and nickel

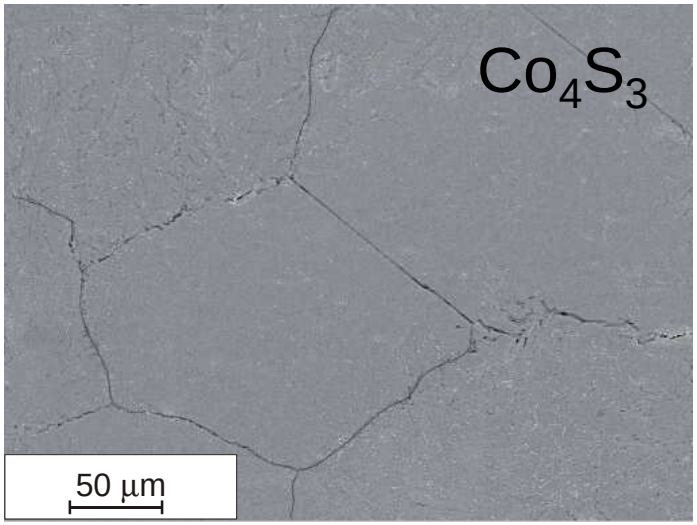

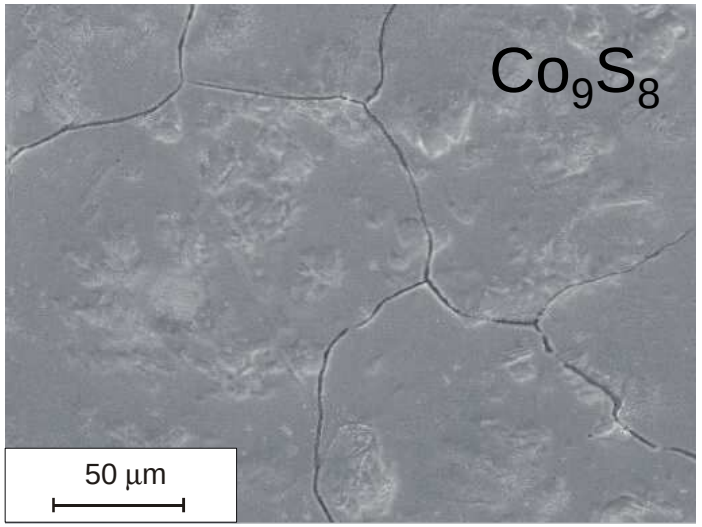

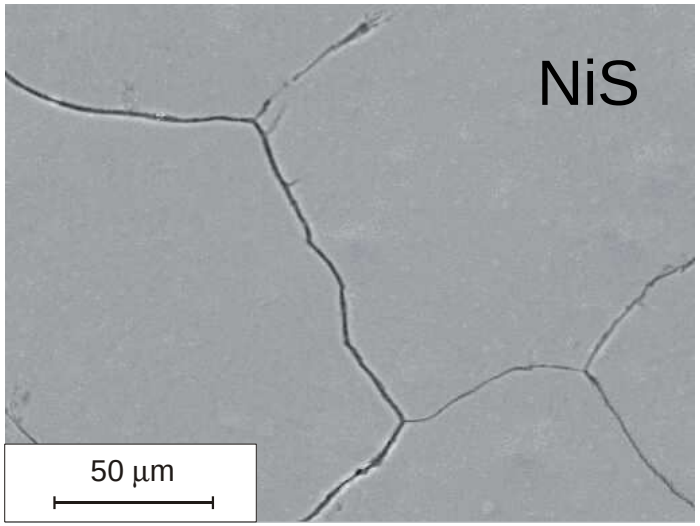

Projection of Co_9S_8 crystallographic structure in the ⟨100⟩ direction

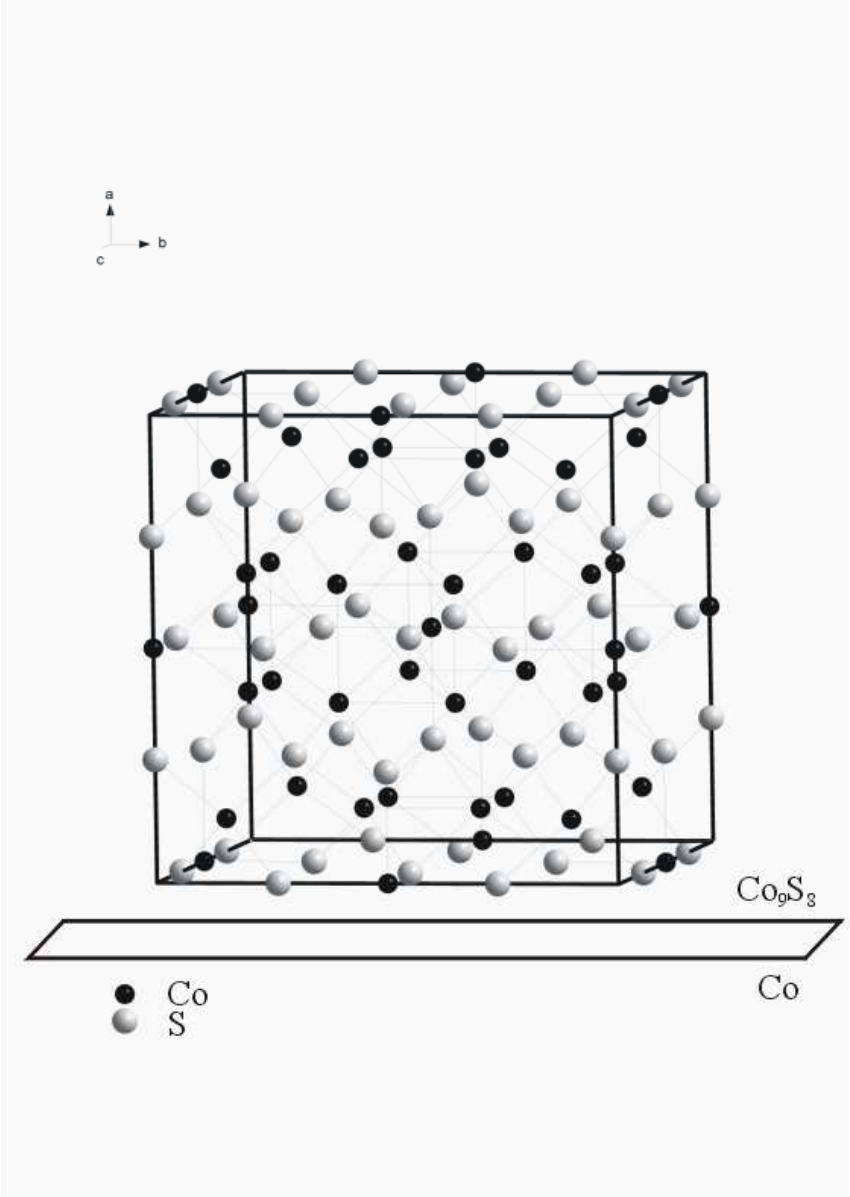

Projection of NiS crystallographic structure in the ⟨100⟩ direction

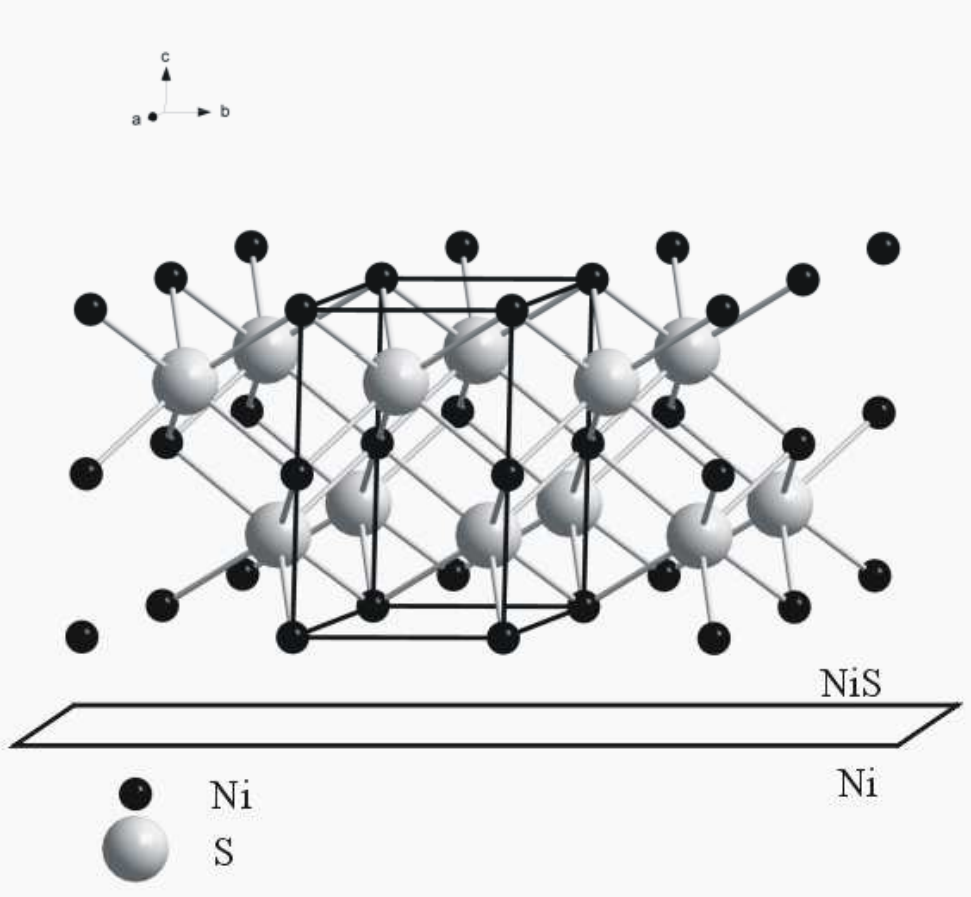

THE END